
# UNIVERSITY OF SOUTHAMPTON

FACULTY OF NATURAL AND ENVIRONMENTAL SCIENCES

School of Ocean and Earth Science

Volume 1 of 1

**Probing rates of growth and mortality in natural coccolithophore populations**

by

**Kyle Mayers**

Thesis for the degree of Doctorate of Philosophy

[April 2018]

**UNIVERSITY OF SOUTHAMPTON**

## ABSTRACT

FACULTY OF NATURAL AND ENVIRONMENTAL SCIENCES

SCHOOL OF OCEAN AND EARTH SCIENCE

Thesis for the degree of Doctor of Philosophy

# PROBING RATES OF GROWTH AND MORTALITY IN NATURAL COCCOLITHOPHORE POPULATIONS

Kyle Michael James Mayers

Coccolithophores are biogeochemically important components of marine phytoplankton communities through the intracellular production and subsequent export of calcium carbonate scales, termed coccoliths. The species *Emiliania huxleyi* is considered the most cosmopolitan and dominant coccolithophore in the modern ocean, having the ability to form extensive blooms. A hypothesis for the evolution and function of coccoliths, as well as for how *E. huxleyi* can form large-scale blooms, is that the presence of coccoliths provides protection against microzooplankton grazers. This thesis sets out to directly test this hypothesis using several lines of evidence.

In this thesis, I show how gradients in nutrients and irradiance control coccolithophore biogeography on spatial and seasonal scales, provide evidence that microzooplankton grazers exert strong controls over coccolithophore populations. I also show that the possession of calcium carbonate coccoliths does not provide a protective function against microzooplankton ingestion of *E. huxleyi*, when grazing rates are compared with other similarly sized, but non-calcified, phytoplankton groups. I also observed no negative impact on community grazing rates by microzooplankton when *E. huxleyi* was dominant within the phytoplankton community.

Although coccoliths do not appear to prevent ingestion of coccolithophores by microzooplankton, evidence is presented that rather the coccoliths may protect the organic cell from dissolution within the vacuole of microzooplankton grazers. Overall, this thesis provides a greater understanding of the role of microzooplankton in coccolithophore growth and mortality. Microzooplankton grazing could also reduce the export of calcite to depth, particularly if dissolution occurs within vacuoles, leading to enhanced $CO_2$ recycling within the upper ocean.

# Table of Contents

# Table of Tables

# Table of Figures

Table of Figures

# Academic Thesis: Declaration Of Authorship

I, Kyle Mayers, declare that this thesis entitled “Probing rates of growth and mortality in natural coccolithophore populations” and the work presented in it are my own and has been generated by me as the result of my own original research.

I confirm that:

1. This work was done wholly or mainly while in candidature for a research degree at this University;
2. Where any part of this thesis has previously been submitted for a degree or any other qualification at this University or any other institution, this has been clearly stated;
3. Where I have consulted the published work of others, this is always clearly attributed;
4. Where I have quoted from the work of others, the source is always given. With the exception of such quotations, this thesis is entirely my own work;
5. I have acknowledged all main sources of help;
6. Where the thesis is based on work done by myself jointly with others, I have made clear exactly what was done by others and what I have contributed myself;
7. Parts of this work have been published as:

Mayers, K. M. J., Poulton, A. J., Daniels, C. J., Wells, S. R., Woodward, E. M. S., Tarran, G. A., et al. (2018). Growth and mortality of coccolithophore during spring in a temperate Shelf Sea (Celtic Sea, April 2015). *Prog. Oceanogr.*, doi:10.1016/j.pocean.2018.02.024.

Signed: .....

Date: .....

# Acknowledgements

I have had the great privilege during my PhD to work with a large number of excellent scientists, people and friends. There are too many to name in this short section, so I apologise to anyone who is not mentioned, but know that you helped get me to this point.

Firstly, I would like to thank my supervisors, Alex Poulton and Toby Tyrrell, as well as my panel chair Anna Hickman. Panel meetings have been a real test of my knowledge and understanding of the subject material, and I thank you for this. It has made me a better scientist, and organiser! A special thanks to Alex, who not only took a chance on an enthusiastic biologist, but also gave me amazing opportunities throughout my PhD. I am sure at times, you wondered if I would ever stay in one place for longer than a month, but your patience, knowledge and just general approach to everything in life has been amazing over the last three and a half years. I hope I did not disappoint you!

A special thank you to all the crew and scientists on board the RRS Discovery, and involved in the SSB project, especially Chris Daniels and Alex who shared many early mornings and late nights with me in the container. Particular shout-outs to the diet BCs (you know who you are) for keeping me sane (debatable) during the two cruises! The spring bloom (#SpringBloom2015) would not have been the same without you. Special thank you to Dagmara for her conversations in the antechamber, and throughout our PhDs! Thank you Amber for your positivity, music, friendship, chocolate coffee beans, and throwing the best container parties! A big thank you to my official and unofficial mentor Clare Davis, for your advice, encouragement and excellent mentoring skills!

A special thanks to Sari Giering and Seòna Wells for teaching me about the joy of zooplankton, carrying out dilution experiments, and deploying nets and finding surprises, still the best birthday card I ever received. R.I.P to the only jellyfish in the Celtic Sea during April, and I will never drop a sample on the docks again. Sari has been an incredible mentor and friend. Thank you for all of our coffee chats, talking about crazy science ideas, the future and just general nonsense. Your laugh is incredibly infectious and always brightens up my day! Thank you to Seòna for her encouragement, and skills in the R and Norwegian languages! Without your advice to attend the Zooplankton conference, my life would certainly be very different to how it is now.

A HUGE thank you to my office pals (Helen, Rosie, Lucie, Chelsey, Vlad and Pri) and for putting up with me, especially my loud and furious typing. I always looked forward to chip Fridays and also the new trend of “crème egg breaks”. Special thank you to the

“NOColithophores” for being a great knowledge source for everything Coccolith-related, including the “post it of intrigue”.

The graduate community at NOCS is really special and unique, and I hope that feeling of community continues into the future. There are too many people to thank here, but a special thanks to my fellow WND’ers (especially Steve, who is always happy to help you forget about a particular crappy day!) I have to pay special homage to the wonderful Manon Duret, who is an incredible friend, scientist and housemate. I have made a truly unique and lifelong friend and have many precious memories that make me smile with you. Thank you for everything, including Flappy the office mascot (Santee-Uhhh). Lucie Munns, thank you for bringing your constant positivity in the world. Even when you have encountered dark times you always manage to shed light, and I am so happy to be your friend and fellow coccolithophore. Hurry up and finish so we can get our tattoos!

The Van Mooy lab at Woods Hole was an amazing place to work! Thank you to Ben for letting me join his lab and for all of the opportunities he has provided me! I look forward to incorporating lipids into my future work, as Kevin says, “any problem can be solved with lipids”! Everyone in Ben’s lab has been an amazing help (Kevin, Jon, Alina, Jamie, Justin), and a special thanks to Helen Fredricks, whose encyclopaedic knowledge of chemistry, constant willingness to help and snack draw is a blessing!

It was a real joy to work with the Harvey and Whalen labs during MesoHux2017, thank you for the great memories (Thais, Carrie, Kristen, Anna, Patrick and Sean). Special thanks to Sean for originally teaching me how to culture dinoflagellates, and being a great sounding board for scientific ideas and life problems! A HUGE thank you to Liz Harvey, who has been a great friend and unofficial supervisor to me! Your scientific approach is amazing, and I look forward to where our collaborations will go in the future! Thank you to the Norwegian divers.

I would also like to say a special thank you to Aud Larsen, Jessica Ray and Gunnar Bratbak at UniResearch and the University of Bergen! It has been a pleasure to be a part of your research group and to work with you. Thank you to Aud for her assistance with the thesis and constant encouragement. Tusen takk til alle i Marin Mikrobiologi!

Finally, I would like to thank my family, who have always supported me, especially my Mum who encouraged me to pursue my passions. Her work ethic and enjoyment for life is something I have learnt, and has allowed me to be where I am today. Lastly, thank you to Ej for your constant support and love, and for making sure I was still happy, healthy, and well fed, even when writing this thesis!

# Definitions and Abbreviations

| | |
|---|---|
| ACD | Aragonite compensation depth |
| ANOSIM | Analysis of Similarities |
| BCP | Biological carbon pump |
| CCD | Carbon compensation depth |
| CCS | Central Celtic Sea |
| Cell-CF | Cell normalised Calcification |
| CM | Chesson-Manly index |
| CP | Calcite Production |
| CS2 | Celtic Shelf Edge station 2 |
| CTD | Conductivity Temperature Depth |
| DIC | Differential Interference Contrast |
| DCM | Dichloromethane |
| DMS | Dimethyl sulphide |
| DMSP | Dimethylsulphoniopropionate |
| DNP-PE | 2,4-dinitrophenyl modified PE |
| DOC | Dissolved Organic Carbon |
| DOM | Dissolved Organic Matter |
| EhV | *Emiliania huxleyi* Virus |
| FSC | Forward Scatter |
| FSW | Filtered Seawater |
| HOLs | Holococcolithophores |
| HPLC | High Performance Liquid Chromatography |
| HPLC-MS | HPLC coupled Mass Spectrometry |
| JGOFS | Joint Global Ocean Flux Study |
| Li | Strauss Linear Index |

| | |
|---|---|
| NGR | Net Growth Rate |
| nMDS | Non-metric multidimensional scaling |
| PAR | Photosynthetically Active Radiation |
| PBS | Phosphate Buffered Saline |
| PERMANOVA | Permutational Analysis of Variance |
| PG | Phosphatidylglycerol |
| PP | Primary Production |
| PRO | *Prochlorococcus* spp. |
| PUFA | Polyunsaturated Fatty Acids |
| RDA | Redundancy Analysis |
| SCM | Sub-surface Chlorophyll Maximum |
| SEM | Scanning Electron Microscopy |
| SSB | Shelf Sea Biogeochemistry |
| SSC | Side Scatter |
| SYN | *Synechococcus* spp. |
| TAG | Tri-acyl glyceride |
| WCO | Western Channel Observatory |
| WSW | Whole Seawater |

# Chapter 1: General Introduction

## 1.1 Phytoplankton

Phytoplankton are mostly single celled plants that drift with the currents of marine and freshwater system. These organisms constitute the base of aquatic food webs. Through the process of photosynthesis, they convert sunlight and $CO_2$ into organic carbon. This process also produces oxygen, with oceanic phytoplankton estimated to produce ~50% of the world's oxygen, as well as half of the carbon fixed by global primary production (Falkowski & Raven, 2007). This organic carbon can be transferred to depth, through a process known as the biological carbon pump (BCP) (Boyd and Trull, 2007; Sigman and Boyle, 2000), where sinking particles are removed from the sunlit surface layers into the deep ocean. Dissolved organic carbon (DOC) released from phytoplankton through growth and mortality processes can be converted to recalcitrant organic matter, which is also exported to depth (Jiao et al., 2010).

Being at the base of the marine food web, phytoplankton are a food source for larger predators, known as zooplankton, these in turn provide a food source for fish, and finally this becomes food for larger marine animals. Phytoplankton also play important roles in the cycling of inorganic nutrients, such as nitrogen and phosphorus. This is achieved via uptake of nutrients for growth and subsequent release through cellular processes and mortality. The populations of phytoplankton are regulated by biotic and abiotic factors, both of which can affect growth and mortality rates.

## 1.2 The marine food web

The transfer of material from primary producers to higher organisms occurs along the marine food web. There are three ways an organism can obtain energy and nutrition (termed trophic strategy). These are:

1. Autotrophy: the process of synthesising organic carbon from inorganic sources using energy from sunlight (photo-autotrophy) or from oxidising inorganic compounds (chemo-autotrophy).
2. Heterotrophy: the process of gaining energy through the uptake of organic matter as dissolved organic matter (DOM, osmotrophy) or ingestion of particles (phagotrophy).
3. Mixotrophy: a mixture of the strategies above. Multiple definitions of mixotrophy have been proposed, and species exist along a continuum from nearly pure autotrophy to pure heterotrophy (Sanders, 1991, Stoecker et al., 2017). Mixotrophy

can include ingestion of chloroplasts and utilisation for photoautotrophy (kleptoplastidy) or the ingestion of bacteria (bacterivory) as an energy source.

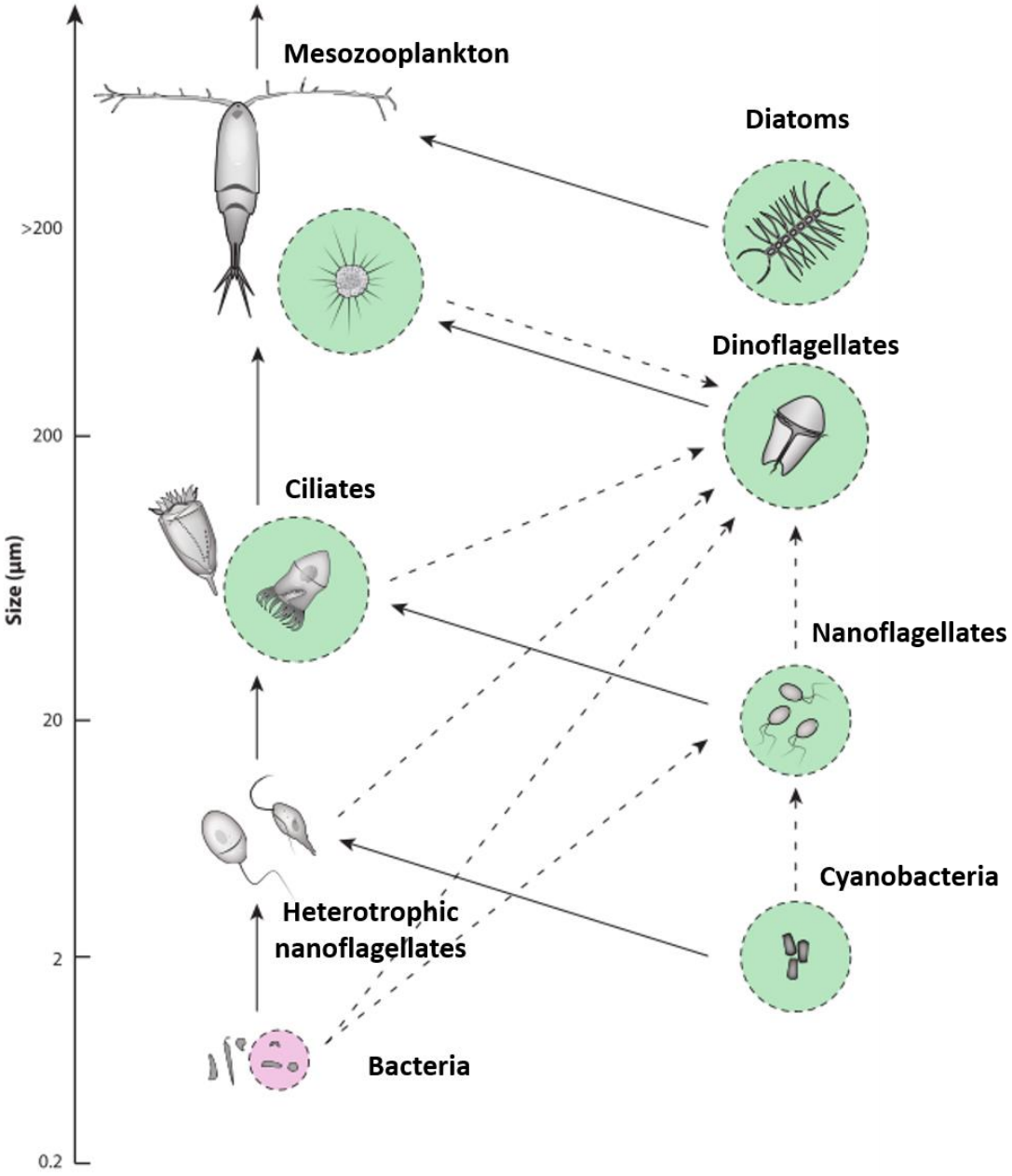


**Figure 1.1** Food web diagram showing the different modes of trophic transfer. Photosynthesis is shown by green circles; photoheterotrophy is shown by the pink circle in bacterioplankton. Solid arrows indicate ingestion of prey by heterotrophs and dashed lines by mixotrophs. Figure adapted from Stoecker et al., 2017.

A generalised food web diagram is displayed in Fig 1.1, showing the various pathways by which energy and nutrients can move through the marine environment. Regional differences in marine food webs exist due to the composition of the phyto- and zooplankton communities, which can be affected by the physiochemical characteristics. Diatom-dominated ecosystems generally have shorter food webs, and higher faecal pellet

production by copepods favouring vertical export of carbon (Henson et al., 2012). Whereas, a longer microbial food web, with smaller autotrophs and many linkages to copepods is expected to allow more organic carbon to be remineralized in the euphotic zone, reducing vertical export (Henson et al., 2012).

## 1.3 Phytoplankton groups

Phytoplankton are diverse in size, shape and extracellular coatings. They are commonly divided into size categories, of picophytoplankton (0.2-2 µm), nanophytoplankton (2-20 µm ) and microplankton (>20 µm ) (Fig 1.2) (Finkel et al., 2010).

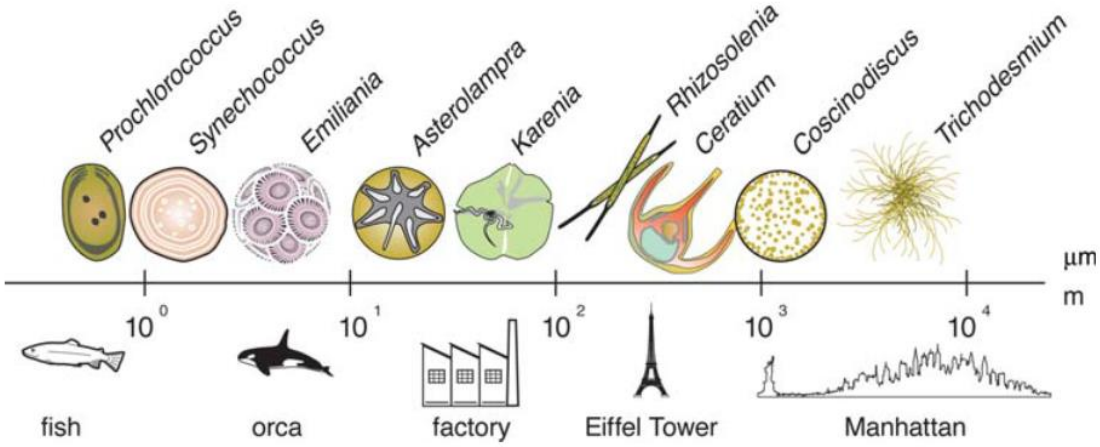


**Figure 1.2** Comparison of phytoplankton size ranges (maximum linear dimension) relative to macroscopic objects (taken from Finkel et al., 2010).

As this thesis focuses on the phytoplankton group, the coccolithophores, we will present a short overview of other components of marine communities, before focusing deeper into the coccolithophores.

Picoplankton (0.2 - 2 µm) can be sub-divided into prokaryotes (cyanobacteria and bacteria) and pico-eukaryotes. Cyanobacteria are photosynthetic prokaryotes, the primary constituents of this group within the oceans are *Prochlorococcus* (PRO), *Synechococcus* (SYN) and the filamentous *Trichodesmium*. Within the ocean, PRO and SYN appear to occupy different ecological niches, with PRO primarily being found in oligotrophic open waters, and extending deeper in the water column than SYN (Chisholm et al., 1988, Campbell et al., 1994). Pico-eukaryotes have been demonstrated as important components of the phytoplankton in oligotrophic (Ishizaka et al., 1997), coastal (Not et al., 2004) and Arctic environments (Lovejoy et al., 2007). It has also been shown that an increase in pico-eukaryote abundance can precede the spring diatom bloom in Norwegian coastal waters (Larsen et al., 2004). Being a small size (0.2 - 2µm), picoplankton are prey

species for small heterotrophic nano-flagellates (HNFs) and protistian grazers (e.g. ciliates) (Christaki et al., 1999; Evans et al., 2003).

Nanoplankton (2 – 20 µm) are observed to dominate in a large number of marine environments, believed to be due to a balance between the trade-offs related to nutrient requirements, acquisition, and use (Marañón, 2015). Nanoplankton represent a diverse range of taxa, including biomineralised and non-biomineralised forms. Common groups within the nanoplankton include diatoms, haptophytes, chlorophytes and cryptophytes.

Diatoms are purely autotrophic phytoplankton with a casing surrounding them made up of biogenic silica (known as a frustule) (Fig 1.3); they are unicellular but are able to form long chains. Diatoms can range in size from small (2 - 4 µm, e.g. *Minidiscus* sp.) to large forms (> 50 µm, e.g. *Thalassiosira* sp.), with diatom chains sometimes being up to 2 mm long. Diatoms are responsible for up to 20% of global $CO_2$ fixation (e.g., Nelson et al., 1995) and are found in all oceanographic regions. Spring blooms are thought to typically comprise larger diatom species (Guillard & Kilham, 1977), however the role of nano-sized diatoms within spring bloom conditions (Leblanc et al., 2018) has also been highlighted. Diatoms are believed to be the first phytoplankton group to bloom at temperate latitudes when irradiance increases (Margalef, 1978), which then follows an ecological succession to coccolithophores and dinoflagellates. Although enhanced biomass of picoeukaryotes has been observed to precede spring diatom blooms (Larsen et al., 2004). The silica frustules can contribute towards the sinking of organic matter out of the euphotic zone due to a ballasting effect (Dugdale et al., 1995), and thus typical diatom spring blooms can be important times of carbon export due to these organisms.

Haptophytes are a unique group of algae that differ from other eukaryotes due to the possession of a flagellum like organelle known as the haptonema during part of their life-cycle. Another unique feature is seen in the coccolithophores (the Calcihaptophycideae clade) which possess an exoskeleton of calcium carbonate (see below). Molecular evidence has suggested haptophytes originated ~824 million years ago (1,031 - 637 Ma), with the ability to calcify being between 329 – 291 million years ago (Liu et al., 2010), which is earlier than suggested by fossil evidence (~185 Ma, Bown, 1998). One of the most abundant coccolithophores, *Emiliania huxleyi* only appeared in the fossil record relatively recently (291,000 years ago; Raffi et al., 2006)). Haptophytes are globally distributed and include a number of bloom-forming species, such as *Prymnesium parvum*, *Phaeocystis globosa, Haptolina* (formerly *Chrysochromulina*) *hirta,* and *E. huxleyi*. They have been observed to numerically constitute 2.5 to 65% of nano-phytoplankton cells (Estep and MacIntyre 1989, Hajdu et al., 1996). Some members are toxic (e.g. *P. parvum*) (Roelke et al., 2011) and many are believed to be mixotrophic (Anderson et al., 2017; Skovgaard et al., 2003; Unrein et al., 2014), indeed this has been a proposed function of

the haptonema (Kawachi et al., 1991). This grazing function gives haptophytes the dual role of grazers and prey within marine systems.

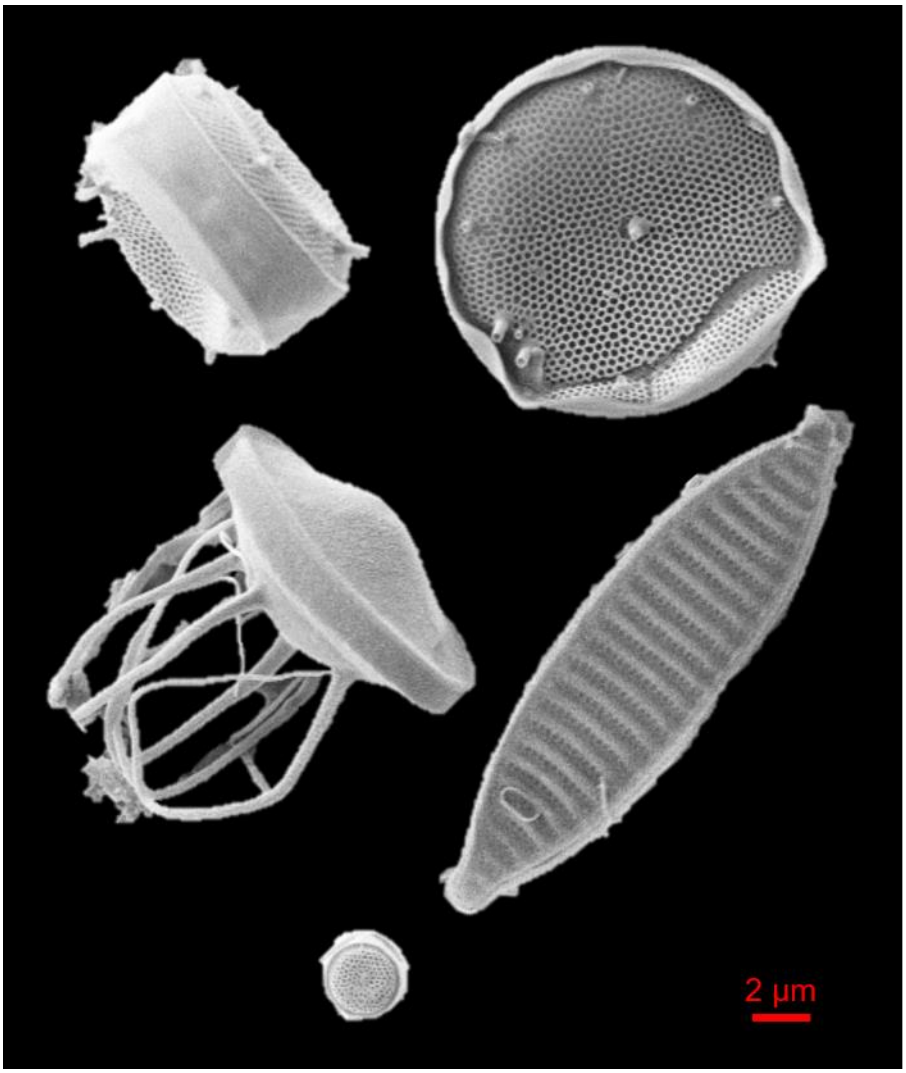


**Figure 1.3.** Different diatom species (unidentified) sampled from the Celtic Sea in April 2015 and Iceland Basin, in June 2015. Red scale bar = 2 µm.

## 1.4 Micro- and mesozooplankton

Microzooplankton are eukaryotic protists between 20 to 200 µm, they can be autotrophic, heterotrophic or mixotrophic in their mode of nutrition and include the dinoflagellates, ciliates, rotifers, and some nauplii stages of mesozooplankton organisms (Gifford, 1988) (Fig 1.4). Microzooplankton are important consumers of phytoplankton in all oceanic regions studied, ingesting on average 64 to 67% of primary production per day (Calbet and Landry, 2004; C. Schmoker et al., 2013). Both dinoflagellates and ciliates have been shown to have growth rates close to their prey species (Franzè and Lavrentyev, 2014), suggesting they are important regulators of certain phytoplankton biomass.

Dinoflagellates are a broad class of planktonic organisms, all capable of motility through the possession of flagellum (“dinoflagellate” literally means “whirling whip”). Dinoflagellates represent the end of the Margalef continuum (highly stratified and low nutrient conditions) (Margalef, 1978), and in temperate latitudes they are usually observed to dominate phytoplankton biomass during summer months and early Autumn (Widdicombe et al., 2010). Certain dinoflagellates are capable of forming blooms, some of which are toxic (e.g. red tide) (Horner et al., 1997), and there are some dinoflagellates capable of bioluminescence (e.g. *Noctiluca scintillans*) (Haddock et al., 2010; Valiadi and Iglesias-Rodriguez, 2013).

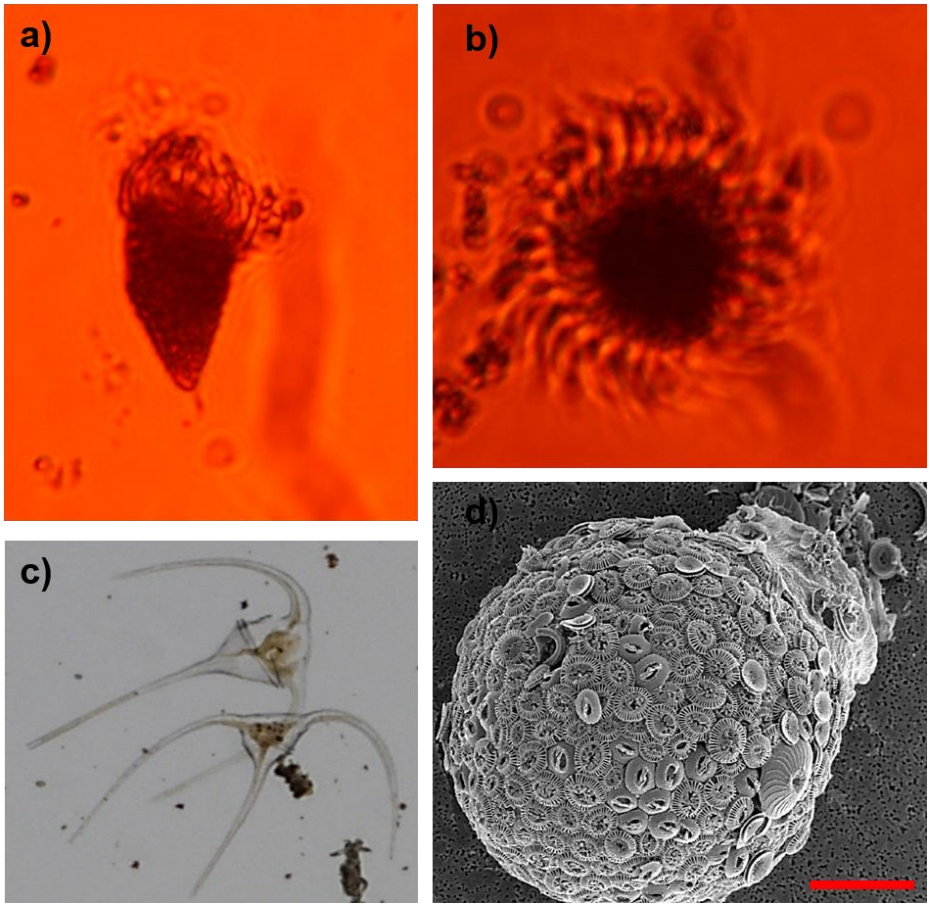


**Figure 1.4.** Microzooplankton images, *Strombidium* sp. (ciliate, a), *Mesodinium rubrum* (ciliate, b) from the Celtic Sea, April 2015, *Ceratium* sp., dinoflagellate (image courtesy of Elizabeth Harvey, Skidaway Institute for Oceanography, c), loricated ciliate with a coccolith coated lorica (image from Mikrotax.org, d). Red scale bar = 20 µm.

Dinoflagellates are particularly important grazers of phytoplankton, having the ability to graze on bacteria, other dinoflagellates and heterotrophic protists (Hansen et al., 1996; Harvey et al., 2015; Jeong et al., 2010). In fact, some dinoflagellates have been observed

to paralyse and consume metazoan prey (Berge et al., 2012). There are three main mechanisms of dinoflagellate feeding, with implications for the size of prey consumed: 1) direct engulfment of prey; 2) Peduncle feeding (extendable organelle which acts like a straw); 3) pallium feeding (a delicate feeding veil which surrounds prey and digestive enzymes are secreted by the pallium) (Jeong et al., 2010). Some species of dinoflagellates have been shown to use two different feeding modes depending on the size of the prey encountered (Berge et al., 2008). It has also been demonstrated that dinoflagellates can better withstand periods of starvation than ciliates (Jakobsen and Hansen, 1997), with some studies showing survival after more than 10 days of starvation in dinoflagellates (Anderson and Menden-Deuer, 2016).

Ciliates contain over 8000 different species (Lynn, 2008) with many different subclasses found within the marine environment. One of the smallest groups of ciliates include the scutiociliates (e.g. *Uronema* sp.), which are voracious grazers of bacteria, cyanobacteria and small picoeukaryotes (Christaki et al., 1999; Schaafsma and Peperzak, 2013). Oligotrich ciliates are common in the marine environment and graze on cyanobacteria (Christaki et al., 1999), coccolithophores (Strom and Bright, 2009), dinoflagellates and cryptophytes (Gifford, 1985).

Tintinnids are a type of ciliate, which are able to accumulate mineral particles on their lorica (a shell-like protective outer covering). The mineral particles on the lorica can be inorganic particles, as well as the biominerals from coccolithophores (Takahashi and Ling, 1984; Winter et al., 1986) and diatoms (Armbrecht et al., 2017). Although it cannot be concluded whether the coccoliths or frustules accumulate due to grazing or direct incorporation from the environment. Tintinnids were observed to have a mean digestion time in the ctenophore *Mnemiopsis leidyii* of ~30 minutes, compared to ~1.4 minutes of aloricated ciliates (Sullivan, 2010), suggesting the lorica may provide protection against digestion by grazers. Many experimental observations using molecular, cellular and pigment-based markers, and idealised food web models have shown that copepods prefer ciliates and large diatoms over small autotrophs as a food source (Larsen et al., 2015; Nejstgaard et al., 2001, 1997; Ray et al., 2016; Saiz and Calbet, 2007).

Mesozooplankton (> 200 µm), in particular copepods are estimated to consume 10 to 40% of primary production (Calbet, 2001). The most substantial component of copepod diets has been shown to be microzooplankton (Fileman et al., 2007; Nejstgaard et al., 1997). For example, even when microzooplankton constituted 3% of total carbon, they made up 41% of the copepods diet (Gifford and Dagg, 1988).

Mesozooplankton are unable to synthesise essential polyunsaturated fatty acids (PUFAs), so they must obtain them from algal prey, along with other lipid compounds (e.g. sterols).

Heterotrophic dinoflagellates (e.g. *Oxyrrhis marina*) has been shown to enhance the biochemical "quality" from algal prey, a process known as trophic upgrading (Klein Breteler et al., 1999). However, in a study of the marine ciliate *Strombidium sulcatum*, no evidence for trophic upgrading was seen (Klein Breteler et al., 2004) which may have implications for higher trophic levels.

## 1.5 Coccolithophores

Coccolithophores are a group of nanoeukaryotes with size ranges from 2 to 20 µm (Young et al., 2003). They are a member of the haptophyte clade of algae, and are believed to have evolved the ability to calcify and diverged between 321 to 291 million years ago (Liu et al., 2010). Coccolithophores produce an exoskeleton made up of calcium carbonate plates, termed coccoliths. These interlock around a cell to produce a variety of different morphologies (Young, 2003) (Fig 1.5). The production of coccoliths occurs within an intracellular vesicle and is then extruded onto the outside of the cell (Young & Henriksen, 2003). This group of organisms is responsible for ~10 to 40% of marine primary production (Poulton et al., 2007) and potentially a large proportion of pelagic calcium carbonate production and export (Broecker and Clark, 2009). As a particularly dense material, calcite sinks rapidly, and when associated with other particles can actually ballast material to the deep ocean, enhancing the BCP (Balch et al., 2016; Klaas and Archer, 2002). Although, only ~9% of pelagic produced calcite is estimated to be preserved in sediments (Balch, 2018), suggesting there is high dissolution within the water column. Calcification produces $CO_2$ as a by-product, and this process has been termed the calcium carbonate counter pump, as high abundances of coccolithophores can enhance $CO_2$ emissions, compared with non-calcite producing phytoplankton (Rost and Riebesell, 2004). Coccolithophores are also important producers of the gas dimethyl sulphide (DMS) through the production of the precursor molecule dimethylsulphide-proprionate (DMSP) (Malin et al., 1993), thus playing important roles in oceanic sulphur cycling (Fig 1.6).

The production of DMSP, and subsequent cleavage to dimethylsulphide (DMS) and acrylate within the marine environment has been proposed to play a number of roles in coccolithophore ecology, including; as an antioxidant, an osmolyte (assisting in the regulation of cellular osmolarity) and a possible chemical deterrent against grazers (Sunda et al., 2002; Archer et al., 2001). However, DMS has been observed in the laboratory to act as a chemoattractant to possible microzooplankton grazers (Seymour et al., 2010; Breckels et al., 2011) suggesting this compound could act to increase the predator-prey encounter radius. Although a link between cellular DMSP-content and grazing pressure by heterotrophic dinoflagellates was not found between different *E.*

*huxleyi* strains (Harvey et al., 2015; Strom et al., 2017). In addition, in natural communities, a difference in growth rates of DMSP-containing algae was observed, but not in microzooplankton grazing rates (Salo et al., 2010), suggesting a complex relationship between the chemical ecology of coccolithophores and predation.

Coccolithophores comprise, on average, ~10% of carbon biomass in the ocean, however during large bloom events this can be up to 40% of local carbon fixation (Mayers et al., 2018; Poulton et al., 2013). Coccolithophores follow a succession of phytoplankton along environmental gradients of decreasing nutrients and increasing water column stabilisation (Margalef, 1978; Balch, 2004, 2018). Different coccolithophore species have been observed to show separate ecological niches within marine environments, across spatial and temporal scales (Charalampopoulou et al., 2011, 2016; Poulton et al., 2017a; Smith et al., 2017). In general, coccolithophores are believed to occupy one of four niches: 1) bloom-forming species in coastal and upwelling waters; 2) oligotrophic, blue-water sites in subtropical latitudes; 3) deep dwelling (150 – 200m) species in stratified low to mid latitude waters; and 4) rarer species other than those in the first three (Young, 1994). Recently, Poulton et al. (2017) used morphological measurements of coccolithophore populations across the Atlantic Ocean to characterise tropical and sub-tropical species. Patterns were strongly influenced by vertical, rather than horizontal gradients, including some species within the sub-euphotic zone, suggesting some coccolithophore species can be mixotrophic (Poulton et al., 2017a; von Dassow et al., 2009).

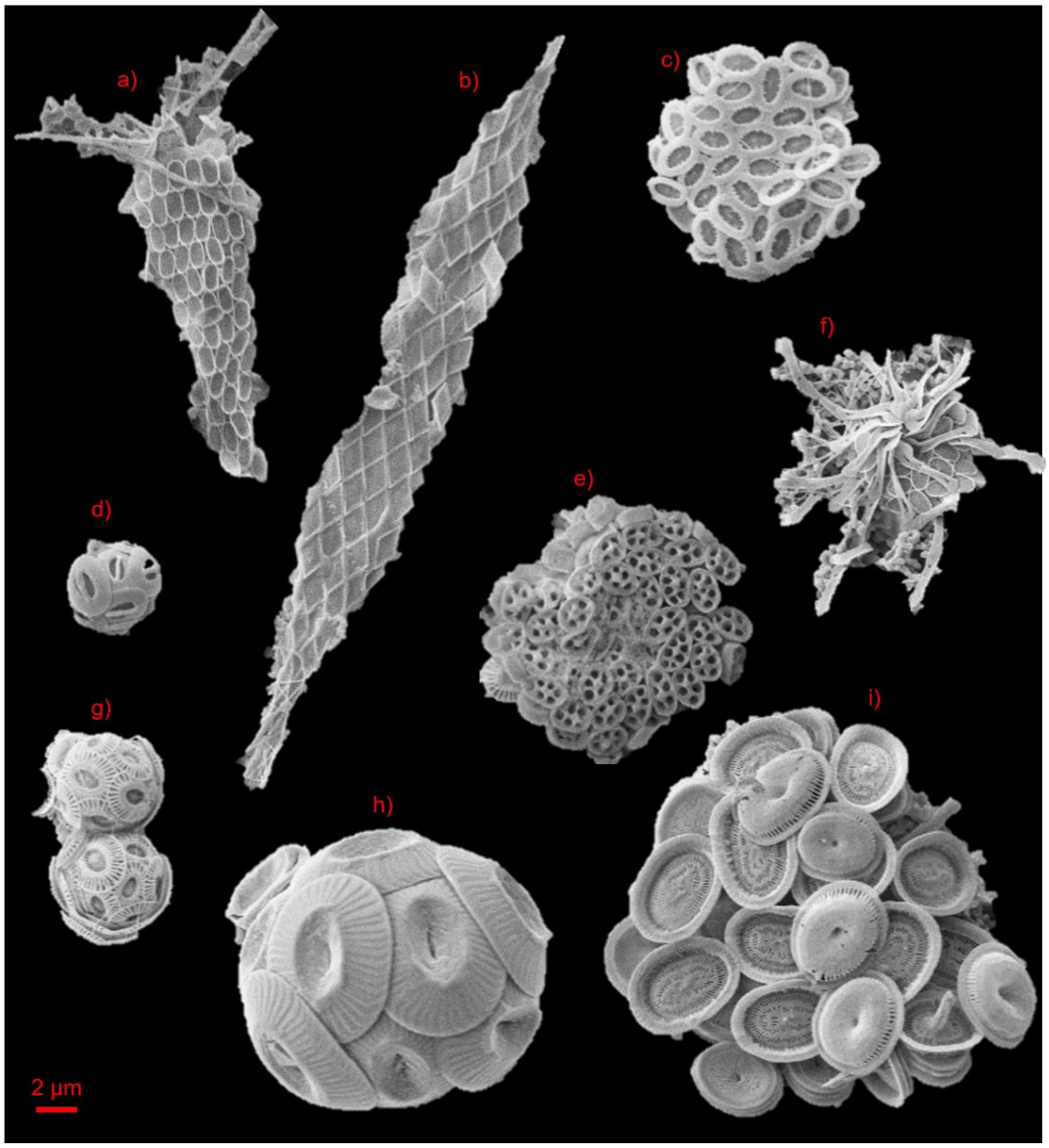


**Figure 1.5.** Coccolithophore species identified within this thesis. *Calciopappus caudatus* (a), *Calciosolenia* sp. (b), *Syracosphaera* sp. (c), *Gephyrocapsa muellerae* (d), Holococcolithophore (unidentified species) (e), *Ophiaster* sp. (f), *Emiliania huxleyi* (g), *Coccolithus pelagicus* (h) and *Coronasphaera mediterranea* collapsed coccosphere (i). Red scale bar = 2 µm.

Within coastal and shelf environments, coccolithophores show the highest abundance during summer months, as observed through cell counts and satellite data (Iglesias-Rodriguez et al., 2002; Smyth et al., 2004; Widdicombe et al., 2010). Within the Mediterranean sea, the highest abundance of coccolithophores is between December and February, during the winter mixing event with a secondary peak in May to June (Cerino et al., 2017a). The peaks are representative of different species, in the winter *Emiliania huxleyi*, and in late spring lightly calcified *Syracosphaera* spp. and holococcolithophores

(HOLs). HOLs represent a haploid life stage of particular coccolithophore species (Geisen et al., 2004). It has been suggested that this life stage exists to allow an adaptation to a wider range of environmental conditions (Houdan et al., 2006), such as seasonal changes (e.g. low nutrients, high temperature) (D'Amario et al., 2017) or strong vertical gradients (e.g. low nutrients-high light, high nutrients-low light) (Cros and Estrada, 2013; Poulton et al., 2017a). A greater understanding of environmental drivers of coccolithophore populations across both spatial and seasonal scales is required to better understand coccolithophore biogeography. Particularly in continental shelf regions, where the most intense coccolithophore blooms are often observed (Iglesias-Rodriquez et al., 2002; Tyrrell & Merico, 2004). Within chapter 2, I will quantify the vertical, horizontal and seasonal distribution of coccolithophores within the north-west European Shelf, and using multivariate statistics, analyse for associations between different species and environmental variables.

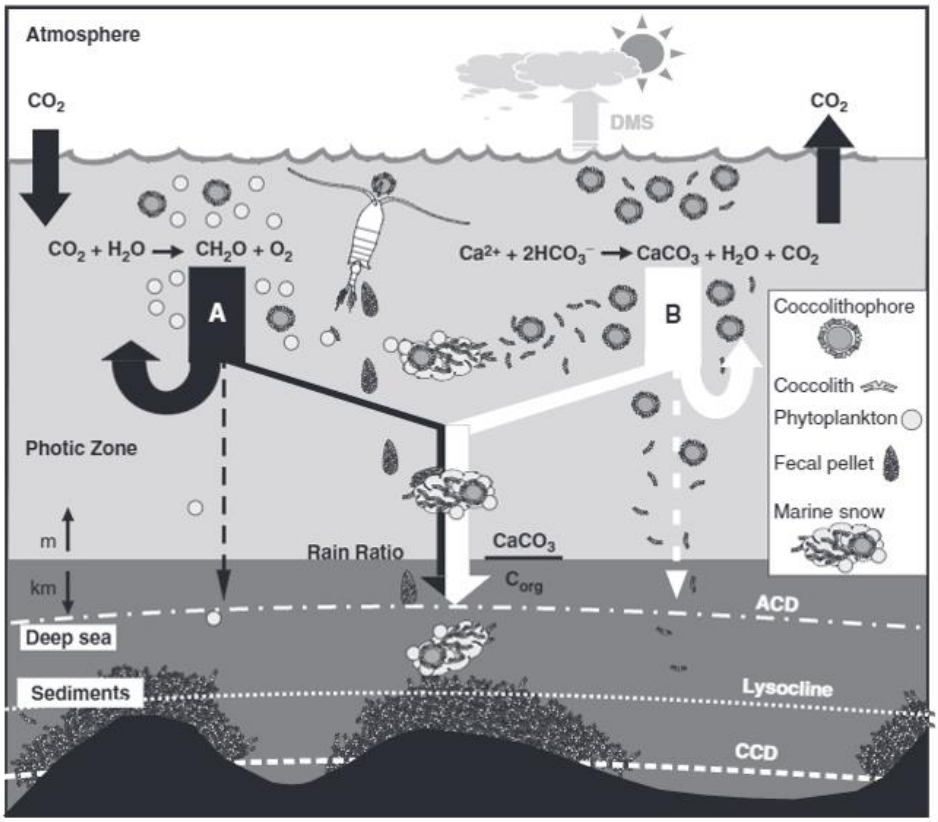


**Figure 1.6.** Illustration of the role that coccolithophores play in ocean carbon cycling. Figure is taken from de Vargas et al., 2007. ACD = aragonite compensation depth, CCD = calcite compensation depth (depth at which aragonite and calcite are undersaturated in the water column respectively and dissolution occurs below this regions).

The main bloom forming coccolithophore is *E. huxleyi*, which can produce bloom features up to 200,000 $km^2$ in area, and due to the shedding of coccoliths and subsequent light

backscattering, allow these features to be viewed from space (e.g., Balch et al., 1991, 2005). Blooms have been observed in the open ocean (Holligan et al., 1993), along continental shelves (Holligan et al., 1983; Poulton et al., 2013), and in coastal shelf seas (e.g., Buitenhuis et al., 1996; Krueger-Hadfield et al., 2014; Mayers et al., 2018; Robinson et al., 2002). There are many hypotheses as to how *E. huxleyi* can form such large-scale blooms, including nutrient conditions (nitrate to phosphate ratios), low silicic acid (reduced diatom competition), high light intensities (due to a lack of photo-inhibition in this species, and reduced mortality due to microzooplankton grazers (see review by Tyrrell & Merico, 2004).

## 1.6 Growth and mortality of coccolithophores

Enhanced concentrations of $CO_2$ can differently impact coccolithophore growth and calcification rates (Bach et al., 2015; Krumhardt et al., 2017; Raven and Crawfurd, 2012). Reports have suggested coccolithophores are expanding their ranges (Winter et al., 2013; Neukermans et al., 2018), or increasing in abundance (e.g., Widdicombe et al., 2010; Rivero-Calle et al., 2015; Krumhardt et al., 2016) hypothesised to be due to increased $CO_2$ concentrations. Other reports have suggested coccolithophores may be impaired by future oceanic conditions (e.g., Riebesell et al., 2017). Studies in the laboratory on the cosmopolitan coccolithophore *E. huxleyi*, have reported different responses to enhanced $CO_2$ (e.g., Riebesell et al., 2000; Iglesias-Rodriguez et al., 2008), $CO_2$ and temperature (e.g., Müller et al., 2014), and light (e.g., Zondervan et al., 2002; Perrin et al., 2016; Feng et al., 2016). However, when considering multiple effects of climate change, particularly enhanced nutrient limitation, the response of coccolithophores to $CO_2$ is different (e.g., Müller et al., 2017). These studies show there is still much uncertainty in how coccolithophores will respond to climate change. The differences observed may also be due to the high genetic diversity between *E. huxleyi* strains (Read et al., 2013).

In many regions of the ocean, nutrients can be limiting, particularly nitrogen in many oceanic regions, although phosphorus can also be the limiting nutrient in other regions (e.g. the Mediterranean and Sargasso Sea) (Moore et al., 2013). The bloom-forming *E. huxleyi* has been shown to utilise a variety of different nitrogen sources (e.g. nitrate, ammonia) (Strom and Bright, 2009). Different strains of *E. huxleyi* were able to grow mixotrophically on all organic nutrient sources tested, whereas *Coccolithus pelagicus* and *Calcidiscus leptoporus* only grew on 70% and 30% of the tested nutrients, respectively (Benner and Passow, 2010). The enzyme alkaline phosphatase (APA) enhances a cell's ability to scavenge inorganic phosphorus during periods of phosphate stress; *E. huxleyi* has been shown to possess both constitutive and inducible APA activity (Dyhrman and Palenik, 2003). It has also been demonstrated that *E. huxleyi* can substitute non-

phosphorus lipids for phosphorus containing lipids in response to low P environments (Van Mooy et al., 2009), a process not yet observed for other coccolithophore species. These studies suggest that *E. huxleyi* is able to rapidly respond to an increase in nutrient conditions within the water column. In bioassays, coccolithophores on the north-west European shelf showed enhanced growth rates when nitrate and phosphate were added, aside from in a mixed community in the off-shelf Bay of Biscay which displayed no response, possibly due to light limitation or different grazing pressure (Poulton et al., 2014).

Phytoplankton, including coccolithophores, also require minor elements, such as trace metals, for their growth requirements. In the Iceland Basin, evidence has suggested that coccolithophores could be iron limited (Nielsdóttir et al., 2009; Poulton et al., 2010) and in the Southern Ocean once silicate becomes depleted, coccolithophores are able to thrive at the ambient iron levels and outcompete diatoms (Hopkins et al., 2015; Balch et al., 2014, 2016). Culture experiments with *E. huxley*i have also shown a requirement for zinc and cobalt (Boye et al., 2017; Brand et al., 1983). It was believed coccolithophores did not require silicate for growth, given that a hypothesis is that they are able to outcompete diatoms once the silicic acid concentration has become limiting to diatom growth (Egge and Asknes, 1992; Tyrrell and Merico, 2004). However, it has recently been shown that different coccolithophore species had requirements for silica in culture (Durak et al., 2016). Although, this requirement was not observed in the bloom forming *E. huxleyi* or the closely related species *Gephyrocapsa oceanica*, it was seen in *Coccolithus braarudii* and *Calcidiscus leptoporus*.

As discussed above, microzooplankton grazing is an important loss factor for phytoplankton populations. The technique commonly employed to provide estimates of both phytoplankton intrinsic growth rates (i.e. growth in the absence of mortality) and microzooplankton grazing rates is known as the *dilution technique* (Landry et al., 1995; Landry and Hassett, 1982). This technique involves producing sequential dilutions of whole seawater (WSW) with ~0.2 µm filtered seawater (FSW). Typically, four dilutions are used, however recent evidence has displayed a two-point dilution method can provide accurate rate estimates (Morison and Menden-Deuer, 2017), and by reducing the time and resources needed to set up a multiple point dilution allows examination of more variables in the environment. Macro-nutrients (nitrogen and phosphorus) are also commonly added to dilution bottles to ensure measured phytoplankton growth rates are not limited during the incubation times (24 hours) used (Landry et al., 1995), unless nutrients are determined to be replete (for growth) in the environment.

The dilution technique relies on two main assumptions (Landry et al., 1995; Landry and Hassett, 1982):

1. Phytoplankton growth rate is independent of dilution (i.e. at any dilution point the rate of population change is equal);
2. Grazing rate varies proportionally with dilution and the probability of a phytoplankton cell being consumed is a function of the rate of encounter.

The dilution technique has been extensively used across the oceans including polar, tropical, coastal and open ocean regions (Calbet and Landry, 2004; C. Schmoker et al., 2013). In certain circumstances the assumptions of the dilution technique can be invalidated, and produce a variety of responses which are sometimes hard to interpret (Calbet and Saiz, 2013). For instance, during certain phytoplankton blooms, the preparation of FSW may lead to a release of allelochemicals which inhibit phytoplankton growth, thus in dilute treatments the phytoplankton growth rate is depressed (violating assumption 1) and leads to underestimates of growth and mortality rates (Stoecker et al., 2015).

The second assumption is more difficult to quantify, firstly because dilution can impact microzooplankton in different ways to phytoplankton populations, for instance through grazer mortality in dilute treatments, particularly for planktonic ciliates (Dolan et al., 2000). Converting rate estimates to consumption per microzooplankton cell have also occasionally displayed unrealistically high clearance rates (Dolan and Mckeon, 2005). The filtration step to produce diluent can also release metabolites and other cellular components into the water, which can impact on bacterial production rates (Pree et al., 2016a).

However, even given these issues, the dilution technique has and continues to provide a wealth of data on the role of microzooplankton grazing in food webs and the cycling of carbon and nutrients. As suggested by Dolan et al. (2000, 2005), a greater appreciation of microzooplankton within dilution experiments, and within marine ecology is required to fully elucidate ecological and evolutionary relationships.

Copepods in laboratory and mesocosm experiments have also been shown to feed on *E. huxleyi* (Harris, 1994; Nejstgaard et al., 2008, 1997; Sikes and Wilbur, 1982), however faecal pellets produced from a mono-diet of the coccolithophore species *Calcidiscus leptoporus,* are very fragile (Langer et al., 2007), and likely do not contribute significantly to carbon export. Although when copepods were fed *E. huxleyi*, there was no report on fragility of faecal pellets (Harris, 1994), it was mentioned that incomplete quantitative recovery was possible, and could have led to the high estimates of dissolution in Harris (1994) (27 – 50%), which were not observed in Langer et al. (2007) (only ~7%). During mesocosm experiments with *E. huxleyi* blooms, it was estimated that the sinking rate was

enhanced by ~35 to 40% when coccoliths were present (Bach et al., 2016), suggesting coccolith calcite can enhance calcite flux in natural communities.

However, given the small cell size of *E. huxleyi* (<10 µm) compared to copepods (>200 µm), it is unlikely to make up a significant proportion of their diet. The main functional link from copepods to *E. huxleyi* may be through trophic cascades (Calbet and Saiz, 2013) where enhanced grazing pressure on the microzooplankton grazers of *E. huxleyi* may free it from mortality and allow biomass accumulation of this coccolithophore to occur. This has been observed for autotrophic nano-flagellates in mesocosm experiments with added copepods (Pree et al., 2016b; Zöllner et al., 2009), though neither author examined for the presence of coccolithophores in the community.

## 1.7 Biomineralisation as a protective function against grazers

The biomineralisation of both diatoms and coccolithophores has been suggested to provide mechanical protection against grazers (Sikes and Wilbur, 1982). Within diatoms, micro-crush-tests and feeding experiments with copepods have shown a correlation between the size and mechanical properties of the frustule and feeding success (Friedrichs et al., 2013; Hamm et al., 2003). Within coccolithophores, the presence of interlocking coccoliths and the polysaccharide matrix have suggested the coccosphere may provide a mechanical protective function (Young, 1994; Jaya et al., 2016; see review by Monteiro et al., 2016). However, this was only for the species *E. huxleyi*, and no evidence has been observed in a reduced grazing rate by copepods on calcified vs non-calcified strains of *E. huxleyi* (Sikes and Wilbur, 1982).

Generally, the major grazers of many coccolithophores species are likely to be the microzooplankton, due to the small size (2 - 20 µm) of this algal group. Coccoliths have been hypothesised to act as a deterrent against grazing by microzooplankton (Monteiro et al., 2016), particularly for “spiky” morphologies (e.g. *Calciopappus caudatus,* Fig 1.5) (Young et al., 2009). In laboratory experiments, there has been no evidence that calcified *E. huxleyi* cells are ingested less than non-calcified variants (Harvey et al., 2015; Strom et al., 2017), and in one study calcified cells appeared to be selectively grazed on due to the increased cell size (Hansen et al., 1996). Harvey et al. (2015) observed that the ingestion rate of *E. huxleyi* varied depending on the strain (with highest and lowest rates observed on calcified cells); however, the growth rate of the dinoflagellate grazer was significantly reduced when grazing on calcified over naked cells. This suggest that calcification could act as a population-level defence, with the overall aim of reducing grazing pressure on the *E. huxleyi* population due to reduced predator growth rates, possibly caused by the negative effect of calcite buffering the pH of the food vacuole causing digestive problems

(Harvey et al., 2015). This could also be an example of kin selection altruistic behaviour within microbes (Lewin-Epstein et al., 2017), whereby slowing the predator of your offspring (in this case clones of cells due to asexual reproduction) can lead to persistence of kin. In diatoms, lower ingestion rates were observed by a heterotrophic dinoflagellate and ciliate on high silica content cells, which also displayed longer clearance rates, suggesting the frustule enhanced digestion times (Zhang et al., 2017).

Within the marine environment there has been evidence for reduced microzooplankton grazing rates during *E. huxleyi* blooms, through the observation of lower phytoplankton community grazing rates (Olson and Strom, 2002), with suggestions that this can lead to the formation and persistence of these bloom features (Fileman et al., 2002). However, there is currently no clear consensus on whether this is due to coccolithophore populations within the environment, with most data being from pigment analyses, rather than direct coccolithophore enumeration. Within chapter 3, I will show how using microscopy counts of coccolithophores it is possible to quantify the impact of microzooplankton grazers on coccolithophore populations. There has also been no direct comparisons of coccolithophore grazing rates relative to other phytoplankton groups. In chapter 4, I present flow cytometry data, which allows us to directly compare growth and grazing rates on coccolithophores and other similarly (cell) sized, non-calcified phytoplankton.

## 1.8 Other agents of mortality

Phytoplankton mortality can also be caused by much smaller agents, including marine bacteria and viruses. Viruses are obligate intracellular parasites, meaning they require a host cell in order to replicate. Viruses are the most abundant biological entity in the ocean, with $10^{31}$ viruses estimated within the oceans. If converted to a carbon biomass, this is more carbon than 75 million blue whales, and if assuming an average size of 100 nm they would stretch further than the diameter of the Milky Way (Suttle, 2005). Viruses generally have two life phases, the lytic and lysogenic. In the lytic cycle, a virus enters a cell, replicates and then causes the cell to lyse (burst open) and release progeny virus. In the lysogenic stage, a virus is able to integrate itself into the genome of the organism and lay dormant. A lysogenic virus is able to revert to a lytic phase when there is a change in environmental conditions or a host response. The lysis of cells leads to a significant release of dissolved organic matter (DOM) into the marine environment, where it can be incorporated by microbial communities, this process is termed the viral shunt, as it increases respiration and reduces transfer of material further up the food web (Suttle, 2005).

The coccolithophore *E huxleyi* has a well-characterised virus. The *E. huxleyi* virus (EhV) is a large (~180 nm diameter) double-stranded DNA virus, which has been implicated in the termination of coccolithophore blooms (Bratbak et al., 1993; Brussaard et al., 1996; Martinez Martinez et al., 2007; Vardi et al., 2012). This host-virus system has been co-evolving for at least 7,000 years (Coolen, 2011), and there is also evidence of horizontal gene transfer between host and virus, with almost all of the genes for the full sphingolipid biosynthesis pathway present within the virus (Monier et al., 2009), suggesting a high level of genetic transfer between host and virus.

There are other forms of mortality in coccolithophores, of which much less is currently known about. For instance, bacterial mediated mortality can occur within *E. huxleyi* (Mayers et al., 2016). The scutiociliate *Uronema marinum* has also been observed to cause lysis of *E. huxleyi*, potentially due to toxin secretion (Schaafsma and Peperzak, 2013). Although these other modes of mortality are not directly considered within this thesis, it is important to keep these in mind, as mortality pathways do not act alone, and may act in concert; for instance enhanced grazing on infected *E. huxleyi* cells has been observed by a heterotrophic dinoflagellate (Evans and Wilson, 2008) .

## 1.9 Thesis goals and objectives

The overall goal of this thesis was to investigate how the rates of coccolithophore growth and mortality can affect natural population dynamics, including calcite production, and lead to changes in spatial and temporal biogeography. The specific objectives were to (a) investigate the role of microzooplankton grazers in controlling coccolithophore populations, and (b) to examine if the presence of calcium carbonate coccoliths acts as an effective protective mechanism against grazing mortality. To do this I used natural spatial (cross-shelf) and temporal (seasonal) gradients, as well as mesocosm experiments.

The specific hypotheses of this thesis are:

1. A relationship between nutrients and irradiance and coccolithophore biogeography will be observed across seasonal and spatial scales, within Shelf Sea environments (Chapter 2).
2. Coccolithophores will display low growth rates during the spring bloom, as other phytoplankton dominate the community (Chapter 3).
3. Microzooplankton grazing exerts little control on coccolithophore communities due to the protection conferred by calcification (Chapter 3).
4. Coccolithophores, such as *E. huxleyi*, due to their possession of a coccosphere, are grazed at significantly lower rates by microzooplankton than similar-sized phytoplankton groups (Chapter 4).

5. Greater proportions of *E. huxleyi* in the environment will cause a reduction in community grazing rate, due to the negative impact calcite has on microzooplankton growth rates (Chapter 4).

## 1.10 Thesis outline

Chapter 2 is a field study, where coccolithophore abundance and species composition were examined at two sites within the Celtic Sea during autumn, spring and summer. In this chapter, I investigated the distribution of species relative to environmental variables, including light, nutrients, temperature and salinity. These results were then compared to coccolithophore data collected from the long-term time series station in the English Channel (Western Channel Observatory; L4) to produce a cross-shelf perspective of seasonal changes in coccolithophore populations. Using multivariate statistics, I tested the environmental variables which best correlated with the variability in coccolithophore species composition across these spatial and seasonal gradients (Hypothesis 1).

Chapter 3 is an investigation into the growth and mortality rates of coccolithophores during a spring cruise (April) to the Celtic sea. Rate measurements of calcification, net growth, and intrinsic growth and grazing rates were carried out in order to measure the variability in growth and mortality rates at the central Celtic Sea during the spring phytoplankton bloom. In this chapter, I tested whether coccolithophores showed lower growth rates while other phytoplankton species “bloomed” (Hypothesis 2). I also examined intrinsic growth and grazing rates within a spring bloom of *E. huxleyi* at another site in the Celtic Sea (station J2) and explored the role of microzooplankton grazing on controlling coccolithophore population dynamics (Hypothesis 3). This chapter has been published as:

Mayers, K. M. J., Poulton, A. J., Daniels, C. J., Wells, S. R., Woodward, E. M. S., Tarran, G. A., et al. (2018). Growth and mortality of coccolithophores during spring in a temperate Shelf Sea (Celtic Sea, April 2015). *Prog. Oceanogr.*, doi:10.1016/j.pocean.2018.02.024.

Chapter 4 is a synthesis of 45 dilution experiments conducted in mesocosms in a Norwegian Fjord (Raunefjord, western Norway) that explored the role of growth and microzooplankton grazing on phytoplankton population dynamics. Using flow cytometry, I compared such rate measurements for coccolithophores and other phytoplankton groups, including similarly sized but non-calcified pico- and nano-eukaryotes. Here, I tested the hypothesis that calcification acts as a protective mechanism against microzooplankton grazing (Hypothesis 4). I also put these results within the context of the community grazing rate using chlorophyll-*a* to examine if higher abundances of *E. huxleyi* lead to a reduced grazing rate by slowing predator growth rates (Hypothesis 5).

Chapter 5 brings together the results from chapters 2, 3 and 4 to further explore the factors affecting the distribution of coccolithophore populations. In this chapter, I summarise the impact of grazing on coccolithophores and what this means for their biogeochemistry. Firstly, I introduce a novel method for measuring mortality using high-throughput lipid analysis ('lipidomics') and look at differences in the lipidomes of *E. huxleyi* and the dinoflagellate *Oxyrrhis marina* with calcified and non-calcified prey. Secondly, I combine the intrinsic growth rates calculated from dilution experiments with the measured rates of calcification to draw suggestions on the fate of grazed calcite. Finally, the wider implications of the thesis's main findings, along with the limitations and future directions this research could take are discussed.

# Chapter 2: Cross-shelf environmental drivers of coccolithophore abundance and species composition in a temperate shelf sea

This chapter is in preparation for publication as “Cross-shelf environmental drivers of coccolithophore abundance and species composition in a temperate shelf sea”. Kyle M, J. Mayers[1], Chris J. Daniels[2], E. Malcolm S. Woodward[3], Claire E. Widdicombe[3], Alex J. Poulton[4].

[1] Ocean & Earth Sciences, University of Southampton, Southampton, UK

[2] National Oceanography Centre Southampton, Southampton, UK

[3] Plymouth Marine Laboratory, Prospect Place, West Hoe, Plymouth, PL1 3DH, UK

[4] The Lyell Centre for Earth and Marine Science and Technology, Heriot-Watt University, Research Avenue South, Edinburgh, EH14 4AS, UK

KMJM conducted data analysis, data collection on DY018 (November 2014) and DY029 (April, 2015), coccolithophore counts for all three cruises and wrote the manuscript. CJD collected data from DY029 and DY033 (July, 2015), EMSW provided nutrient data, CEW provided coccolithophore data from station L4, AJP collected data from cruise DY018 and DY033 and provided feedback on the manuscript. We also thank Tim Smyth (Plymouth Marine Laboratory) for providing photosynthetically active radiation data from L4.

## 2.1 Abstract

Coccolithophores are important components of shelf sea phytoplankton communities, contributing to the production of pelagic calcium carbonate, although factors, which affect their distributions through space and time in these regions, are not well known. Measurements of coccolithophore abundances, biomass and community composition were made during November, April and July at three stations within the north-west European Shelf, from a coastal station (L4), to the central Celtic Sea (CCS) and shelf edge (CS2). Differences between light depths in communities at CS2 and CCS were not found to be significant, apart from during July at CCS, along with a well-defined subsurface chlorophyll maximum. At CCS, coccolithophore biomass ranged from 9.0 to 123.2 nmol C $L^{-1}$ with the highest biomass observed during November, representing 4.9 to 6.9% of phytoplankton carbon. Coccolithophore communities varied with season and site, with *Emiliania huxleyi* being the greatest contributor to coccolithophore biomass (52.5 ± 34.5%), followed by *Syracosphaera* spp. (22.6 ± 28.3%) and *Calciopappus caudatus* (6.2 ± 11.3 %). These species showed different ecological niches throughout this study, with *Syracosphaera* spp. associated with environments with high nutrients and low light. During summer, *E. huxleyi* appeared to be most dominant in environments where intermittent nutrient inputs occur, such as following storms, internal tides at the shelf break, and riverine input. This study suggests that gradients in nutrients and light conditions can control the biogeographical distribution of coccolithophore species across the north-west European shelf, and intermittent nutrient supply during summer months may contribute to the observation of *E. huxleyi* blooms during this time of year.

## 2.2 Introduction

Shelf seas represent less than 10% of the global ocean in terms of area, but are responsible for up to 30% of primary production (Simpson and Sharples, 2012). Annually, shelf seas go through significant seasonal variations in physical and biological characteristics. During spring stratification of the water column and increasing irradiance and high nutrients allow high biological production. The summer brings stronger stratification and low nutrient levels in surface waters, along with a sub-surface chlorophyll maximum at depth (Hickman et al., 2009). Into autumn, stratification breaks down and the water column becomes fully mixed. These physical and chemical changes in the water column influence shelf sea plankton communities in terms of primary and secondary production, nutrient uptake and recycling, export of material to depth, species composition and diversity.

Coccolithophores are unicellular calcifying phytoplankton, present in marine environments from polar oceans to tropical waters. They are major contributors to pelagic calcite production due to the intracellular synthesis, as well as the export of calcium carbonate coccoliths (Bach et al., 2016; Klaas and Archer, 2002). They are a common feature of shelf seas (Poulton et al., 2014), and often form annual blooms, for instance on the North-west European shelf, Patagonian shelf, North Sea and Barents Sea (Iglesias-Rodriguez et al., 2002). In general, coccolithophores constitute between around 1 to 10% of phytoplankton biomass (Poulton et al., 2010, 2007); however, in coccolithophore blooms, typically of the species *Emiliania huxleyi*, they can represent up to 30 to 40% of carbon production (Mayers et al., 2018; Poulton et al., 2013). Coccolithophores typically show two main annual peaks in abundance, during spring and a larger peak within the summer period (Balch et al., 2008; Widdicombe et al., 2010; Hopkins et al., 2015) in most ocean basins, aside from the Southern Ocean, where coccolithophore abundance peaks are only during the austral summer months (December – January) (Iglesias-Rodriguez et al., 2002).

Several previous studies have investigated environmental drivers of in-situ coccolithophore populations along strong spatial gradients (Charalampopoulou et al., 2016, 2011; Poulton et al., 2017a; Smith et al., 2017) and temporally (Cerino et al., 2017). Major environmental factors believed to impact coccolithophores include sea surface temperature, low silicic acid concentrations (low competition with diatoms), light availability and carbonate chemistry. A possible role for microzooplankton grazing has also been suggested from field and laboratory experiments (Harvey et al., 2015; Holligan et al., 1993; Strom et al., 2017). Different coccolithophore species have also been shown to display different ecological niches within the water column (D'Amario et al., 2017; Poulton et al., 2017a) and between different seasonal gradients (Cerino et al., 2017). However, little data exists on seasonal drivers, particularly in contrasting shelf sea environments such as the shelf edge, central shelf and coastal waters.

Understanding the drivers of coccolithophore abundance is important as species can contribute differently to calcite production based on calcite content, relative abundance and growth rates (Daniels et al., 2014, 2016). Such understanding can also provide us with important information to interpret palaeo-oceanographic records as to why certain species are located in specific areas along gradients of shelf sea sediments (Gibbs et al., 2016). It is important to consider coccolithophores in terms of carbon biomass, rather than cell abundances as coccolithophores span a range of cell sizes (2-30 µm), from the common *E. huxleyi* (~5 µm) to larger species such as *Coccolithus pelagicus* (~15 µm) (Daniels et al., 2014).

The long-term Western Channel Observatory (WCO) time series of coccolithophores at the L4 station has suggested coccolithophores have increased in abundance by almost 20% since 1991 (Widdicombe et al., 2010). This is supportive of other studies providing evidence for an increase in coccolithophores from continuous plankton recorder (Rivero-Calle et al., 2015) and pigment data from Bermuda (Krumhardt et al., 2016). However, the latter study used prymnesiophyte specific pigments, so it is difficult to link directly to coccolithophore increase.

In this paper, we analysed: 1) the abundance, biomass and community structure of coccolithophores from a central shelf and shelf edge site sampled at different light depths within the euphotic zone, 2) the seasonal changes in these populations during autumn, spring and summer and, 3) the environmental drivers of coccolithophore populations within shelf seas. Within this chapter, I aim to test the hypothesis that gradients in nutrients and irradiance control coccolithophore biogeography and diversity across seasonal and spatial scales, from near-coastal, to mid-shelf and Shelf-edge stations. We compare our data with coccolithophore biomass from the L4 time series collected within the same seasons. Station L4 is within the English Channel sector of the NW European Shelf but much more shallow and closer to shore, providing an opportunity to analyse cross-shelf variability in coccolithophores from coastal shelf seas to the shelf edge (Fig 2.1).

## 2.3 Methods

### 2.3.1 General sampling

Sampling within the Celtic Sea stations (CCS and CS2, Fig. 2.1) was carried out during three cruises on board the *RRS Discovery* from 2014 to 2015: November 2014 (DY018: 9$^{th}$ November to 2$^{nd}$ December), April 2015 (DY029: 1$^{st}$ April to 29$^{th}$ April) and July 2015 (DY033: 11$^{th}$ July to 2$^{nd}$ August). These three time periods focused key points in the annual cycle of ecosystem production and seasonal drivers: the breakdown of summer stratification in autumn (November); the development of the spring phytoplankton bloom (April); and the nutrient depleted strongly stratified summer period (July). Two sites were sampled on all three cruises, the Central Celtic Sea (CCS; 49 $^{o}$24'N, 8$^{o}$ 36'W; 150m water depth) and the Shelf Edge (CS2; 48$^{o}$ 34.26'N, 9$^{o}$ 30.58'W; 203m water depth) (Fig. 2.1). Over the three cruises, these sites were sampled repeatedly but at different frequencies, CCS ($n$ = 15) and CS2 ($n$ = 6). Water sampling was carried out using a conductivity-temperature-depth (CTD) profiler with a rosette sampler fitted with twenty-four 20 L niskin bottles.

Sampling at the Western Channel Observatory (WCO) site L4 (50º 15.00'N, 4º 13.02'W; 51m water depth) has been conducted on a weekly basis (weather permitting) since 1992 (Smyth et al., 2015). To coincide with the cruise dates within the Celtic Sea, we selected data from the WCO-L4 site to analyse samples conducted at a similar seasonal time period at station L4 (*n* = 12). These time periods match generally well with the annual coccolithophore abundances at L4 from 1992 – 2015, with only April showing slightly higher than normal abundances (Fig. 2.2). Temperature and salinity data were measured at L4 using a SeaBird SBE19+ CTD.

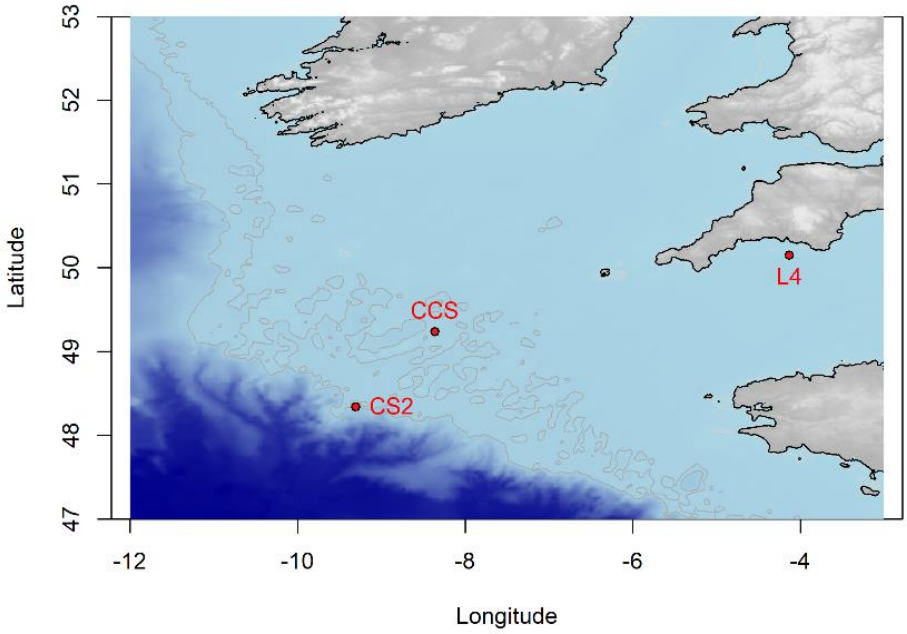


**Figure 2.1.** Map of the Celtic Sea showing the location of sampling sites. Depth contours are 100m, and blue shading representing on and off shelf waters (light and dark blue respectively). CCS = Central Celtic Sea, CS2 = Shelf Edge site.

### 2.3.2 Nutrient and chlorophyll quantification

Water samples at CCS and CS2 for nutrient determination (nitrate+nitrite, nitrite, phosphate, silicic acid and ammonia) were collected from the CTD into aged, acid-washed and MilliQ-rinsed 60 mL HDPE Nalgene™ bottles. Where possible, sampling was carried out according to the International GO-SHIP nutrient manual recommendations (Hydes et al., 2010). Nutrient samples were analysed on board using a Bran and Luebbe segmented flow colourimetric auto-analyser with techniques from Woodward and Rees (2001). Nutrient reference materials (KANSO, Japan) were run daily to check performance and guarantee data quality. Nitrate concentrations were calculated by subtracting nitrite from the combined nitrate plus nitrite concentration. The typical uncertainty of results was between 2-3% with detection limits of 0.02 µM for nitrate and phosphate and 0.01 µM for nitrite.

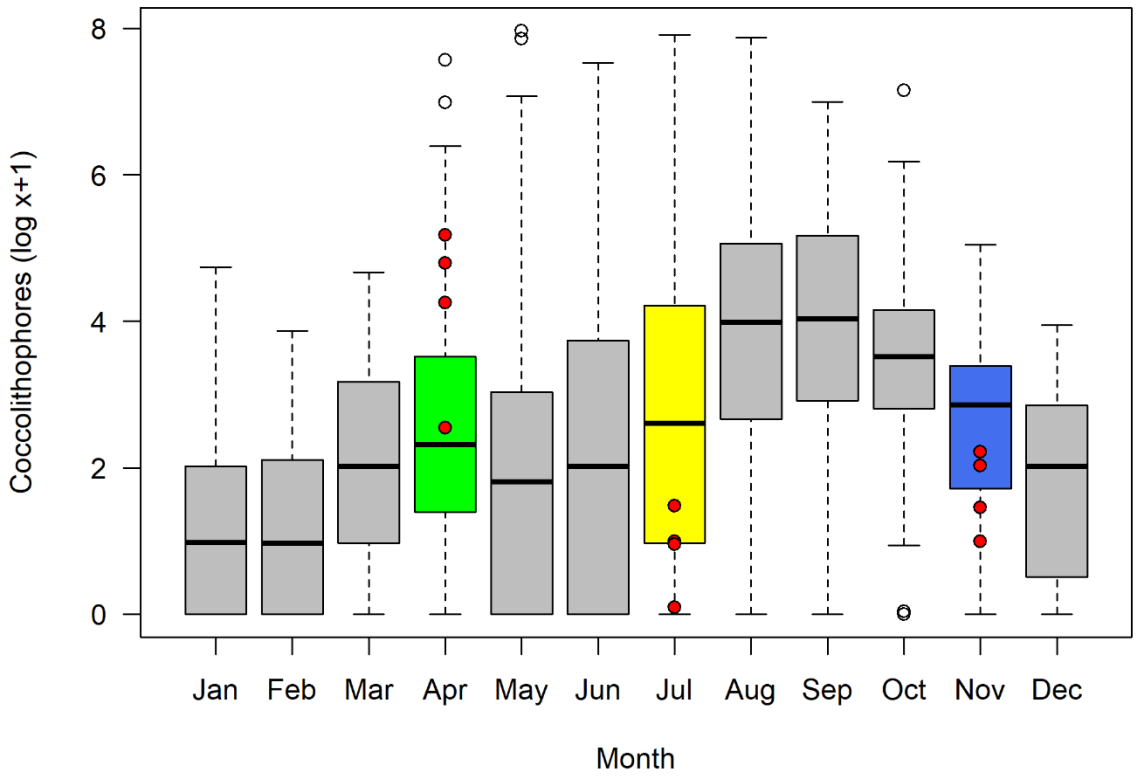


**Figure 2.2** Boxplots of monthly coccolithophore samples (log (x+1)) at station L4 from 1992 – 2015. White circles represent outlier samples (more or less than $\frac{3}{2}$ times the upper or lower quartile), filled red circles are the 4 data used from each of November 2014, April and July 2015.

Water samples for chlorophyll-*a* extraction (0.2 – 0.25 L) were filtered onto 25-mm diameter Whatman GF/F® or Fisherbrand MF300 glass fibre filters (effective pore sizes 0.7 µm) and extracted in 6-10 mL 90% acetone (HPLC grade, Sigma-Aldrich, UK) at 4°C for 18 to 24h (Poulton et al., 2014). Fluorescence was measured on a Turner Designs Trilogy fluorometer using a non-acidification module and calibrated with a solid standard and a pure chlorophyll-*a* standard from spinach extract (Sigma-Aldrich, UK).

At L4, nutrients and chlorophyll-*a* were collected as in Smyth et al. (2010). Briefly, nutrients were collected from 10 L Niskin bottles and analysed at Plymouth Marine Laboratory within 3 to 4 hours of collection. All nutrient concentrations were determined following analytical techniques as in Woodward and Rees, 2002. Chlorophyll-*a* concentration at L4 was from 0.1 L of seawater filtered onto Whatman GF/F® filters in triplicate. The JGOFS (JGOFS, 1994) protocols were adhered to.

### 2.3.3 Coccolithophore abundance and diversity

Seawater samples at CCS and CS2 were obtained at six light depths within the upper euphotic zone determined as 60, 40, 20, 10, 5 and 1% surface irradiance (see Poulton et al., 2017b). Seawater (0.2 – 1 L) was filtered under gentle pressure through 25 mm 0.8 µm pore size Nucleopore™ cellulose nitrate filters with a Whatman GF/F® backing filter to aid in equal distribution of material. Filters were oven dried for 12 hours at 50 to 60°C and stored in Millipore petri-slides prior to analysis. Filters were made into permanent slides on board by mounting the filters using Norland Optical Adhesive 074 (Poulton et al., 2010, Mayers et al., 2018). Samples were analysed under cross-polarized light using an Olympus BX51 x1000 (oil immersion) objective. Either 300 fields of view, or 300 cells (whichever was reached first) were counted with a minimum of 50 fields of view counted. Coccolithophores were identified following the taxonomy of Frada et al. (2010) to the lowest possible taxonomic unit. Cell numbers (cells $mL^{-1}$) were calculated based on the filter area examined, cells counted and volume filtered (mL). Standard errors in cell counts were calculated using:

$$\frac{(\sqrt{C})}{(FOV\ x\ \frac{V}{A})} \qquad \text{(Equation 1)}$$

Where C is the number of cells counted, A is the area investigated ($mm^2$), FOV is the number of fields of view counted and V is the volume of water filtered (mL) (Taylor, 1982). For a small number of samples (usually the 40% surface irradiance depth, and subsurface chlorophyll maximum in July) further species identification and cell counts were carried out using scanning electron microscopy (SEM) and following the taxonomy of Young et al. (2003).

Coccolithophore abundance was converted into carbon biomass using coccosphere (cell) diameter, minus the thickness of coccoliths to assume the size of the underlying cell. Cell diameter was then used to calculate the cell volume and the organic carbon conversion factor of 0.216 x $volume^{0.939}$ from Menden-Deuer & Lessard (2000) was used.

At station L4, coccolithophore enumeration was by inverted light microscopy. Seawater was sampled from a depth of 10 m using a 10 L niskin bottle. A 200 mL subsample was removed and preserved in neutral formaldehyde (2%) before being returned to Plymouth Marine Laboratory. Samples were stored in cool and dark conditions until analysis using the Utermöhl technique (Utermöhl, 1958), according to guidance procedures within “Water Quality – Guidance standard for routine microscopic surveys of phytoplankton using inverted microscopy (Utermöhl technique)” (BS EN 15204:2006). Samples were gently homogenized before a 100 mL subsample was removed and settled for more than 48 h,

all cells were identified where possible to species level at either x200 or x400 magnification under differential interference contrast (DIC) or polarised light with a Leica DM IRB or Olympus DMI4000B inverted microscope (Widdicombe et al., 2010).

### 2.3.4 Statistical analysis

Multivariate statistics were carried out in R (v. 3.3.2) using the vegan (v.2.4-5) package (Oksanen et al., 2016, R Core Team, 2015). Bray-Curtis dissimilarity matrices were calculated on standardised coccolithophore biomass with certain taxa considered at such a low biomass contribution as to be "rare" (here defined as on average <5% of total cell biomass at each site) being removed (loss of ~10% biomass on average). Data was transformed as log ($x$+1) to reduce the influence of dominant taxa. To explore biodiversity, Pielou's evenness index (J') was conducted on untransformed data. ANOSIM (Analysis of Similarity) and SIMPER (Similarity of Percentages) tests were conducted on transformed data to explore differences driven by light depth within sites (CCS and CS2) and between sampling periods (seasons). The differences in species composition between light depths were tested using non-parametric multivariate analysis of variance (PERMANOVA) using the 'Adonis' function with 999 random permutations, the data was transformed log ($x$+1) as before for the analysis. Bray-Curtis dissimilarity indices were calculated using the 'vegdist' function on log ($x$+1) transformed data.

Averages of standardised coccolithophore biomass were calculated for all light depths at CS2 and CCS in November and April, in July we calculated an upper euphotic zone (60,40 and 20% PAR) and a lower euphotic zone (10,5 and 1% PAR) average, to reflect the different communities (see Results). A nonmetric multidimensional scaling (nMDS) plot using a Bray-Curtis dissimilarity matrix was used to display coccolithophore population differences. A SIMPER routine was used to statistically determine the species which defined the differences within coccolithophore populations between different seasons.

Environmental data were tested for skewness, with heavily left-skewed variables (all nutrients, temperature, salinity, chlorophyll-*a* and mixed layer depth) being log transformed (log (x+1)) to reduce skewness and stabilise variance. Due to the high correlation between nitrate and phosphate ($R^2$ = 0.98, $p$ < 0.001), nitrate was considered to be representable of both nutrients. All environmental data were then normalised to a mean of zero and standard deviation of 1 before a redundancy analysis (RDA) was run, using the log ($x$+1) transformed community matrix data, to analyse environmental drivers of coccolithophore populations across the Celtic Sea shelf.

## 2.4 Results

### 2.4.1 Seasonal coccolithophore populations

Coccolithophores were observed at all sites sampled within the Celtic Sea and English Channel during November, April and July. At CCS, they showed differences in biomass, with highest values in November (102.56 ± 23.08 nmol C $L^{-1}$, *n* = 24), followed by April (–44.90 ± 34.71 nmol C $L^{-1}$, *n* = 35) and finally July (24.01 ± 28.53 nmol C $L^{-1}$, *n* = 28) (Fig. 2.3a-c). By plotting Pielou's evenness (J') with light depth, we can see if there is a shift in species composition (dominance by particular taxa) with a changing light environment. During November at CCS there was limited variability in J' (Fig. 2.3d) with values varying from 0.49 to 0.67 (seasonal average 0.59 ± 0.04). April also showed little change in J' with light depth, though there was some variability at CCS throughout the month (0.31 – 0.78, seasonal average 0.56 ± 0.12). In July, CCS displayed very different trends to the other months. Firstly, the range in J' ranged from completely uneven (0.07) to almost completely even (0.99), there was also a clear light driven difference, with the deeper depths (lower irradiances) showing slightly less variability and greater evenness (seasonal average 0.53 ± 0.30). Species richness represents the number of different species identified in a sample. Values in November and April at CCS showed very little variation with depth (5 – 10 species identified), however in July there was an increase with declining irradiance, with more species observed at the lower light depths (deeper in the water-column). Species richness was also lower in July than in the other seasons (2 – 6 species identified) (Fig. 2.3g-i).

To further identify vertical differences in coccolithophore species composition, we analysed Bray-Curtis similarity relative to the top light depth (60% PAR) (Fig. 2.4). At the CS2 site, there was generally little variability in similarity from the surface to the bottom of the euphotic zone, during any season; the one exception to this was the 10% PAR depth during November. In November, there was very little variability in Bray-Curtis similarity at CCS, suggesting populations are almost uniform in composition within the euphotic zone (see also Figs. 2.3 and 2.4). During April though there was some variability within the sampled light depths, there does not appear to be a light-driven trend. However, in July, there was a large deviation from the surface site at the 20% PR depth and below, strongly indicative of variability in species composition with depth.

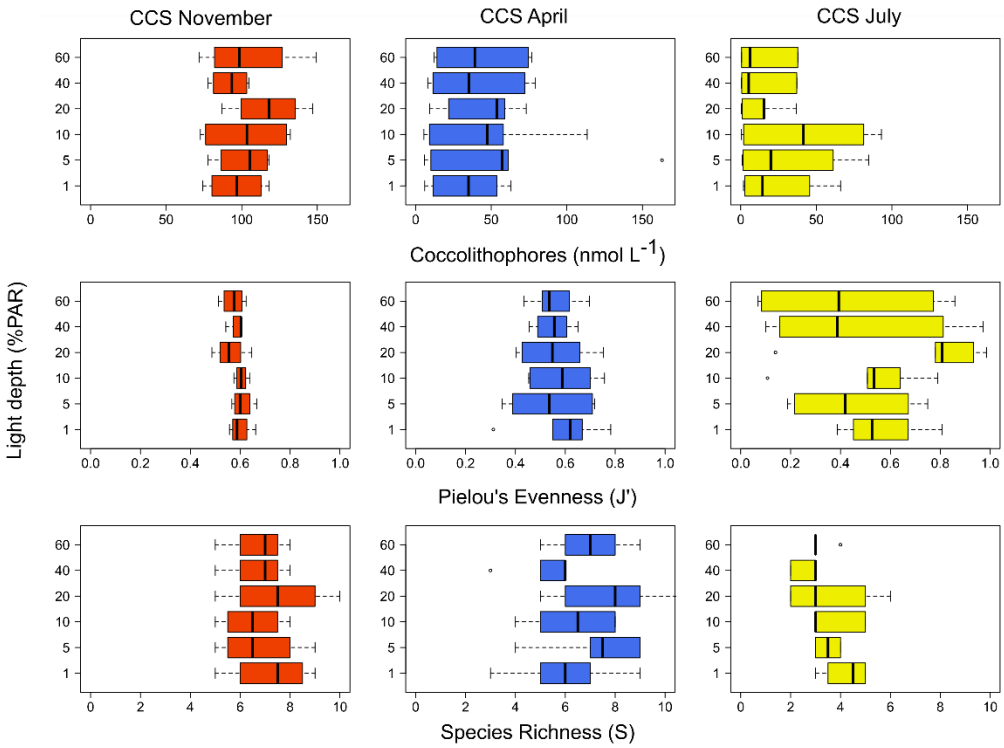


**Figure 2.3.** Boxplots of coccolithophore biomass (top), Pielou's J' evenness (middle) and species richness (bottom) at the Central Celtic Sea during November (red, left), April (blue, middle) and July (yellow, right). For November, April and July *n* = 24, 36 and 30 respectively.

An analysis of similarities (ANOSIM) was conducted on the data at CCS to observe if light depth was responsible for the variability observed. An ANOSIM tests whether the similarity between groups is greater than or equal to the similarity within groups. In November and April there were no significant differences ($p > 0.9$) between depths, however in July a significant difference was observed ($p = 0.05$, ANOSIM $R$ statistic = 0.16). Therefore, to further analyse trends between sites and seasons, the average coccolithophore biomass and environmental parameters was calculated throughout the euphotic zone at CS2 and CCS during November and April. For July, we divided the samples into upper euphotic zone (60, 40 and 20% PAR) and lower euphotic zone (10, 5 and 1%), which included samples within the sub-surface chlorophyll maxima (SCM).

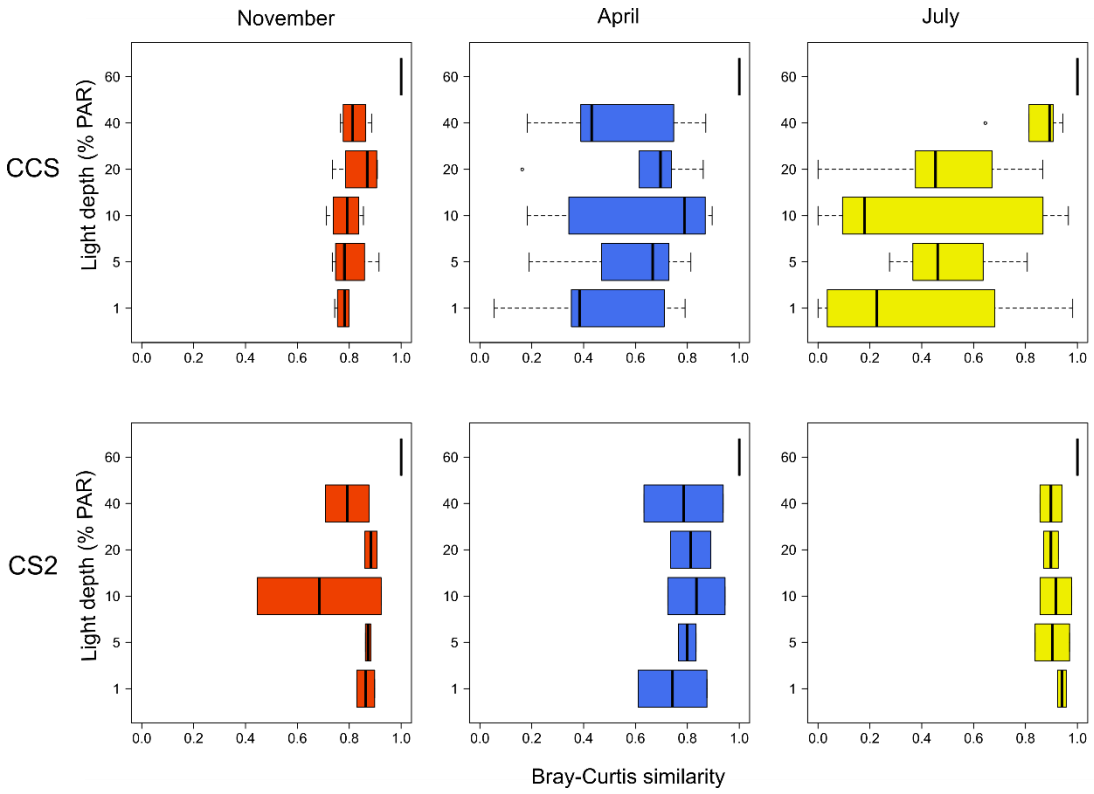


**Figure 2.4.** Box plots of Bray-Curtis similarity relative to the upper light depth (60% photosynthetically active radiation (PAR)) at the Central Celtic Sea (left) and Shelf Edge (right) for November (red, top), April (blue, middle) and July (yellow, bottom).

### 2.4.2 Seasonal and cross-shelf variability

Coccolithophores showed variability in distribution in terms of carbon biomass between sites and seasons. In general, coccolithophore biomass was higher at CS2 than CCS, aside from during November (Table 2.1). Average biomass in November was102.56 ± 23.08nmol C $L^{-1}$ and from 40.10 ± 8.78nmol C $L^{-1}$ for CCS and CS2 respectively, whilst there appeared to be little variability of biomass with depth during this season. Coccolithophore contribution to phytoplankton carbon ranged from 4.9 – 6.9% at CCS, and 3.1 – 4.6 at CS2 (Table 2.1). Biomass at L4 was considerably lower than at Celtic Sea sites (1.5 – 5.6 nmol C $L^{-1}$). In April, biomass showed large ranges at CCS (9.0 – 76.1 nmol C $L^{-1}$), CS2 (40.2 – 138.4 nmol C $L^{-1}$) and L4 (12.6 – 128.8 nmol C $L^{-1}$) (Table 2.1). Contribution to phytoplankton carbon was lower in April than November for CCS (0.2 – 0.8%) and CS2 (1.7 – 2.0%). On average, CS2 had higher biomass (89.34 ± 60.23 nmol C $L^{-1}$) than at CCS and L4 (44.90 ± 34.71 and 71.63 ± 49.61 nmol C $L^{-1}$ respectively) throughout April.

Table 2.1.Euphotic zone averages of environmental and biological parameters (during July at CCS values are for the upper euphotic zone depths (60, 40 and 20% PAR) and values in brackets are from lower euphotic zone depths (10, 5 and 1% PAR). ND = not determined, JD = Julian day.

| Date | Site | JD | $C_{cocco}$ (nmol C $L^{-1}$) | % $C_{phyto}$ | $NO_3$ (µM) | dSi (µM) | $NH_4$ (µM) | Chl-*a* (mg $m^{-3}$) | Temp. ($^oC$) | Salinity | $E_o$ (mol quanta $m^{-2}$ $d^{-1}$) |
|---|---|---|---|---|---|---|---|---|---|---|---|
| | | | | | | *November 2014* | | | | | |
| 10-Nov | CCS | 314 | 95.0 | 4.9 | 2.2 | 0.9 | 0.2 | 1.0 | 13.6 | 35.4 | 8.4 |
| 12-Nov | CCS | 316 | 76.8 | 5.9 | 2.0 | 0.8 | 0.2 | 0.9 | 13.6 | 35.4 | 11.9 |
| 22-Nov | CCS | 326 | 123.2 | 6.8 | 1.5 | 1.0 | 0.1 | 1.1 | 13.1 | 35.4 | 8.1 |
| 25-Nov | CCS | 329 | 115.2 | 6.9 | 2.3 | 1.0 | 0.1 | 1.0 | 13.0 | 35.1 | 12.1 |
| 18-Nov | CS2 | 322 | 47.2 | 4.6 | 3.3 | 1.4 | 0.1 | 0.6 | 13.9 | 35.6 | 7.7 |
| 20-Nov | CS2 | 324 | 33.1 | 3.1 | 2.4 | 1.3 | 0.1 | 0.7 | 14.1 | 35.6 | 9.3 |
| 05-Nov | L4 | 309 | 2.2 | ND | 5.1 | 4.4 | 0.2 | 0.3 | 14.6 | 35.0 | 6.5 |
| 17-Nov | L4 | 321 | 4.8 | ND | 5.9 | 4.1 | 0.2 | 0.2 | 13.9 | 34.9 | 1.7 |
| 24-Nov | L4 | 328 | 5.6 | ND | 4.5 | 2.7 | 0.2 | 0.2 | 13.6 | 35.2 | 4.5 |
| 02-Dec | L4 | 336 | 1.5 | ND | 5.3 | 2.9 | 0.1 | 0.1 | 13.2 | 35.2 | 3.6 |
| | | | | | | *April 2014* | | | | | |
| 04-Apr | CCS | 94 | 9.0 | 0.2 | 6.0 | 2.8 | 0.0 | 1.3 | 10.0 | 35.3 | 20.7 |
| 06-Apr | CCS | 96 | 11.7 | 0.3 | 5.6 | 2.7 | 0.0 | 1.6 | 10.0 | 35.3 | 43.2 |
| 11-Apr | CCS | 101 | 38.9 | 0.4 | 4.0 | 2.6 | 0.1 | 2.5 | 10.3 | 35.3 | 42.3 |
| 15-Apr | CCS | 105 | 73.5 | 0.8 | 2.4 | 2.6 | 0.2 | 4.5 | 10.6 | 35.3 | 20.0 |
| 20-Apr | CCS | 110 | 59.1 | 0.7 | 2.1 | 2.5 | 0.2 | 2.8 | 10.6 | 35.3 | 41.4 |
| 25-Apr | CCS | 115 | 76.1 | 0.8 | 0.8 | 2.2 | 0.2 | 3.2 | 11.0 | 35.3 | 42.0 |
| 10-Apr | CS2 | 100 | 40.2 | 1.7 | 8.2 | 3.2 | 0.1 | 0.8 | 11.3 | 35.6 | 18.1 |
| 24-Apr | CS2 | 114 | 138.4 | 2.0 | 6.1 | 2.4 | 0.2 | 1.9 | 11.6 | 35.6 | 45.4 |
| 07-Apr | L4 | 97 | 54.9 | ND | 2.8 | 1.2 | 0.7 | 1.9 | 9.5 | 35.2 | 41.0 |
| 13-Apr | L4 | 103 | 128.8 | ND | 1.3 | 1.2 | 0.2 | 3.0 | 9.8 | 35.2 | 15.3 |
| 20-Apr | L4 | 110 | 12.6 | ND | 1.3 | 1.5 | 0.9 | 0.9 | 10.1 | 35.2 | 48.2 |
| 27-Apr | L4 | 117 | 90.3 | ND | 0.0 | 0.9 | 0.3 | 1.2 | 10.4 | 35.3 | 16.1 |
| | | | | | | *July 2015* | | | | | |
| 14-Jul | CCS | 195 | 0.7 (9.1) | < 0.1 | 0.01 (0.79) | 0.7 (1.6) | 0.0 (0.0) | 0.25 (0.72) | 16.2 (12.9) | 35.4 (35.3) | 23.2 (5.6) |
| 15-Jul | CCS | 196 | 0.5 (30.0) | 0.6 | 0.01 (2.81) | 0.6 (2.0) | 0.1 (0.1) | 0.33 (0.79) | 16.2 (12.6) | 35.4 (35.4) | 33.2 (5.6) |
| 24-Jul | CCS | 205 | 8.9 (28.1) | 2.0 | 0.01 (4.3) | 0.2 (2.4) | 0.1 (0.1) | 0.31 (0.82) | 16.9 (11.7) | 35.4 (35.4 | 26.2 (5.6) |
| 29-Jul | CCS | 210 | 37.2 (48.4) | 2.7 | 0.01 (2.9) | 0.2 (1.8) | 0.0 (0.1) | 0.32 (0.88) | 16.3 (12.9) | 35.4 (35.4) | 41.5 (5.6) |
| 30-Jul | CCS | 211 | 30.1 (93.1) | ND | 0.01 (0.01) | 0.2 (0.2) | <0.1 (<0.01) | 0.29 (0.30) | 16.3 (16.3) | 35.4 (35.4) | 49.4 (5.6) |

| | | | | | | | | | | | |
|---|---|---|---|---|---|---|---|---|---|---|---|
| 19-Jul | CS2 | 200 | 38.8 | 1.3 | 0.3 | 0.2 | 0.2 | 0.9 | 15.7 | 35.5 | 26.1 |
| 20-Jul | CS2 | 201 | 82.6 | ND | 0.2 | 0.2 | 0.1 | 0.7 | 16.3 | 35.6 | 49.8 |
| 06-Jul | L4 | 187 | 1.1 | ND | 0.1 | 0.3 | ND | 0.9 | 14.2 | 35.3 | 11.1 |
| 14-Jul | L4 | 195 | 2.3 | ND | 0.0 | 0.5 | 0.1 | 1.7 | 14.9 | 35.2 | 6.4 |
| 20-Jul | L4 | 201 | 1.1 | ND | 0.1 | 0.8 | 0.2 | 1.8 | 15.0 | 35.3 | 10.2 |
| 28-Jul | L4 | 209 | 0.4 | ND | 0.3 | 1.0 | 0.7 | 1.2 | 14.8 | 35.2 | 18.8 |

During July, increased biomass at CCS was generally observed at the lower light depths (33.85 ± 36.19 nmol C $L^{-1}$) than higher in the water column (15.48 ± 16.70nmol C $L^{-1}$). At CS2 the biomass was similar to the lower light depths but higher than the upper euphotic zone at CCS (60.73 ± 71.63 nmol C $L^{-1}$), with the lowest biomass seen at L4 (1.23 ± 0.81nmol C $L^{-1}$). Contribution to phytoplankton carbon was slightly higher towards the end of July at CCS than CS2 (<0.1 – 2.7% and 1.3% respectively) (Table 2.1).

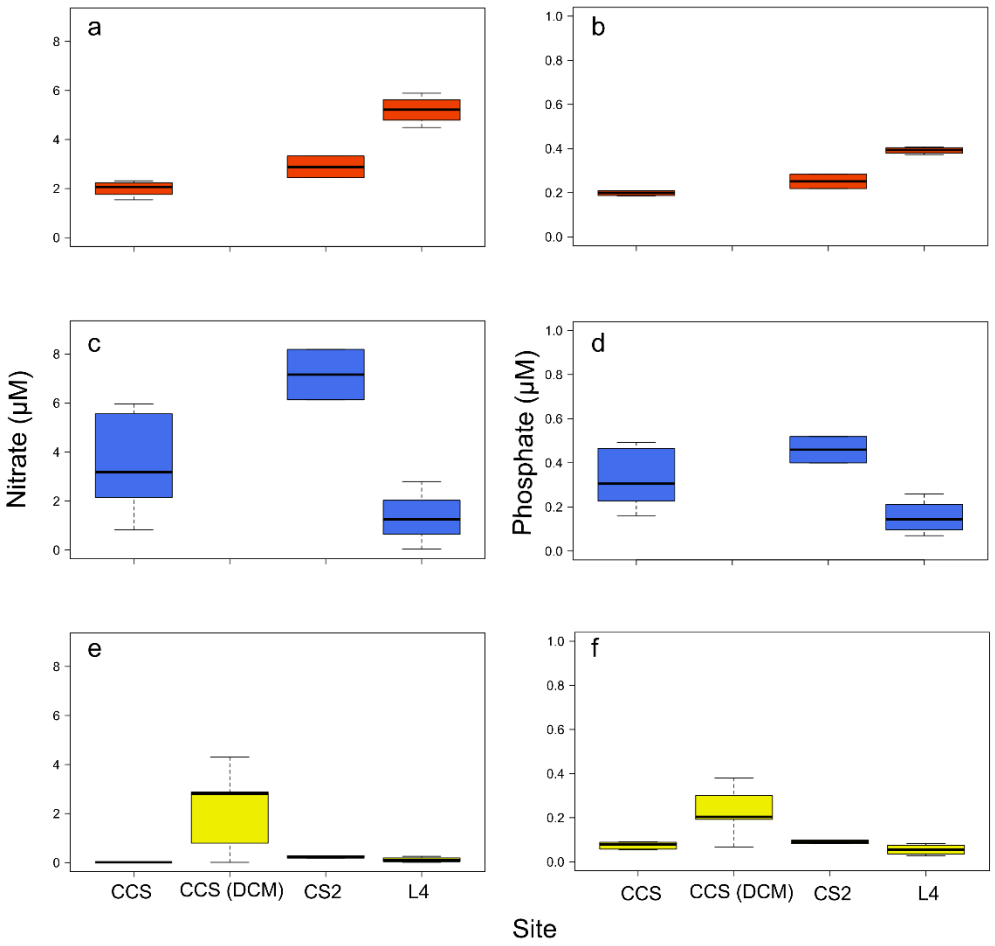


**Figure 2.5.** Concentrations of the macronutrients nitrate (a, c and e) and phosphate (b, d and f) during November (red, top), April (blue, middle) and July (yellow, bottom). For CCS in November, April and July (*n* = 24, 36 and 30), for CS2 in each month (*n* = 12) and for L4 in all months (*n* = 4).

The average seasonal concentrations of the macronutrients nitrate and phosphate at the different sites varied between seasons. Nutrients were generally highest at CCS during April (Fig 2.5 c and d) (3.5 ± 1.8 and 0.3 ± 0.1 µM nitrate and phosphate respectively), compared with November (2.0 ± 0.3 and 0.2 ± <0.1 µM) and July (<0.1 ± <0.1 and 0.1 ± <0.1 µM). However, the deep chlorophyll maximum had slightly higher values in July (2.2 ± 1.7 and 0.3 ± 0.1 µM) (Fig 2.5 e and f). The highest nutrient concentrations at CS2 were also in April (7.2 ± 1.5 and 0.5 ± 0.1 µM for nitrate and phosphate respectively), but for L4

the highest concentrations were observed in November (5.2 ± 0.6 and 0.4 ± <0.1 µM for nitrate and phosphate respectively) (Fig 2.5a and b).

The species composition of CCS, CS2 and L4 throughout all three months is shown in Fig 2.6 as stacked bar charts. During November at CCS, *E. huxleyi* was present but declined in relative biomass throughout the month (42.5 – 6.8%), with a relative increase in *Syracosphaera* spp. (up to 60%). The coccolithophore *Calciopappus caudatus* was also consistently >15%, and up to 42.0% of total coccolithophore biomass during November at CCS (Fig 2.6). In April, there appeared to be a gradual progression throughout the season. This included a gradual decline in the biomass of *Coronasphaera meditteranea* and *Syracosphaera* spp. and an increase in *E. huxleyi* up to ~60% by the end of the month. Towards the end of April, *C. caudatus* became more abundant, with *Alisphaera unicornis* showing an initial increase in abundance towards mid-April (~5 to ~35%) before becoming absent by the end of April. The species *Coccolithus pelagicus* was also present at low biomass (<9%) throughout that month.

At CS2, the most abundant coccolithophore was almost always *E. huxleyi*, aside from one date (24 April). In November, *E. huxleyi* relative biomass ranged from ~50 to 65%, with a small contribution (~10 - 20%) from *Syracosphaera* spp. The coccolithophore *Calcidiscus leptoporus* was only found during November at this site (Fig. 2.6), and *Gephyrocapsa muellerae* contributed ~15% at the later sampling date. In April, *E. huxleyi* showed its lowest contribution to coccolithophore biomass (< 45%), with a higher contribution from *Syracosphaera* spp. (30 – 60%). There were also small contributions (<10%) from *C. pelagicus, G. muellerae, C. caudatus* and *C. meditteranea* throughout April.

Station L4, located further inland within the English Channel (Fig. 2.1), displayed a high dominance by *E. huxleyi* during November (> 75%), with small contributions (7 - 23%) from *C. pelagicus*. In April, there were three species identified at this site, *C. pelagicus* (5 – 30%), *G. muellerae* (5 – 20%) and *E. huxleyi* (40 - 80%). During July, the coccolithophore community was almost exclusively composed of *E. huxleyi* (100%), aside from the 28th July when the community was completely composed of *C. pelagicus*.

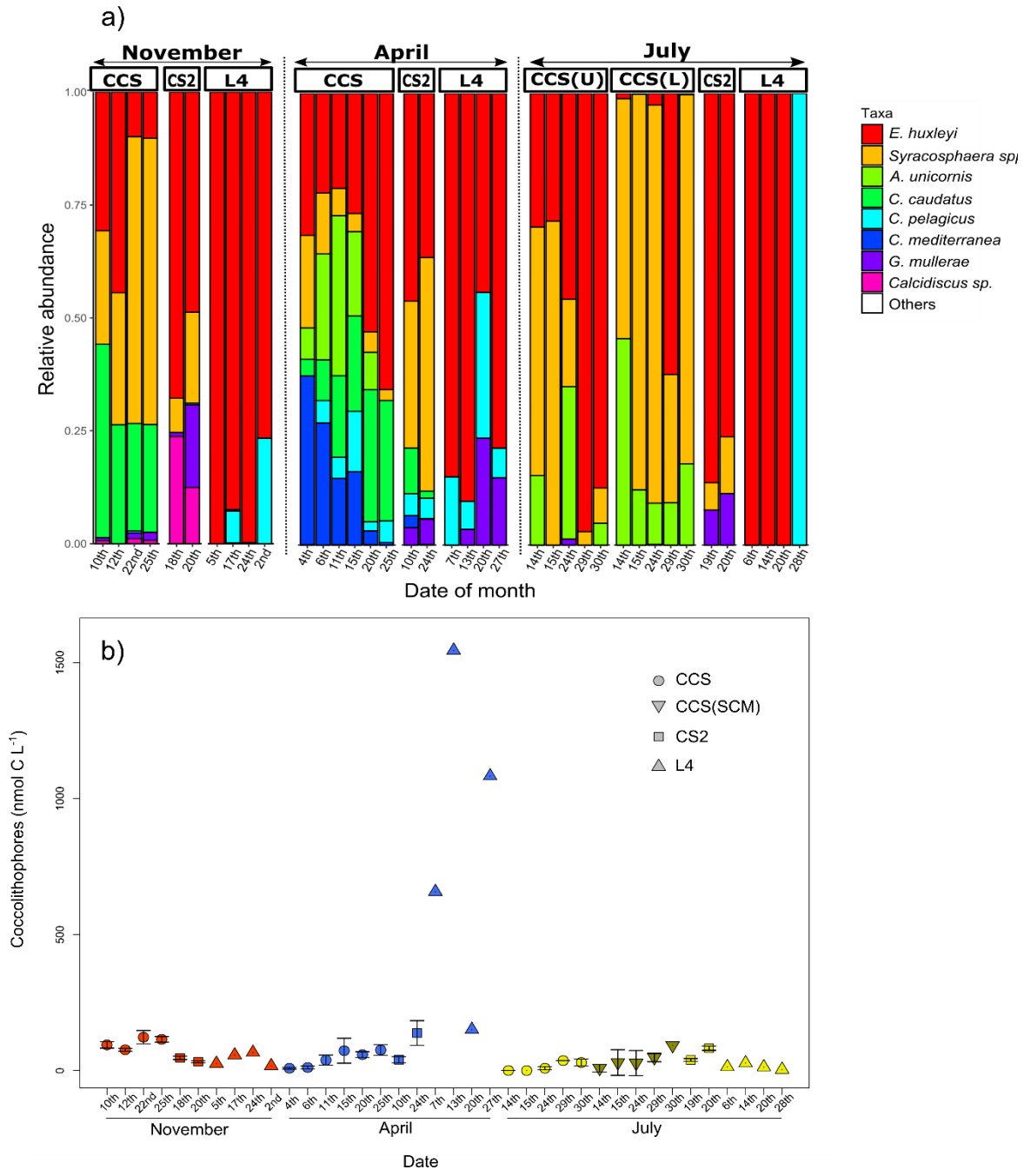


**Figure 2.6.** Relative abundance of species composition at CCS, CS2 and L4 during November, April and July (a) and absolute abundance of coccolithophores at the same sites (b), error bars represent ± standard deviation (*n* =3 on each date at CCS, CCS (SCM) and CS2 and *n* = 1 at L4). In November the 2nd at L4 is the 2nd of December.

To further test the clustering of samples, a similarity of percentages (SIMPER) analysis was conducted between the different seasons (Table 2.2). This analysis determines the contribution of each species to the observed differences between the sample groupings. The species which demonstrated high contributions to the differences between seasons (17.2 – 30.2%) was *Syracosphaera* spp., particularly between the upper and lower euphotic depths of summer (Table 2.2). The species *E. huxleyi* was also a significant

driver between the upper and lower depths in summer, and between summer and autumn (32.7 and 14.9% respectively). Between all seasons, *C. caudatus* contributed significantly to the variation observed (15.5 – 16.9%). Other species which made contributions to the seasonal differences include; *C. pelagicus*, *C. meditteranea, G. muellerae* and *A. unicornis* (Table 2.2).

An nMDS is a non-parametric approach to ordinate samples based on a dissimilarity matrix; it attempts to represent pairwise dissimilarity between samples with the distance between samples indicative of the dissimilarity in their species compositions. The nMDS clustering of samples in the Celtic Sea and English Channel displayed some interesting trends (Fig 2.7). The L4 samples clustered closely together and independently from the other samples from the Celtic Sea, irrespective of season, aside from one summer sample being distributed away from the others (this station was 100% dominated by one species, *C. pelagicus*). Samples from the lower euphotic zone in July at CCS also clustered away from the upper euphotic zone summer samples, aside from one sample which clustered with the upper euphotic zone summer samples (Fig. 2.7). CCS autumn and spring samples clustered together, along with spring CS2 samples (Fig 2.7b). The CS2 samples from autumn and summer clustered also closely with the upper euphotic zone samples in summer.

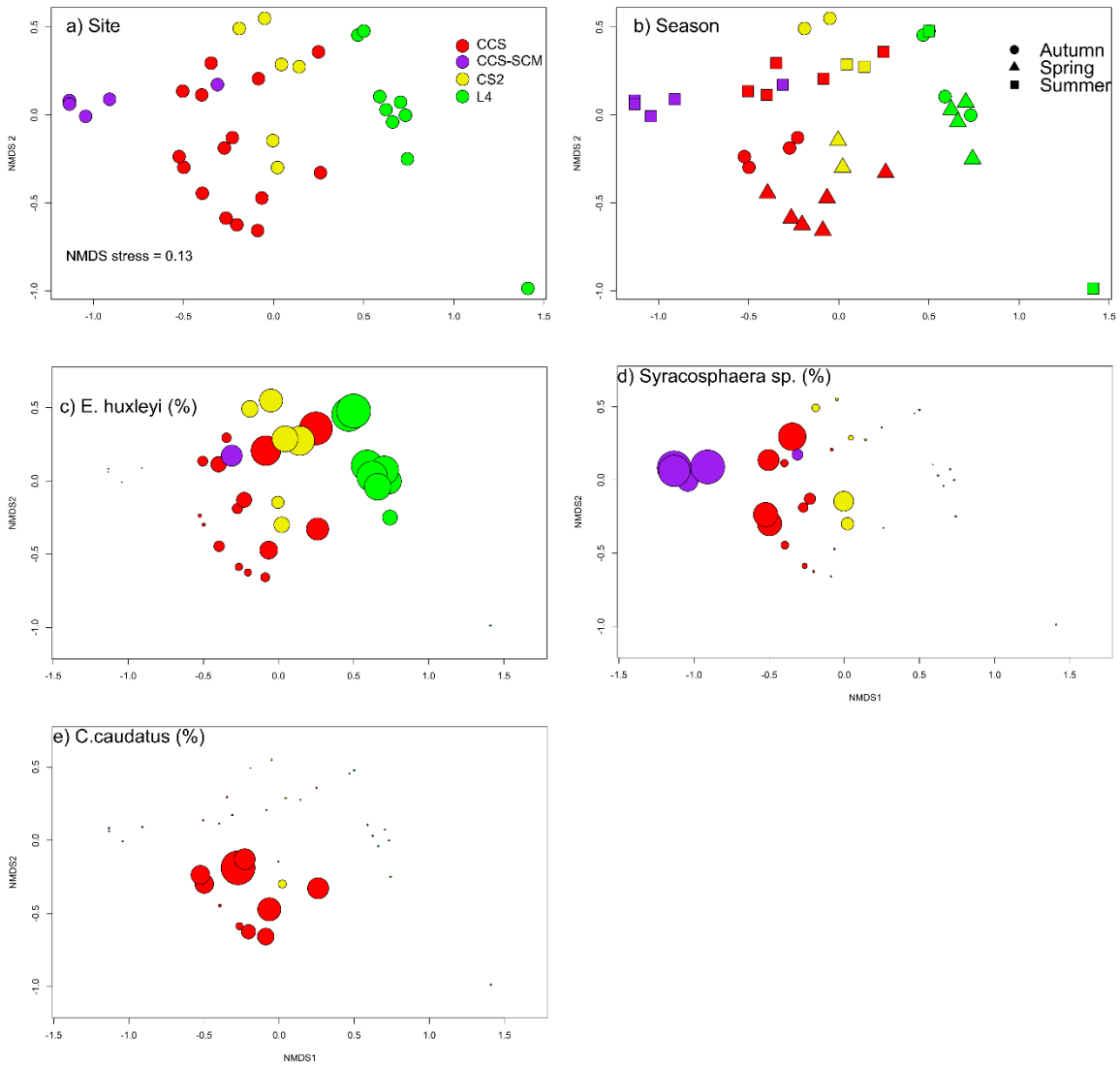


**Figure 2.7**. NMDS plots of SSB data set from CCS, CS2, L4 and CCS-DCM. Colours represent sites, a) shows sites, b) displays seasons as shapes, c) bubble size represents proportion of *E. huxleyi*, d) proportion of *Syracosphaera* spp. and, e) proportion of *C. caudatus*

Table 2.2: Results from SIMPER analysis between seasons. Summer (U) and Summer (L) are for the upper euphotic and lower euphotic zones, with Summer (L) only at CCS.

| Species | Standardised biomass (%) | Average standardised biomass (%) | Contribution to dissimilarity |
|---|---|---|---|
| **Autumn-Spring average dissimilarity = 46.9%** | | | |
| *Syracosphaera* spp. | 20.7 | 16.4 | 18.1 |
| *C. pelagicus* | 5.6 | 19.0 | 17.5 |
| *C. caudatus* | 13.9 | 16.6 | 16.6 |
| *C. meditteranea* | 0.0 | 13.2 | 11.7 |
| *G. muellerae* | 6.1 | 9.2 | 11.3 |
| | | | Total = 75.3% |
| **Spring-Summer (U) average dissimilarity = 50.6%** | | | |
| *C. pelagicus* | 19.0 | 4.2 | 21.2 |
| *Syracosphaera* spp. | 16.4 | 17.7 | 17.2 |
| *C. caudatus* | 11.7 | 0.0 | 15.5 |
| *A. unicornis* | 13.2 | 7.4 | 12.7 |
| *C. meditteranea* | 9.2 | 0.0 | 11.8 |
| | | | Total = 78.3% |

| | | | |
|---|---|---|---|
| **Autumn-Summer (U) average dissimilarity = 44.8%** | | | |
| *Syracosphaera* spp. | 20.7 | 17.7 | 25.7 |
| *C. caudatus* | 13.9 | 0.0 | 16.9 |
| *E. huxleyi* | 38.2 | 38.5 | 14.9 |
| *C. pelagicus* | 5.6 | 4.2 | 13.9 |
| *G. muellerae* | 6.1 | 5.0 | 10.6 |
| | | | Total = 82.1% |
| **Summer (U) - Summer (L) average dissimilarity = 58.5%** | | | |
| *E. huxleyi* | 38.5 | 13.2 | 32.7 |
| *Syracosphaera* spp. | 17.7 | 41.5 | 30.2 |
| *A. unicornis* | 7.4 | 28.0 | 26.5 |
| *C. pelagicus* | 4.2 | 0.0 | 5.6 |
| *G. muellerae* | 5.0 | 0.3 | 5.1 |
| | | | Total = 100% |

In terms of the species driving this distribution, we replotted the nMDS with the proportion of *E. huxleyi* (Fig. 2.7c), *Syracosphaera* spp. (Fig. 2.7d) and *C. caudatus* (Fig. 2.7e) represented as the size of the data points (these three species were identified as contributing to the nMDS variation by the SIMPER analysis; Table 2.2). The largest proportion of *E. huxleyi* was observed at L4 during multiple sampling time points, as well as at CS2, the upper euphotic zone of summer at CCS, and in some spring CCS samples. The distribution of *Syracosphaera* spp. in samples was almost directly opposite to *E. huxleyi*, with the highest proportions seen within the lower euphotic zone of summer at CCS, autumn at CCS and being completely absent at station L4. Finally, the species *C. caudatus* was found at CCS during autumn and spring, with little to none observed in the summer or at stations L4 or CS2.

### 2.4.3 Environmental drivers

The variation of environmental variables with respect to the coccolithophore community was analysed using a redundancy analysis (RDA). An RDA essentially extracts and attempts to summarise the variation in a set of response variables (here coccolithophore species), which can be explained by a set of explanatory variables (here environmental variables) by using multiple linear regression. We found that two RDA axes accounted for 49 and 23% of the variability in species occurrence, respectively. RDA1 was strongly influenced by bottom depth and salinity (Fig 2.8, Table 2.3), and can therefore be considered as a pseudo-spatial (cross-shelf) axis, whereas RDA2 showed a positive relationship with Julian Day and a negative relationship with incidental irradiance (E0), nitrate, chlorophyll-*a* and silicate (Fig 2.8, Table 2.3), and can therefore be considered to represent a pseudo-temporal (seasonal) axis.

Coccolithophore species which showed strong scores against RDA1 (Table 2.3), and likely relate to cross-shelf variability, include *E. huxleyi* (0.74), *Syracosphaera* spp. (-1.92), *C. caudatus* (-1.05) and *A. unicornis* (-0.77). With RDA2, *Syracosphaera* spp. and *C. caudatus* also showed strong scores (0.52 and -1.17, respectively), as well as *C. mediterranea* (-0.85) and *C. pelagicus* (-0.8) suggesting strong influence of seasonal environmental variability. This supports the results from the SIMPER analysis (Table 2.2) Interestingly, *E. huxleyi* showed one of the lowest (-0.24) scores with RDA2.

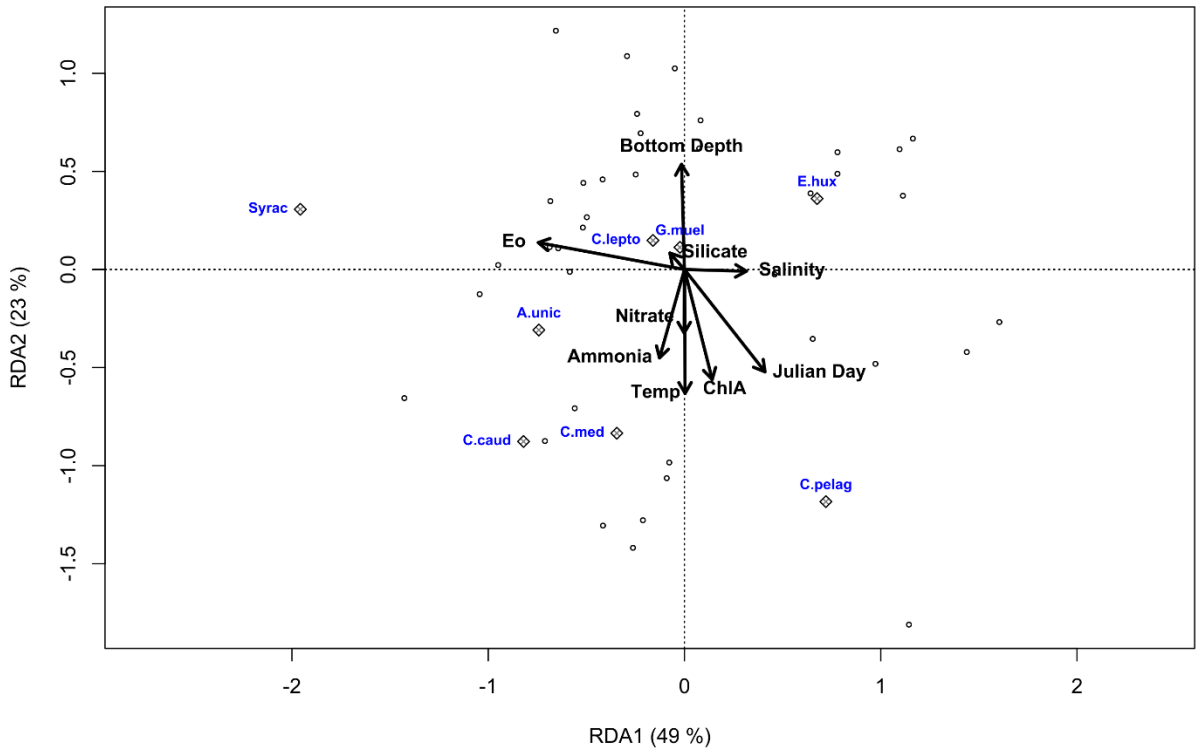


**Figure 2.8.** Redundancy analysis (RDA), of environmental variables and species data averaged for all sampled sites, upper and lower euphotic zones for CCS in July. Species are labelled as E.hux (*E. huxleyi*), C.pelag (*C. pelagicus*), C.med (*C. meditteranea*), C.caud (*C. caudatus*), A.unic (*A. unicornis*), Syrac (*Syracosphaera.* Spp.), C. lepto (*C.* leptoporus) and G.muel (*G. muellerae*)

**Table 2.3**. Species scores for the redundancy analysis against redundancy axis 1 and axis 2

| Species | RDA1 (49%) | RDA2 (23%) |
|---|---|---|
| *E. huxleyi* | 0.74 | -0.24 |
| *G. mullerae* | 0.15 | 0.24 |
| *Syracosphaera.* spp | -1.92 | 0.52 |
| *C. caudatus* | -1.05 | -1.17 |
| *Calcidiscus* sp. | -0.05 | 0.20 |
| *C. meditteranea* | -0.44 | -0.85 |
| *A. unicornus* | -0.77 | -0.14 |
| *C. pelagicus* | 0.69 | -0.80 |

## 2.5 Discussion

### 2.5.1 Seasonal variability in coccolithophore populations

Using carbon biomass rather than cell counts allows us to investigate coccolithophore populations with respect to their differing cell sizes (~2 - >20 µm; Young et al., 2003) and contribution to community biomass rather than only their cellular abundance. Importantly, consideration of biomass rather than cell abundance changes the relative proportions of the different species, with large species making a greater contribution (e.g. *C. pelagicus* average contribution increased from 0.9 – 3.2%) than smaller celled species such as *E. huxleyi*. Even though there is a noticeable decline in *E. huxleyi* contributions (from 61.3% of total cells to 46.3% of total community biomass), it remained the dominant coccolithophore in the Celtic Sea. This is in accordance with studies across the entire north-west European shelf in summer (>60%) (Poulton et al., 2014), a coastal Scottish Coastal site (>60%) (León et al., 2018), and in spring and summer blooms in this shelf region (Marañón and González, 1997; Mayers et al., 2018; Rees et al., 2002). The other species identified in the SIMPER analysis showed an increase when using biomass, (*Syracosphaera* spp. 18.5 – 25%) as well as a similar contribution (*C. caudatus*, 11.3 – 10.4%).

### 2.5.2 Central Celtic Sea

Coccolithophore populations across a transect of the Atlantic Ocean showed sharpest dissimilarity gradients along vertical rather than horizontal gradients (Poulton et al., 2017a), related to the changing light environment. Our data only showed significant vertical differences during July at the CCS, with strong stratification and a well-defined subsurface chlorophyll maximum (SCM). During summer, there was a striking difference in populations within the upper and lower euphotic depths, with *Syracosphaera* spp. dominating at depth and *E. huxleyi* in the surface (especially towards the latter part of July). In the Mediterranean during summer, *Syracosphaera* spp. are also common (Cerino et al., 2017; Karatsolis et al., 2016), although not typically within the SCM, although the pigment 19'-hexanoyloxyfucoxanthin (19'hex-fuco), a marker for the broader taxonomic class prymnesiophytes, was elevated in this layer in the Celtic Shelf (Hickman et al., 2009) and Aviles Canyon (Latasa et al., 2017). In the latter, high coccolithophore cell counts were also observed in the SCM (although > 90% *E. huxleyi*), however at other stations there was a marked difference between 19'hex-fuco distribution and coccolithophore cell counts. This could be due to the presence of *Syracosphaera* spp., which can be difficult to identify due to their small cell size, low cellular calcite contents, or due to the presence of other unidentified prymnesiophytes.

During July in the upper euphotic zone, coccolithophore biomass was low during the earliest sampling times; however, this increased throughout the season due to an increase in *E. huxleyi*, despite its small cell size and low cellular biomass. This sudden appearance and increase in *E. huxleyi* biomass could be linked to storm conditions, which occurred around the 24$^{th}$ July (Humphreys and Moore, 2015). We can also see this from a deepening of the mixed layer from 22 to 35 m between the 24$^{th}$ and 29$^{th}$ July (Table 2.1). The net growth rate of *E. huxleyi* between 15 and 24$^{th}$ July was 0.39 d$^{-1}$ and between 24$^{th}$ and 29$^{th}$ July was 0.45 d$^{-1}$, indicating *E. huxleyi* was beginning to grow in the upper euphotic layers before a possible storm scenario. These net growth rates were twice as high as the maximum rates measured for *E. huxleyi* during April at CCS (0.21 d$^{-1}$) as the spring phytoplankton bloom developed, and estimated between subsequent visits during an *E. huxleyi* bloom (0.20 d$^{-1}$) (Mayers et al., 2018). This rapid response to nutrient input may be due to the ability of *E. huxleyi* to use multiple nitrogen sources (Benner and Passow, 2010), and its possession of a constitutive (and inducible) alkaline phosphatase activity (Dyhrman and Palenik, 2003; Riegman et al., 2000), allowing the rapid assimilation of nutrients. Thus, *E. huxleyi* may have been able to rapidly respond to a pulse of inorganic nutrients from below the mixed layer provided due to a storm event, a feature which may control its wider shelf sea biogeography (see below).

Highest coccolithophore abundances at CCS were observed during November, as winter mixing broke down the water column stratification. Coccolithophores in the northern Adriatic Sea peak in December to February, however this is mostly due to *E. huxleyi* (Cerino et al., 2017), whereas in our study, the high biomass was due to *Syracosphaera* spp. and *C. caudatus*. In the Gulf of Naples, *C. caudatus* was also observed to have a peak biomass in October as the stratification was breaking down (Ribera d'Alcalà et al., 2004), suggesting this could be an ecological niche for this species.

During incubation experiments in the Celtic Sea in April 2015, *C. caudatus* was observed to consistently display negative growth rates when compared to *E. huxleyi* (Mayers et al., 2018). These authors suggested it may be that *C. caudatus* is only able to efficiently grow and out-compete other coccolithophores when nutrients are abundant. In the Iceland Basin and Norwegian Sea during June, *C. caudatus* represented up to 43% of the total coccolithophore cell numbers, a period of time when inorganic nutrients were replete (Daniels et al., 2016), further supporting this hypothesis. There could also be selection for *C. caudatus* compared to other coccolithophores by (micro-) grazers, particularly as it has a larger cell size (~12 µm) than many other species (e.g. *E. huxleyi*, 5 µm) which may enhance . However, the presence of spines on this species has been suggested as a mechanism for grazing protection and possible selection against this species (Monteiro et al., 2016; Young et al., 2009).

During spring, particularly at CCS and L4, as a phytoplankton bloom developed there were similarities in the presence of *E. huxleyi* and *C. pelagicus* at these sites. These species were also observed at CS2, although in much lower relative proportions and abundances. Both these species were also observed in pre-spring bloom conditions in the North Atlantic, even displaying similar net growth rates as the water column stabilized (Daniels et al., 2015). The abundances of two other large (> 10 µm) coccolithophores, *A. unicornis* and *C. mediterranea* were also high within the pre-spring bloom communities; however these both show a decline throughout April in the Celtic Sea. This suggests either a reduction in competitive advantage as nutrients are depleted, mixed layer irradiance increases, or preferential grazing on these larger cells by microzooplankton grazers. The biomass of planktonic ciliates (63 – 200 µm) did increase throughout April (Giering et al., 2018), which could support these as possible grazers of larger coccolithophores. A peak in *C. meditteranea* was observed during July at a Scottish Coastal site, when inorganic nutrients were low (León et al., 2018), suggesting that other factors, rather than nutrients may have played a role.

### 2.5.3 Shelf edge

Coccolithophore biomass at the shelf edge (CS2) was highest during April, followed by July and finally November, which is the reverse trend as seen at CCS. During November, CS2 showed high proportions of *C. leptoporus* and *G. muellerae,* both of which are species associated with the North Atlantic Ocean (Ziveri et al., 2004). The higher proportions at the shelf edge could be due to the stronger current flows found there during winter (Pingree et al., 1999). During winter in the northern Adriatic Sea, *E. huxleyi* was observed to be the most numerically dominant coccolithophore (Cerino et al., 2017) as it was at CS2 during November.

Throughout April at the shelf edge, *Syracosphaera* spp. was the most dominant species rather than *E. huxleyi*, as was seen at CCS. This could be due to light limitation, as the euphotic zone was 48 m during early April and shallowed by ~20 to 30 m by the second visit, which was slightly later than at CCS. There was little vertical variation in coccolithophore populations at the shelf edge, even during July (Fig. 2.3). This trend could be related to the vertical supply of nitrate from below the mixed layer through tidal mixing (internal tides) (Sharples et al., 2009, 2007), allowing phytoplankton communities access to a reliable source of inorganic nutrients. This may also explain why *E. huxleyi* is the most dominant coccolithophore at the shelf edge during summer, due to a continuous nutrient source and its ability to rapidly respond to nutrient pulses into the euphotic zone.

### 2.5.4 Coastal English Channel

The coastal station L4 in the English Channel was mostly dominated by *E. huxleyi* during all the periods sampled, with *C. pelagicus* being the second most prominent species, even making up 100% of the biomass on 28th July. This is consistent with data from the 1992 to 2007 time-series at L4 which found *E. huxleyi* made up on average 93% (numerically) of the coccolithophore population at L4 (Widdicombe et al., 2010). The presence of both of these species during November could be linked to their positive growth rates in similar laboratory conditions (temperature and light) as to those observed at L4 (0.59 $d^{-1}$ and 0.43 $d^{-1}$ for *E. huxleyi* and *C. pelagicus*, respectively) (Daniels et al., 2014). During April, these two species were observed again, however *G. muellerae* was also present, particularly towards late April.

During July at L4, all samples except one sampling date were completely dominated by *E. huxleyi* in terms of biomass. Nutrient input from riverine sources regularly occurs at L4 (Smyth et al., 2010), providing further support that *E. huxleyi* can dominate in environments where there is an intermittent nutrient sources into depleted conditions. Enhanced alkaline phosphatase activity has been observed in response to high summertime rainfall at L4 (Rees et al., 2009), although no data on coccolithophore responses are reported. Off the coast of Bermuda in the Sargasso Sea, the abundance of *E. huxleyi* was found to have a negative correlation with nitrate concentration (Haidar and Thierstein, 2001), however the nitrate flux is unlikely to be from similar sources in the Celtic Sea.

### 2.5.5 Cross shelf patterns in coccolithophore species variability

The main coccolithophore species driving community differences between the three sites, in terms of coccolithophore populations was *E. huxleyi* followed by *Syracosphaera* spp (Fig 2.5). This difference might be driven by the differing times of *E. huxleyi* dominance at the sites, as well as the absence of *Syracosphaera* spp. from L4. It may be that *Syracosphaera* spp. are present at L4, however using the Utermöhl technique for coccolithophore enumeration can lead to rare and lightly calcified species (such as *Syracosphaera* spp.) being missed. Within the Mediterranean Sea, holococcolithophores (HOLs) are commonly observed (D'Amario et al., 2017), which are the haploid life stage of many coccolithophore species (Billard, 1994). During this study, we observed very low biomass (or numbers) of HOLs, which could be due to their unique ecological drivers, but also due to the difficult nature of observing HOLs, due to their lack of calcified scales. This is especially true given some haploid stages can also be 'naked' or completely un-calcified (Frada et al., 2012). A greater understanding of how to measure and monitor these

different life stages is needed for biogeographical studies (Cros & Estrada, 2013). One possible method, developed for *E. huxleyi* is the use of fluorescent (COD-FISH) and molecular (reverse transcription-PCR) markers (Frada et al., 2012).

There appears to be connectivity between the open-ocean and shelf edge (CS2), and possibly at certain points of the year with the shelf edge and central English Channel (Station L4). Comparably, at CCS data on zooplankton biomass, community composition and iron profiles throughout our study period (Giering et al., 2018, Birchill et al., 2017), suggest that it is a relatively closed system in terms of water circulation. Indeed, drifter trajectories from buoys released in the region of CCS show little horizontal movement at this site, and this conclusion is further supported from predicted density driven currents at CCS (Young et al., 2004). Therefore, water mass movement may influence populations less here than for instance at the shelf edge. For example, during repeated visits to CCS in April there appears to be a progressive change in coccolithophore populations, such as a gradual decline of *C. mediterranea* and increase in *E. huxleyi*. This suggests changes in environmental or biological gradients (e.g. grazers) may be controlling species composition, rather than advection between sites.

This study relied on Eulerian sampling (i.e. fixed point with water parcel movement), which may have biased our measurements. If mesoscale features (e.g. eddies) had passed through our sample sites, these would have biased our measurements (for example station L4 on the 20$^{th}$ and 28$^{th}$ July) and could lead to misinterpretation of biological responses. A possible alternative approach would be Lagrangian studies using inert tracers (such as sodium hexafluoride, see Jickells et al., 2008). This would allow an examination of temporal changes within a water body, and a greater understanding of how biogeochemical (Jickells et al., 2008) and ecological (Burkill et al., 2002) processes interact and shift over time.

The redundancy analyses displays the changes in cross shelf parameters (RDA1, bottom depth and salinity), whereas RDA2 represents changes across seasons. *Syracosphaera* spp. and *C. caudatus* appear to be the species most influenced by RDA1, both being found only at CCS and CS2 (negative species scores), with *C. pelagicus* and *E. huxleyi* displaying positive species scores (Table 2.3). *C. pelagicus* had a much higher score with RDA2 (seasonality) than *E. huxleyi*, being present only in April at all sites on the NW European Shelf, but also in July and November at L4. As the sampling at L4 was only from one depth, there is the possibility that *C. pelagicus* HOL exist at different light depths within L4, (as seen for HOLs in the Atlantic Ocean in deeper layers (Poulton et al., 2017a)), this could explain its presence at multiple points during the year at this site.

From this analyses, a schematic is proposed for coccolithophore populations throughout the year within the Celtic Sea and English Channel (Fig. 2.9). When light is limiting rather than nutrients (e.g. winter and within the SCM), *Syracosphaera* spp. dominates coccolithophore populations at the shelf edge and CCS, with *C. caudatus* being present during winter and early spring, possibly due to a mixotrophic lifestyle (Poulton et al., 2017a). In early spring, large celled coccolithophores are also present (*C. meditteranea, A. unicornis*). As stratification develops and the spring phytoplankton bloom draws down nutrients, *E. huxleyi* dominates due to recycling processes and variable fluxes of inorganic nutrients into the euphotic zone from stochastic mixing events (i.e. storms). In culture conditions, *E. huxleyi* displays increased biomass when N: P was supplied at a high ratio (100:1), particularly when supplied in 3 hours pulses (Riegman et al., 1992), suggesting that a greater competitive ability of *E. huxleyi* at low phosphorus concentrations may be the controlling nutrient. In mesocosm experiments, *E. huxleyi* was reported to form larger abundances when N: P were added at 16:1 and 16:0.2 ratios (i.e. low phosphorus) (Egge & Heimdal, 1994), supporting this hypothesis.

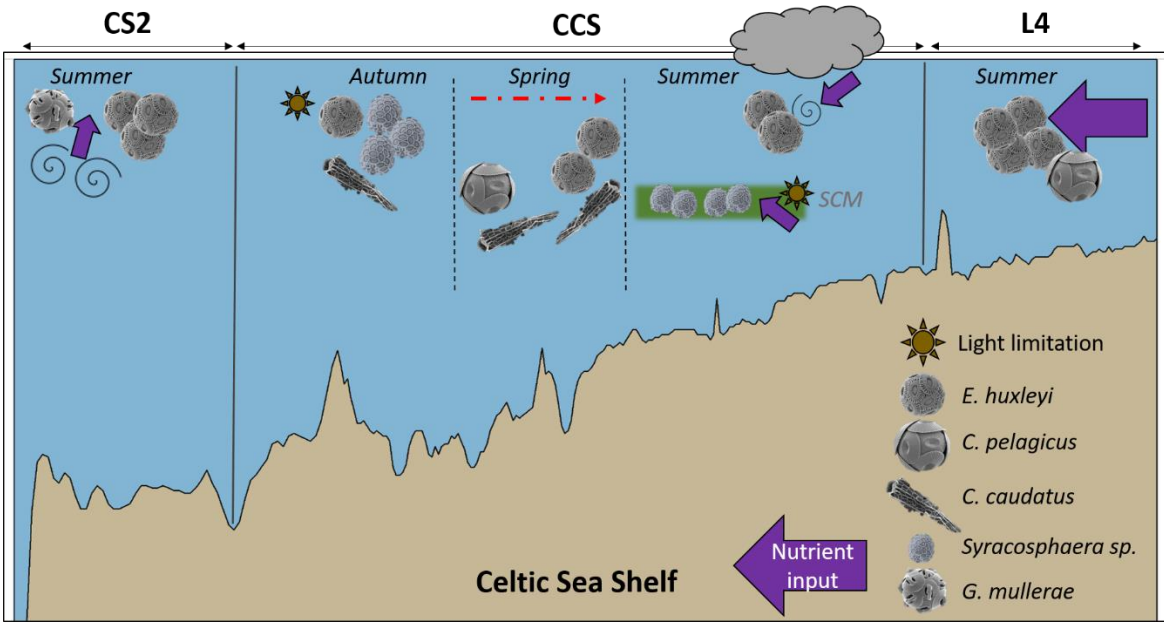


**Figure 2.9.** Schematic of the shelf sea during summer at all sites, and Autumn and Spring at CCS. SCM is the subsurface chlorophyll maximum, red arrow illustrates time. Coccolithophore images were taken from mixrotax.org

## 2.6 Conclusions

The data presented within this chapter are some of the first to present seasonal and spatial coccolithophore biogeography in terms of carbon biomass, rather than direct cell

abundance. This difference displayed a reduced average proportion of *E. huxleyi* and an enhanced contribution of larger coccolithophore species, suggesting these organisms likely have a greater role in carbon flux and food web ecology than previously suggested. This study demonstrates that major seasonal and spatial differences in coccolithophore populations were observed across the Celtic Sea, with vertical differences only being seen within the Central Celtic Sea during July. Within the summer months, *E. huxleyi* makes up a higher proportion of the coccolithophore community within areas where there are intermittent inputs of inorganic nutrients into the environment, providing evidence for possible bloom formation requirements. The observation that lightly calcified species (e.g. *Syracosphaera* spp.) provides further evidence for a possible mixotrophic lifestyle (see Poulton et al., 2018) in order to survive in regions with low light conditions, such as the sub-surface chlorophyll maxima or in late Autumn where biomass is observed to be greatest. Further work is required to understand the biological interactions between coccolithophores and other members of the plankton community (including grazers), especially with regards to species other than *E. huxleyi*, as well as enhanced methodology to quantify the biomass of holococcolithophore life stages, which may be overlooked in usual taxonomic surveys.

# Chapter 3: Growth and mortality of coccolithophores during spring in a temperate Shelf Sea (Celtic Sea, April 2015)

This chapter has been published as: Mayers, K.M.J.[1], Poulton, A.J.[2,†], Daniels, C.J.[2], Wells, S.R.[3], Woodward, E.M.S.[4], Tarran, G.A.[4], Widdicombe, C.E.[4], Mayor, D.J.[2], Atkinson, A.[4], and Giering, S.L.C.[2], (2018). Growth and mortality of coccolithophore during spring in a temperate Shelf Sea (Celtic Sea, April 2015). *Prog. Oceanogr.*, doi:10.1016/j.pocean.2018.02.024.

[1] Ocean and Earth Science, National Oceanography Centre Southampton, University of Southampton, Southampton, UK

[2] National Oceanography Centre, Waterfront Campus, European Way, Southampton, UK

[3] Institute of Biological and Environmental Sciences, University of Aberdeen, Oceanlab, Newburgh, Aberdeenshire, UK

[4] Plymouth Marine Laboratory, Prospect Place, The Hoe, Plymouth, UK

[†] Current address: The Lyell Centre, Heriot-Watt University, Edinburgh, UK

KMJM conducted experiments within this chapter, analysed the data and wrote the manuscript. AJP and CJD conducted rate measurements, EMSW provided nutrient data, SRW and SLCG conducted dilution experiments. All authors provided feedback on the manuscript.

## 3.1 Abstract

Coccolithophores are key components of phytoplankton communities, exerting a critical impact on the global carbon cycle and the Earth's climate through the production of coccoliths made of calcium carbonate (calcite) and bioactive gases. Microzooplankton grazing is an important mortality factor in coccolithophore blooms, however little is currently known regarding the mortality (or growth) rates within non-bloom populations. Measurements of coccolithophore calcite production (CP) and dilution experiments to determine microzooplankton (≤63 µm) grazing rates were made during a spring cruise (April, 2015) to the central Celtic Sea (CCS), shelf edge (CS2) and within an adjacent April bloom of the coccolithophore *Emiliania huxleyi* at station J2.

CP at CCS ranged from 10.4 to 40.4 µmol C $m^{-3}$ $d^{-1}$ and peaked at the height of the spring phytoplankton bloom (peak chlorophyll-*a* concentrations ~6 mg $m^{-3}$). Cell normalised calcification rates declined from ~1.7 to ~0.2 pmol C $cell^{-1}$ $d^{-1}$, accompanied by a shift from a mixed coccolithophore species community to one dominated by the more lightly calcified species *E. huxleyi* and *Calciopappus caudatus*. At the CCS, coccolithophore abundance increased from 6 to 94 cells $mL^{-1}$, with net growth rates ranging from 0.06 to 0.21 $d^{-1}$ from the 4th to the 28th April. Estimates of intrinsic growth and grazing rates, from dilution experiments, at the CCS ranged from 0.01 to 0.86 $d^{-1}$ and from 0.01 to 1.32 $d^{-1}$, respectively, which resulted in variable net growth rates during spring. Microzooplankton grazers consumed 59 - >100% of daily calcite production at the CCS. Within the *E. huxleyi* bloom a maximum density of 1,986 cells $mL^{-1}$ was recorded, along with CP rates of 6000 µmol C $m^{-3}$ $d^{-1}$ and an intrinsic growth rate of 0.29 $d^{-1}$, with ~80% of daily calcite production being consumed.

These results show that microzooplankton can exert strong top-down control on both bloom and non-bloom coccolithophore populations, grazing over 60% of daily growth (and calcite production). The fate of consumed calcite is unclear, but may be lost either through dissolution in acidic food vacuoles, and subsequent release as $CO_2$, or export to the seabed after incorporation into small faecal pellets. With such high microzooplankton-mediated mortality losses, the fate of grazed calcite is clearly a high priority research direction.

## 3.2 Introduction

Coccolithophores are a diverse and biogeochemically important group of marine phytoplankton which contribute towards the marine carbon cycle through the production and subsequent export of cellular scales (coccoliths) formed of calcium carbonate

(calcite). The cellular process of calcite production (calcification) fixes and releases $CO_2$ and hence coccolithophores have an important role in air-sea $CO_2$ fluxes (e.g. Holligan et al., 1993; Buitenhuis et al., 1996). Calcite can also act as a ballast for sinking material, enhancing the deep-sea flux of organic matter (Bach et al., 2016; Klaas and Archer, 2002; Ziveri et al., 2007). Coccolithophores are globally distributed, from polar to tropical low-latitude waters, with the most cosmopolitan and abundant species being *Emiliania huxleyi* (e.g. Winter et al., 1994). *E. huxleyi* often forms extensive, large-scale (>100,000 $km^2$) blooms in the open ocean (e.g. Holligan et al., 1993), along continental shelves (e.g. Holligan et al., 1983; Poulton et al., 2013) in coastal shelf seas (e.g. Buitenhuis et al., 1996; Krueger-Hadfield et al., 2014; Rees et al., 2002).

Phytoplankton blooms are common in shelf sea environments during late spring, when environmental conditions allow growth to exceed mortality and biomass to accumulate. The community structure within these may change with time, as environmental conditions such as nutrient and light availability favour one phytoplankton group over another. Coccolithophore blooms are considered to be favoured under conditions between high-turbulence high-nutrient and low-turbulence low-nutrient environments (Balch, 2004). However, satellite-derived particulate inorganic calcite and chlorophyll-*a* data from open ocean regions suggest that blooms of coccolithophores can also co-occur with blooms of other phytoplankton (e.g. diatoms), and sequential succession between groups may not always occur (Hopkins et al., 2015). In-situ observations made during several phytoplankton blooms support the co-occurrence of coccolithophores with other groups, including diatoms and dinoflagellates in the open ocean and coastal environments (see Daniels et al., 2015; Poulton et al., 2013, 2014; Schiebel et al., 2011), however we currently lack in-situ data from shelf sea environments during spring.

Blooms of *E. huxleyi* have been shown to be important sources of calcite production (CP) (e.g. Balch et al., 2005; Poulton et al., 2007, 2013), primary production (PP) (up to 30-40% (Poulton et al., 2013), $CO_2$ fluxes (e.g. Buitenhuis et al., 1996) and the production of the bioactive gas dimethyl sulphide (e.g. Malin et al., 1993). Within some shelf sea regions, *E. huxleyi* blooms are an annual feature (e.g. English Channel, Patagonian Shelf) whereas in others they appear sporadically though, recently at an increased frequency (e.g. Barent's Sea, Black Sea) (Iglesias-Rodriguez et al., 2002; Smyth et al., 2004). How these blooms fit into global budgets of CP is currently unclear, though they are significant localised sites of CP and export (Holligan et al., 1993; Poulton et al., 2013).

The formation of *E. huxleyi* blooms, which often occur in late summer, is thought to be linked to several environmental factors, including warm, stratified waters, with low silicic acid concentrations (limiting diatoms), high irradiance, low nitrate to phosphate ratios and reduced microzooplankton grazing (see review by Tyrrell and Merico, 2004).

Microzooplankton (<200 µm) are major grazers of phytoplankton, consuming from 49% to 77% of daily PP (Schmoker et al., 2013). The relationship between coccolithophores and microzooplankton grazing is currently unclear, as only a few studies, most of which during coccolithophore blooms, have investigated microzooplankton-induced mortality. A study carried out during an *E. huxleyi* bloom in the Bering Sea found lower grazing rates within bloom waters than outside bloom waters, which led to higher net growth rates compared with outside of the bloom (Olson and Strom, 2002). A similar result was observed in the English Channel (Fileman et al., 2002), suggesting depressed grazing rates on coccolithophores could be a trigger for bloom formation and persistence.

At the cellular scale, calcification accounts for ~30% of photosynthetically fixed energy and hence represents an important fraction of the total cellular metabolism available for key cellular processes such as nutrient uptake and cell division (Monteiro et al., 2016). The ecological or physiological role of calcification is not fully known, though several hypotheses exist such as protection from light stress, enhancement of photosynthesis, buoyancy regulation and as a protection from grazing (Young et al., 1994; Monteiro et al., 2016). A recent modelling study proposed that calcification has different ecological roles across different oceanic provinces (Monteiro et al., 2016). However, experimental results have so far demonstrated less clarity on the role of calcification. For example, culture experiments with the heterotrophic dinoflagellate *Oxyrrhis marina* showed grazing to be higher on calcified *E. huxleyi* cells than naked ones (Hansen et al., 1996). More recently, another culture experiment has shown that grazing rates on *E. huxleyi* appeared to be dependent on the strain studied rather than cell calcite content, although growth rates of the heterotrophic dinoflagellate and their overall grazing impact were also depressed due to the cellular degree of calcification (Harvey et al., 2015).

The aim of our study was to examine the variability in the rates at which coccolithophore communities grow and are being grazed by microzooplankton and how these relate to environmental conditions and the microzooplankton community. We carried out our study during April, as this is the key period in temperate shelf seas for the spring phytoplankton bloom, and not generally associated with coccolithophore blooms that typically occur in late summer. We measured coccolithophore growth and mortality rates, alongside observations of coccolithophore species composition and CP, during April at three sites in the Celtic Sea in order to examine: (1) the role of coccolithophores in carbon cycling during spring, (2) coccolithophore growth rates during the spring bloom, and (3) the role of microzooplankton grazing in coccolithophore population dynamics.

## 3.3 Methods

### 3.3.1 Study site

Sampling was carried out on-board the *RRS Discovery* (cruise number DY029) from 1st April to 29th April 2015 in the Celtic Sea (Fig. 3.1; NW European Shelf) as part of the UK Shelf Sea Biogeochemistry (SSB) research programme. Water sampling was carried out at 10 pre-dawn stations (02:00 – 03:30 h GMT) using a conductivity-temperature-depth (CTD) profiler with rosette sampler fitted with twenty-four 20 L Niskin bottles. Seawater samples were obtained from six light depths within the upper 100 m, determined as 60, 40, 20, 10, 5 and 1% of surface irradiance (see Poulton et al., 2017b for full methodology) for rate measurements (primary production (PP), calcite production (CP)), phytoplankton biomass (chlorophyll-*a*) and coccolithophore community structure. The main sampling stations in this study were the Central Celtic Sea (CCS; 150m water depth), the Celtic Shelf Edge (CS2; 203m water depth) and station J2 (Fig.3.1). Throughout this paper, the term 'spring bloom' is used to refer to a peak in chlorophyll-*a* biomass (~6 mg $m^{-3}$) in the middle (15$^{th}$) of April at CCS, and 'coccolithophore bloom' to refer to the high cellular coccolithophore abundances at J2.

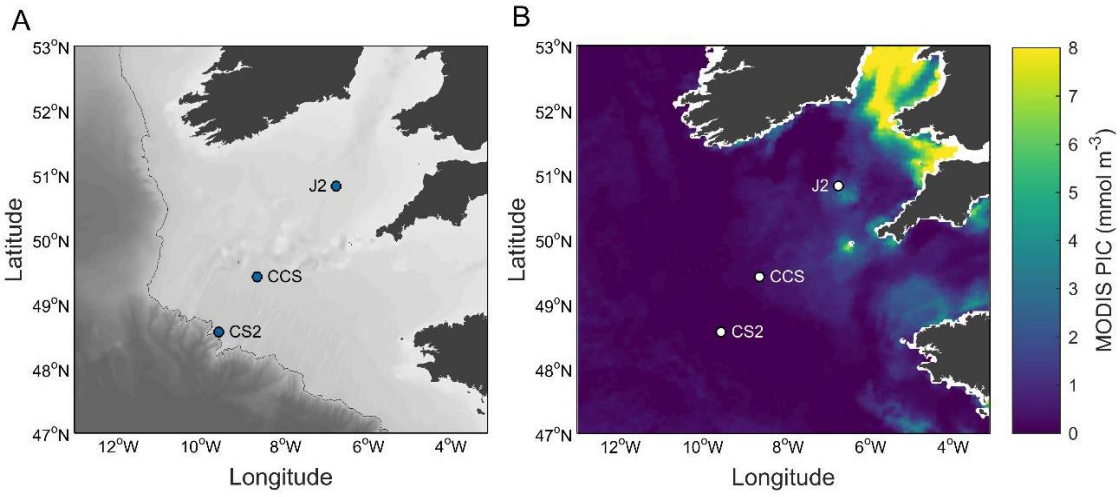


**Figure. 3.1.** Sampling locations within the Celtic Sea superimposed onto depth (left) with dark colours corresponding to deep waters and MODIS particulate inorganic carbon (PIC) concentration for April 2015. Central Celtic Sea (CCS), Shelf Edge (CS2), and station J2.

### 3.3.2 Nutrients and chlorophyll measurements

Water samples for determination of nutrient concentrations (nitrate+nitrite, nitrite, phosphate, and silicic acid) were collected directly from the CTD into aged, acid-washed

and Milli-Q-rinsed 60 mL HDPE Nalgene™ bottles. Clean sampling and handling techniques were employed during the sampling and manipulations within the laboratory, and where possible carried out according to the International GO-SHIP nutrient manual recommendations (Hydes et al., 2010). Nutrient samples were all analysed on board the *RRS Discovery* using a Bran and Luebbe segmented flow colorimetric auto-analyser using techniques described in Woodward and Rees (2001). Nutrient reference materials (KANSO Japan) were run each day to check analyser performance and to guarantee the quality control of the final reported data. The typical uncertainty of the analytical results were between 2 to 3%, and the limits of detection for nitrate and phosphate was 0.02 µmol $L^{-1}$, nitrite 0.01 µmol $L^{-1}$, whilst silicic acid was always higher than the limits of detection. Further details of the nutrient analysis and seasonal variability in nutrient inventories can be found in Humphreys et al. 2017.

Water samples (0.2-0.25 L) for chlorophyll-*a* extraction were filtered onto 25 mm diameter Whatman GF/F or Fisherbrand MF300 glass fibre filters (effective pore sizes 0.7 µm) and extracted in 6-10 mL 90% acetone (HPLC grade, Sigma-Aldrich, UK) at -4°C for 18-24 h (Poulton et al., 2014). Fluorescence was measured on a Turner Designs Trilogy fluorometer using a non-acidification module and calibrated with a solid standard and a pure chlorophyll-*a* standard (Sigma-Aldrich, UK).

### 3.3.3 Coccolithophore community enumeration and composition

Samples for coccolithophore cell counts and community composition were sampled as described by Poulton et al. (2010). Briefly, samples were collected from the six light depths, seawater samples (0.2 – 0.5 L) were filtered under gentle pressure through 25-mm diameter, 0.8-µm pore size Nuclepore™ cellulose nitrate filters with a Whatman GF/F backing filter to aid in equal distribution of material across the filter. Filters were rinsed with trace ammonia solution (pH ~10-11), oven dried for ~12 hours at 50 to 60°C and stored in Millipore petri-slides. Permanent slides of the filters were prepared on board by mounting the filters using low viscosity Norland Optical Adhesive 074 (Poulton et al., 2010). Samples were analysed under cross-polarized light using an Olympus BX51 (x1000, oil immersion). Either 300 individual cells or 300 fields of view (whichever was reached first) were counted per sample with a minimum number of 50 fields of view being counted. Cell numbers (cells $mL^{-1}$) were calculated based on the area of filter examined (total area of filtered material divided by the number of fields of view multiplied by area of 1 field of view), cells counted and volume filtered (mL). Full coccospheres were identified following the taxonomy of Frada et al. (2010) to the lowest possible taxonomic unit. Standard errors in cell counts were calculated using equation 1:

$$\frac{(\sqrt{C})}{(FOV\ x\ \frac{V}{A})} \qquad \text{(Equation 1)}$$

Where C is the number of cells counted, A is the area investigated ($mm^2$), FOV is the number of field of views counted and V is the volume of water filtered (mL) (Taylor, 1982).

For a small number of samples (usually taken at the depth of 40% surface irradiance) further species identification and cell counts were carried out using scanning electron microscopy (SEM) following Young et al. (2003) to identify species. Coccolithophore community diversity was determined and expressed as species richness (total number of species in a sample, S) and Pielou's evenness (J'), which is a measure of how evenly distributed species are in a community (high values represent dominance by a one or a few species). J' was calculated as described by Charalampopoulou et al., (2011, 2016).

### 3.3.4 Primary production and coccolithophore calcification rates

Daily rates (24 hours from dawn to dawn) of primary production (PP) and calcite production (CP) were determined for each of the 10 stations sampled using the methodology described by Balch et al. (2000) (see also Poulton et al., 2010, 2013, 2014). Seawater samples were collected before dawn (02:00 – 03:00 local time), and subsamples from the six light depths decanted into four 70 mL polycarbonate (Corning™) flasks: 3 light replicates and 1 formalin-killed control. All samples were spiked with 34 to 44 $\mu$Ci of $^{14}$C-labelled sodium bicarbonate and placed in dedicated incubation chambers with a combination of LED light panels (Powerpax, UK) and neutral density light filters (Lee Filters™, UK) to replicate the absolute daily light doses at the depths of collection (see Poulton et al., 2017b). Formalin killed blanks were prepared by adding 1 mL of 0.2-µm filtered borate-buffered formalin solution.

Incubations were ended by filtering through polycarbonate filters (25-mm diameter, 0.4-µm nominal pore size, Nucleopore™, USA), with extensive rinsing to remove unfixed $^{14}$C-labelled sodium bicarbonate. Organic (PP) and inorganic (CP) carbon fixation were determined using the micro-diffusion technique (Paasche and Brutak, 1994; Balch et al., 2000; Poulton et al., 2014), the filters were then placed in fresh glass scintillation vials with 12 mL of Ultima Gold™ (Perkin-Elmer, UK) liquid scintillation cocktail added. The activity on the filters was then determined using a Tri-Carb 3100TR Liquid Scintillation Counter on-board. The spike activity was checked by the removal of triplicate 100 µL subsamples directly after the spike addition and mixing with 200 µL of β-phenylethylamine (Sigma, UK) followed by Ultima Gold™ and liquid scintillation counting (Poulton et al., 2014). The average coefficient of variation (standard deviation/mean x 100) of triplicate PP

measurements was 13% (1 – 59%) and 47% (1 – 143%) for CP measurements. The formalin-killed blank represented 27% (<1 – 600%) of the CP signal on average, with higher contributions observed at the base of the euphotic zone.

### 3.3.5 Coccolithophore net growth rates

Net growth rates of coccolithophores were determined from 24 h incubations. Water was collected before dawn as described above. Water samples (250 mL) from the 40% incident irradiance depth were taken directly from the CTD. Three samples were filtered immediately ($T_0$ counts), whilst three more samples were placed in a dedicated incubation chamber (as described above; see also Poulton et al., 2017b) for 24 hrs, and then filtered. Samples were filtered under gentle vacuum through cellulose nitrate filters (25 mm diameter, 0.8 µm pore size Nuclepore™) with a Whatman GF/F backing filter to aid in equal distribution of material across the filter. Filters were treated as discussed above and coccospheres identified. Net growth rates (µ, $d^{-1}$) of coccolithophores were determined using equation 2:

$$\mu = \left(\frac{1}{t}\right) LN \left(\frac{n24}{n0}\right) \qquad \text{(Equation 2)}$$

Where t is time in days, $n_{24}$ is the number of cells $mL^{-1}$ at the end of the incubations and $n_0$ the number of cells $mL^{-1}$ taken directly from the CTD.

### 3.3.6 Coccolithophore growth and microzooplankton grazing

Daily rates of coccolithophore growth and mortality were estimated using the dilution technique (Landry and Hassett, 1982; Landry et al., 1995). Seawater samples from the upper mixed layer (5-10 m water depth) were collected in 10 L acid-clean carboys passed through a 63 µm mesh to exclude larger zooplankton. Use of a 63 µm mesh in this study was aimed at excluding larger grazers and focusing on grazing by microzooplankton on coccolithophores and phytoplankton ≤63 µm. A proportion of the seawater was filtered through 0.2 µm cartridge filters using gravitational filtration. Sequential dilutions were made of 100, 70, 40 and 20% ambient seawater. Samples were gently agitated prior to sampling to ensure they were well mixed. Nutrients were not added to incubation bottles as there is evidence this may impact on microzooplankton abundance (Gifford, 1988) and phytoplankton growth (Lessard and Murrell, 1998). Furthermore, nutrient levels (nitrate, phosphate, silicate) remained in replete concentrations throughout most of the sampling period (>2 µmol $kg^{-1}$ for nitrate and silicate, and >100 nmol $kg^{-1}$ for phosphate; see Humphreys et al., 2017 and Poulton et al., 2017b). During the entire setting up procedure,

seawater was kept in a temperature-controlled laboratory set to in situ temperatures (± 2ºC), and was handled in near darkness to minimise exposure to light.

Samples for nutrients, coccolithophores (by cell counts, see Section 2.3), microzooplankton (by FlowCAM, see below) and chlorophyll-*a* (see Section 2.2), were taken for initial measurements from 63 µm screened water. Twelve 3 L glass jars were filled with the seawater dilutions (triplicates of each dilution), sealed without a bubble present, and incubated for 24 h in a controlled temperature (CT) refrigeration container (see Richier et al., 2014 and Poulton et al., 2017b). After 24 h, the samples were removed from the incubators and the same suite of measurements taken as for the initial measurements (cell counts, microzooplankton abundance, chlorophyll-a), ensuring samples were mixed before sub-sampling. For coccolithophore cell abundances, 250 mL of seawater was filtered through a 0.4 µm pore size Nuclepore™ cellulose nitrate filters with a Whatman GF/F backing filter to aid in equal distribution of material across the filter, filters were then treated the same as for CTD samples (see Section 3.2).

Growth rates were calculated as in equation 2. Changes in coccolithophore cell numbers, measured by cross-polarized light microscopy (see Section 3.2) were used to calculate apparent growth rates, assuming:

$$NGR = k - cg = \frac{1}{t}\, LN\, (\frac{Pt}{Po}) \qquad \text{(Equation 3)}$$

where $P_0$ and $P_t$ are the initial and final cell numbers, *k* is the intrinsic growth rate of coccolithophores (Y-intercept), *g* is the coefficient of grazing mortality (the slope of the linear regression) and *c* is the dilution factor (1, 0.7, 0.4, and 0.2) (Landry and Hassett, 1982; Landry et al., 1995). Two main assumptions of the dilution technique are that phytoplankton growth rates are unaffected by dilution, and that the rate of grazing mortality is proportional to the dilution impact on grazer abundance (Landry and Hassett, 1982; Landry et al., 1995).

We calculated the percentage of daily growth consumed by microzooplankton as intrinsic growth rate ($\mu$) divided by the coefficient of grazing mortality (g). As we will be discussing the consumption of calcite-bearing phytoplankton, we also refer to this as the fraction of calcite production consumed per day rather than primary production.

### 3.3.7 Microzooplankton abundance

Sub-samples (10-20 mL) of preserved microzooplankton in acidic Lugol's Iodine (2% final concentration) collected at T0 and T24 from dilution experiments were analysed using FlowCAM VS-IVc (Fluid Imaging Technologies Inc.) fitted with a 300 µm path length flow cell and x4 microscope objective. Images were collected using auto-image mode at a rate

of 6-12 frames per second. Image files were manually classified to determine the abundance of dinoflagellates and ciliates using Visual spreadsheet software (Version 3.2.3).

### 3.3.8 Data analysis and statistics

All statistical analyses were carried out in SigmaPlot (v12.5). Growth rate errors for incubation experiments were calculated using error propagation and linear regressions. An F-test was used to look for differences in the linear regressions within dilution experiments for total coccolithophore communities and *E. huxleyi*.

## 3.4 Results

### 3.4.1 General Oceanography

Samples were taken during April 2015 at the three sites in the Celtic Sea: Central Celtic Sea (CCS), the shelf edge (CS2), and a shallower station (J2) (Fig. 3.1). Throughout April, CCS was more frequently sampled ($n$ = 5) than CS2 ($n$ = 2) and J2 ($n$ = 2). Hydrographic conditions varied during spring at CCS, with sea surface temperature varying from 9.8$^{o}$C to 11.2$^{o}$C and mixed layer depth (MLD) (determined as an increase of 0.01 kg m$^{-3}$ from the potential density at 10 m; Hopkins, pers. comms) shoaling from 51 m at the beginning of April to 16 m by the end of the month. The shelf-break (CS2) showed slightly higher temperatures than CCS with little variability between subsequent visits (11.4 – 11.8$^{o}$C) and a small decrease in MLD from 27 m to 24 m. The shallower J2 site had sea surface temperatures between 9.8$^{o}$C and 10.4$^{o}$C and a slightly shallower MLD than CS2 (20-22 m; Table 3.1). Poulton et al., 2017b gives details of the seasonal variability in absolute irradiance across the euphotic zone.

**Table 3.1 .** Environmental conditions for calcification and coccolithophore cell experiments conducted in the Celtic Sea during April 2015. Euphotic depth was determined during the cruise to be the depth of 1% photosynthetically active radiation (PAR). Not determined (ND).

| | | | Surface macronutrients | | | | | | |
|---|---|---|---|---|---|---|---|---|---|
| Sampling sites | Day in April | SST (°C) | $NO^3$ (µM) | $PO^4$ (µM) | $Si(OH)^4$ (µM) | $NH^4$ (µM) | N:P ratio | Euphotic depth (m) | Mixed layer depth (m) |
| CCS | 4 | 9.8 | 6.0 | 0.5 | 2.8 | <0.1 | 12 | 37 | 51 |
| CCS | 6 | 10 | 5.6 | 0.4 | 2.7 | <0.< | 14 | 37 | 47 |
| CCS | 11 | 10.3 | 3.8 | 0.3 | 2.6 | 0.1 | 13 | 32 | 22 |
| CCS | 15 | 11.1 | 1.4 | 0.2 | 2.6 | 0.1 | 7 | 28 | 25 |
| CCS | 20 | 10.8 | 2.0 | 0.2 | 2.4 | 0.2 | 10 | 28 | 24 |
| CCS | 25 | 11.2 | 0.4 | 0.1 | 2.2 | 0.2 | 4 | 35 | 16 |
| CS2 | 10 | 11.4 | 8.2 | 0.5 | 3.1 | <0.1 | 16 | 48 | 27 |
| CS2 | 24 | 11.8 | 6.1 | 0.4 | 2.3 | 0.2 | 15 | 30 | 24 |
| J2 | 14 | 9.8 | 4.2 | 0.4 | 3.5 | 0.1 | 11 | ND | 20 |
| J2 | 27 | 10.4 | 0.6 | 0.1 | 2.9 | 0.4 | 6 | ND | 22 |
| **Mean** | | | 3.8 | 0.3 | 2.7 | 0.2 | 11 | 34 | 28 |
| **Min** | | | 0.4 | 0.1 | 2.2 | <0.1 | 4 | 28 | 16 |
| **Max** | | | 8.2 | 0.5 | 3.5 | 0.4 | 16 | 48 | 51 |

Surface nitrate (NOx) and phosphate decreased throughout April from 6 to 0.4 µmol $kg^{-1}$ and 0.5 to 0.1 µmol $kg^{-1}$, respectively, at CCS (Table 3.1). Between each subsequent visit to CCS, NOx declined, apart from between the 15th and 20th April (1.4 – 2.0 µmol $kg^{-1}$), which coincided with a slight drop in sea surface temperature (11.1 – 10.8$^{o}$C) and likely indicates a mixing event, though there was no noticeable change in MLD (25 – 24 m). At J2, NOx was also drawn down between subsequent visits (4.2 – 0.6 µmol $kg^{-1}$), though only to a limited degree at CS2 (8.2 – 6.1 µM). The same pattern was observed for phosphate at J2 (0.4 – 0.1 µM) and CS2 (0.5 – 0.4 µM). Silicic acid remained relatively high at all stations during spring, ranging from 3.5 to 2.2 µmol $kg^{-1}$, with an April average of 2.7 (± 0.4) µmol $kg^{-1}$. At both CCS and CS2, ammonia concentrations increased from less than 0.1 to ~0.2 µmol $kg^{-1}$, but showed a larger increase at J2 from 0.1 to 0.4 µmol $kg^{-1}$ (Table 3.1).

Integrated euphotic zone chlorophyll-*a* ranged from 35.2 to 132.1 mg $m^{-2}$ in the Celtic Sea during spring, with the highest values found at the CCS on 15th April and the lowest at the shelf edge (CS2) on the 10th April (Table 3.2). At CCS, from 4th to 15th April, euphotic zone integrated chlorophyll-*a* concentrations increased 3-fold, associated with a 4-fold increase in primary production (Table 3.2). At CS2, euphotic zone integrated chlorophyll-*a* increased from 35.2 to 59.8 mg $m^{-2}$ between visits and had a higher integrated PP (81.1-155.1 mmol C $m^{-2}$) (Table 2). J2 was the site of an *Emiliania huxleyi* bloom on 27th April, however sampling on the 14th April found higher chlorophyll-*a* (121.4 and 45.2 mg $m^{-2}$, respectively). Euphotic zone integrated PP was significantly higher during the *E. huxleyi* bloom than on the 14th April (524.2 and 112.3 mg $m^{-2}$, respectively) (Table 2).

### 3.4.2 Coccolithophore abundances and species composition

Measurements of upper euphotic zone (60,40 and 20% PAR light depths) coccolithophore cell abundances at CCS ranged from 7.6 to 91.0 cells $mL^{-1}$, with a positive trend observed throughout April (Fig. 3.2b). Over the entire euphotic zone, average coccolithophore abundance also continually increased throughout April (6.3 – 96.0 cells $mL^{-1}$) (Fig. 3.3). The first visit to J2 on the 14th April showed high cell numbers (155.6 cells $mL^{-1}$), which had increased to 1986 cells $mL^{-1}$ (*E. huxleyi*) cells 13 days later on the 27th April.

At CCS the coccolithophore community was dominated (>49% by abundance) by *E. huxleyi*, with this dominance becoming more pronounced later in April (up to 76%) (Table 3). Increasing *E. huxleyi* dominance coincided with an increase in the relative abundance of the coccolithophore *Calciopappus caudatus.* (5-26%) and a decline in “other” species (34-2%) (Table 3), such as the larger coccolithophore *Coronosphaera mediterranea* (7-<1%). This trend is also seen in Pielou’s evenness (J’) which declined from 0.7 to 0.4, as

well as species richness (the number of different species present) which declined from 11 to 6, with lowest values observed on the 25th April. The shelf-edge site CS2 was also dominated by *E. huxleyi*, however this site showed a lower abundance of *C. caudatus.* (10-2%) and a higher abundance of other species (30-42%), which coincided with high values of J' (0.5-0.6) and species richness (9-10). At J2, the community was almost exclusively (99%) *E. huxleyi*, with J' and species richness both extremely low during both visits to this site (0.1-0 and 2-1, respectively). Morphotype A of *E. huxleyi* (after Young et al., 2003) dominated the J2 bloom and was the common morphotype throughout the spring bloom in the CCS in April (see Supplementary Figure 3.1).

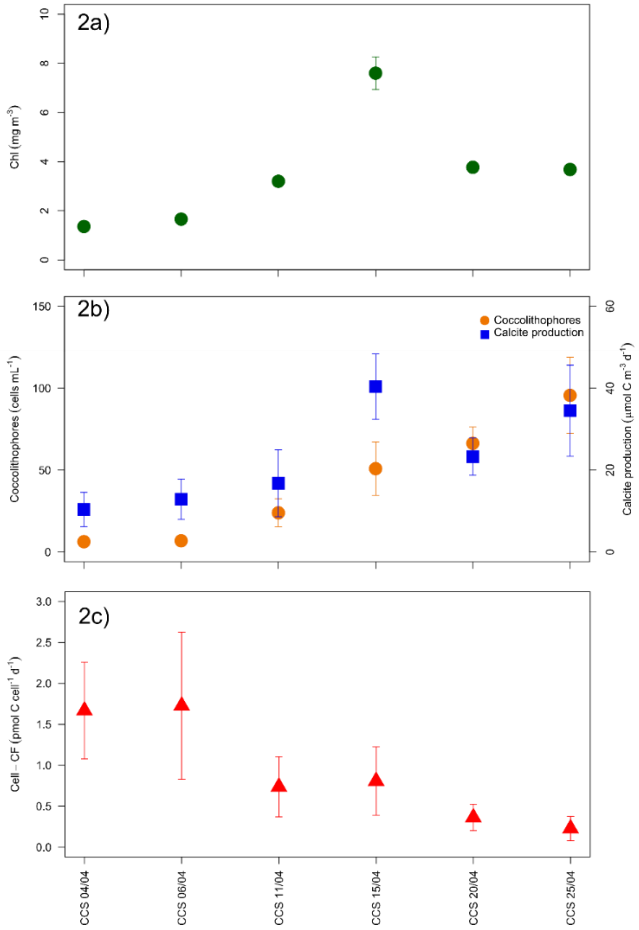


**Figure. 3.2.** Average chlorophyll-*a* (mg $m^{-2}$) (2a), coccolithophore cell numbers (circles, cell $mL^{-1}$) and calcite production (squares, µmol C $m^{-3}d^{-1}$) (2b) and cell normalised calcification rates (2c), averaged over the top 3 light depths (60, 40 and 20% photosynthetically active radiation) at the Central Celtic Sea (CCS). Error bars show ± 1 standard deviation.

**Table 3.2**: Euphotic zone integrated measurements of chlorophyll-*a*, primary production and calcite production.
* Calculated based on the assumption all coccolithophores were *E. huxleyi* and contained 0.34 pg chl-a cell-1 (Daniels et al., 2014)

| | | Chlorophyll-*a* | | | Primary and calcite production | | | |
|---|---|---|---|---|---|---|---|---|
| Sampling sites | Day in April | Total Chl *a* (mg $m^{-2}$) | 2-20µm fraction (%) | Coccolithophore contribution (%)* | PP (mmol C $m^{-2}$) | Coccolithophore contribution (%) | CP (mmol C $m^{-2}$) | CP:PP ratio |
| CCS | 4 | 46.8 | 58 | 0.1 | 101.7 | 0.3 | 0.4 | <0.01 |
| CCS | 6 | 57.8 | 53 | 0.1 | 54.4 | 0.7 | 0.4 | 0.01 |
| CCS | 11 | 102.6 | 67 | 0.2 | 137.3 | 0.3 | 0.5 | <0.01 |
| CCS | 15 | 132.1 | 91 | 0.2 | 435.1 | 0.2 | 1.0 | <0.01 |
| CCS | 20 | 105.2 | 73 | 0.5 | 220.6 | 0.3 | 0.7 | <0.01 |
| CCS | 25 | 112.2 | 64 | 0.6 | 326.9 | 0.2 | 0.7 | <0.01 |
| CS2 | 10 | 35.2 | 46 | 1.0 | 81.1 | 1.8 | 1.5 | 0.02 |
| CS2 | 24 | 59.8 | 72 | 1.4 | 155.1 | 0.7 | 1.1 | 0.01 |
| J2 | 14 | 121.4 | 67 | 1.0 | 112.3 | 8.6 | 10.6 | 0.09 |
| J2 | 27 | 45.2 | 69 | 18.8 | 524.2 | 30.6 | 239.8 | 0.46 |
| **Mean** | | 81.8 | 66 | 2.4 | 214.9 | 4.4 | 25.7 | 0.1 |
| **Min.** | | 35.2 | 46 | 0.1 | 54.4 | 0.2 | 0.4 | <0.01 |
| **Max.** | | 132.1 | 91 | 18.8 | 524.2 | 30.6 | 239.8 | 0.46 |

Discrete measurements of coccolithophore cell numbers within the Celtic Sea ranged from 3.4 (± 0.1) to 150.5 (± 2.2) cells $mL^{-1}$ (Fig. 3.3), with the abundance patterns showing good agreement with average euphotic zone cell numbers (Table 3). Maximum cell numbers at CCS were found below the 60% incidental irradiance depth at all sites, though there was variability in the depth where this maximum occurred. For example, at CCS on the 11th and 25th April maximum cell numbers appeared to coincide with the MLD (Fig. 3.3).

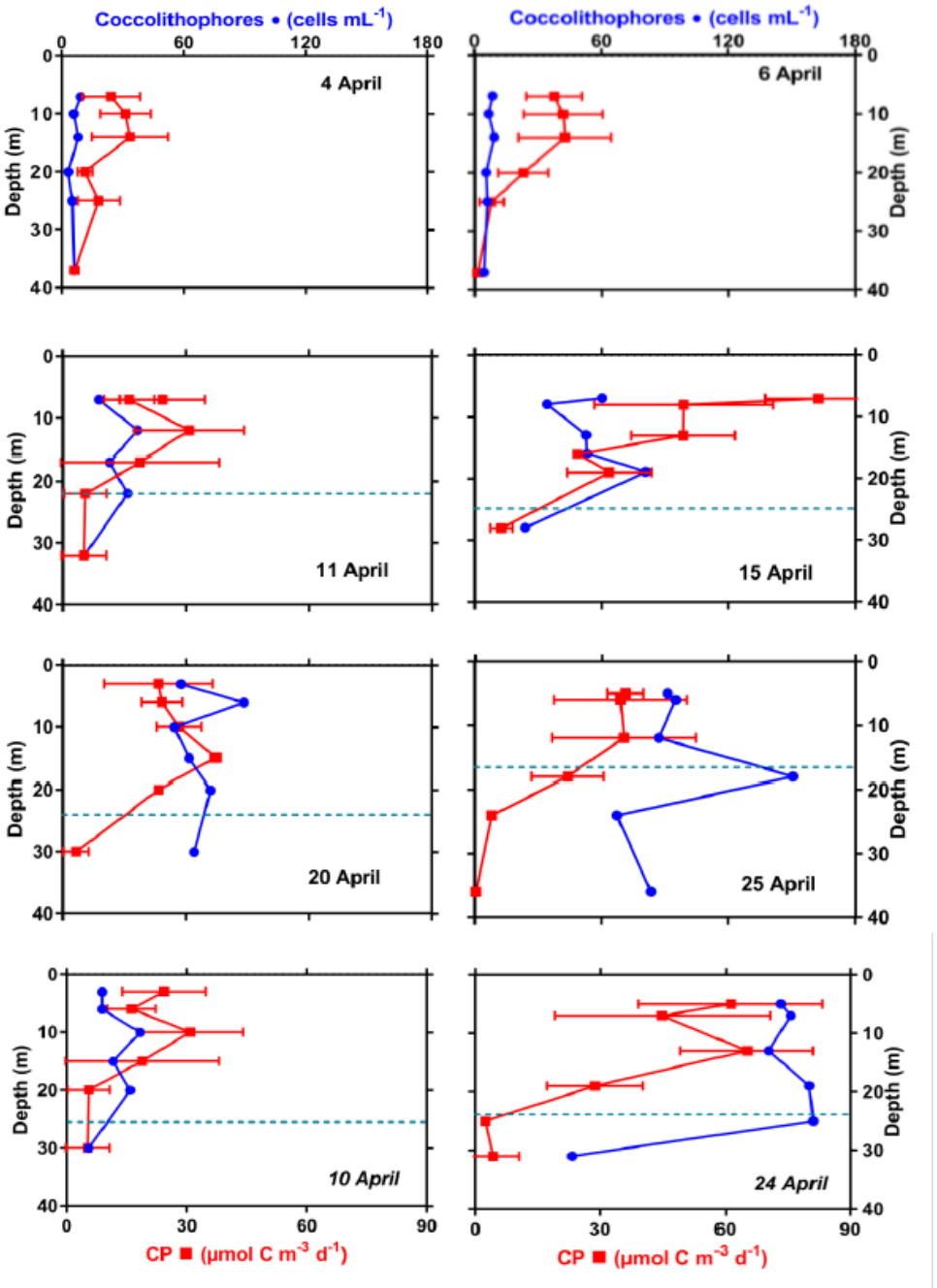


**Figure.3.3**. Vertical profiles of coccolithophore abundance (cells, $mL^{-1}$) and calcite production (CP, µmol C $m^{-3}$ $d^{-1}$) over the euphotic zone at the Central Celtic Sea (CCS) and Shelf Edge (CS2 – italicised dates). Dashed line indicates mixed layer depth.

### 3.4.3 Calcite production and Primary production

Rates of calcite production (CP) sampled at discrete depths within the euphotic zone ranged from 0.7 to 81.3 µmol C $m^{-3}$ $d^{-1}$ at CCS and from 2.4 to 65.2 µmol C $m^{-3}$ $d^{-1}$ at CS2 (Fig. 3.3). Vertical profiles of CP (Fig. 3.3) consistently showed minimum values at the base of the euphotic zone and maximum rates in the upper euphotic zone (aside from a maximum at 15 m at CCS on 20th April). There also appeared to be a declining trend in CP with depth in association with decreasing irradiance, with this decline seen below the MLD (Fig. 3.3). Euphotic zone integrated CP at CCS varied from 0.4 to 1 mmol C $m^{-2}$ $d^{-1}$, with a ratio of CP to PP consistently less than 0.01 (Table 3.2). At station J2, integrated euphotic zone CP was consistently higher (14th April, 10.6 mmol C $m^{-2}$ $d^{-1}$; 27th April, 239.8 mmol C $m^{-2}$ $d^{-1}$) with CP: PP ratios of 0.09 and 0.46, respectively (Table 3.2). Integrated CP showed a similar peak to integrated chlorophyll-*a* on the 15th April (Fig. 3.2b). Normalising CP to coccolithophore cell numbers, to give cell specific CP (Cell-CF; Poulton et al., 2010; Table 3.3, Fig. 3.2c), showed high values in the CCS at the beginning of April (2.0-2.5 pmol C $cell^{-1}$ $d^{-1}$), which declined throughout April to reach a minimum of ~0.4 pmol C $cell^{-1}$ $d^{-1}$ on the 25th (Fig 3.2c).

Euphotic zone integrated primary production (PP) showed a similar temporal trend to integrated chlorophyll-*a* and CP. Integrated PP at CCS ranged from 54.4 to 435.1 mmol C $m^{-2}$ $d^{-1}$, with the peak on the 15th April, the same date as the highest chlorophyll-*a* biomass (Table 3.2). Overall, integrated PP was highest on the 27th April at the site of the *E. huxleyi* bloom (J2; 524.2 mmol C $m^{-2}$ $d^{-1}$), which was a five-fold increase from earlier measurements on the 14th April (112.3 mmol C $m^{-2}$ $d^{-1}$). In contrast to CCS and J2, CS2 had comparatively low integrated PP throughout April (81.1-155.1 mmol C $m^{-2}d^{-1}$).

### 3.4.4 Net growth rate comparison

Net coccolithophore growth experiments were conducted four times at CCS and once at station J2 on the 27th April for 24 h from the 40% PAR depth. On the 11th April net growth rates (NGR) were 0.31 $d^{-1}$ (Table 3.4). On the 15th April coccolithophore NGRs were negative (-0.15 $d^{-1}$), and positive on both the 20$^{th}$ April (0.16 $d^{-1}$) and the 25$^{th}$ April (0.20 $d^{-1}$). During the *E. huxleyi* bloom at J2, coccolithophore NGRs were observed as 0.11 $d^{-1}$ (Table 3.4). At CCS, net growth rates of 0.04 $d^{-1}$ were observed in early April, ~0.20 $d^{-1}$ on the 11th and 15th April and 0.06 $d^{-1}$ at the end of April. At J2 a net growth rate of 0.20 $d^{-1}$ was observed between the 14 and 27 April. This calculation does not take into account advective processes, which likely impacts coccolithophore populations.

**Table 3.3**. Averaged euphotic zone and sampled coccolithophore abundance, relative % abundance of E. huxleyi, calcite production (CP) and cell normalised calcification (Cell-CF) for all sites during DY029, Central Celtic Sea (CCS), shelf edge (CS2) and J2 (± represents standard deviation).

| Sampling site | Day in April | Coccolithophore abundance (cells $mL^{-1}$) | Growth rate between visits ($d^{-1}$) | Relative abundance of *E. huxleyi* (%) | Relative abundance of *C. caudatus* (%) | Other species (%) | Cell-CF (pmol C $cell^{-1}$ $d^{-1}$) |
|---|---|---|---|---|---|---|---|
| CCS | 04-Apr | 6.3 (± 2) | - | 66 (± 12) | 5 (± 3) | 29 (± 10) | 1.7 (± 0.7) |
| CCS | 06-Apr | 6.9 (± 1.9) | 0.04 (±0.02) | 53 (± 13) | 13 (± 9) | 34 (± 5) | 1.7 (± 1.1) |
| CCS | 11-Apr | 23.9 (±10.4) | 0.23 (±0.12) | 49 (± 10) | 27 (± 7) | 24 (± 6) | 0.7 (± 0.4) |
| CCS | 15-Apr | 50.9 (±20) | 0.22 (±0.13) | 54 (±11) | 29 (± 5) | 17 (± 7) | 0.8 (± 0.5) |
| CCS | 20-Apr | 66.4 (± 12.3) | 0.05 (±0.02) | 68 (±7) | 26 (± 6) | 6 (± 2) | 0.4 (± 0.2) |
| CCS | 25-Apr | 95.6 (±28.5) | 0.07 (±0.02) | 76 (± 5) | 21 (± 5) | 2 (± 1) | 0.2 (± 0.2) |
| CS2 | 10-Apr | 40.3 (± 11.8) | - | 60 (± 2) | 10 (± 4) | 30 (± 4) | 0.9 (± 0.8) |
| CS2 | 24-Apr | 134.5 (± 43.9) | 0.09 (±0.04) | 56 (± 7) | 2 (± 1) | 42 (± 8) | 0.2 (± 0.2) |
| J2 | 14-Apr | 155.6 (-) | - | 99 (-) | 0 | 1 (-) | 3.4 (-) |
| J2 | 27-Apr | 1986.1 (±42.5) | 0.18 (±0.00) | 100 (± 0) | 0 | 0 | 3.0 (± 0.1) |

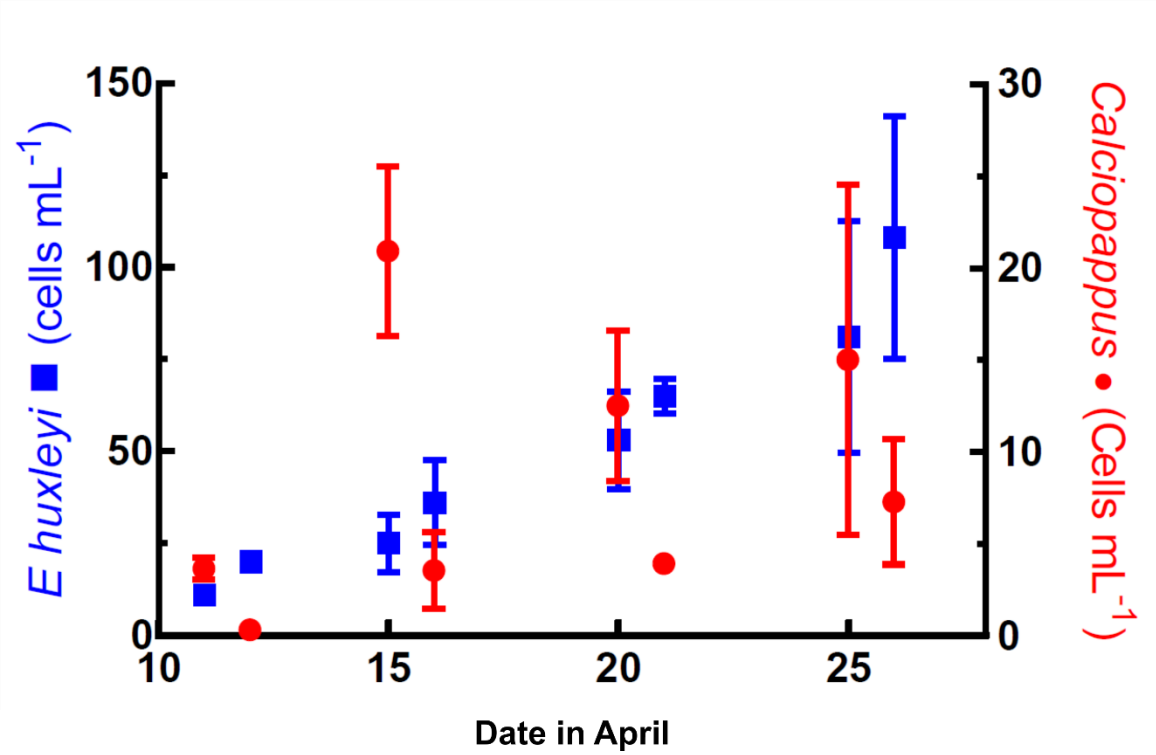


**Fig 3.4.** Cell numbers of *Emiliania huxleyi* (circle) and *Calciopappus caudatus* (squares) from net growth incubation experiments.

**Table 3.4**. Coccolithophore net growth rates and changes in nitrate concentration (µM $d^{-1}$) from incubation experiments. Not determined (ND). * nitrate determined from T24 incubation

| Date in April | Incubation | Coccolithophores (cells $ml^{-1}$) | Growth rate ($d^{-1}$) | ΔNO3 (µM $d^{-1}$) (T0 – T48/2) |
|---|---|---|---|---|
| 11 | T0 | 19.2 (± 0.8) | - | ND |
| | T24 | 26.2 (± 3.7) | 0.31 (±0.05) | ND |
| 15 | T0 | 53.5 (± 12.1) | - | 0.59 |
| | T24 | 46 (± 17) | -0.15 (±0.06) | (1.20 – 0.02) |
| 20 | T0 | 71.9 (± 17.4) | - | 1.15 |
| | T24 | 74.6 (± 4.6) | 0.04 (±0.01) | (2.05 – 0.02) |
| 25 | T0 | 97.8 (± 35.2) | - | 0.20 |
| | T24 | 118.9 (± 29.7) | 0.20 (±0.09) | (0.41 – 0.01) |
| 27 | T0 | 2175.9 (± 145.5) | - | 0.62 |
| | T24 | 2431.5 (± 193.8) | 0.11 (±0.01) | (0.65 – 0.03*) |

### 3.4.5 Growth and mortality rates from dilution experiments

Based on dilution experiments conducted during April all regression slopes were found to be significantly different from zero ($p \leq 0.02$) (Fig. 3.5), apart from on the 4th April at CCS and on the 9th April at CS2, with all other dilution experiments showing a good correlation coefficient for the linear regression ($R^2 \geq 0.44$) (Table 3.5). From all experiments, a positive slope was only encountered at CCS on the 20th April (Fig. 3.5), whilst all others were negative. Due to the negative growth rate also found on 20th April (-0.39 $d^{-1}$), and the violation to the assumptions of the dilution technique (Landry et al., 1995; Landry and Hassett, 1982), we will not comment on this result further. The lack of nutrient addition within the experiments did not appear to negatively impact coccolithophore growth rates, even during late April experiments (see Supplementary Fig. 3.2).

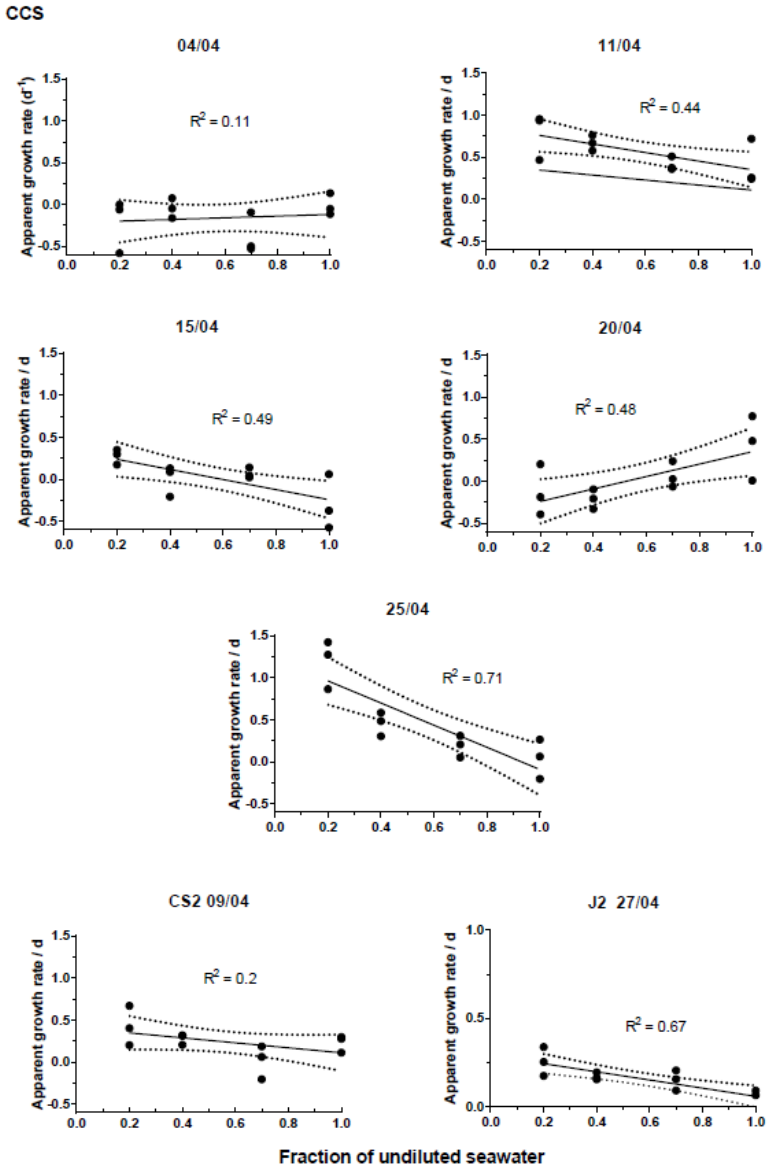

**Figure 3.5.** Plots of the coccolithophore net growth rate ($d^{-1}$) versus dilution factor from microzooplankton (≤63 µm) grazing experiments from the Central Celtic Sea, Shelf Edge (CS2) and J2 during an *E. huxleyi* bloom.

**Table 3.5**. Intrinsic growth (k), grazing mortality (g) and net growth rates of coccolithophores for dilution experiments conducted at CCS, CS2 and J2. * p <0.02 ** p<0.002

| Site | Date in April | Growth *k* ($d^{-1}$) | Grazing *g* ($d^{-1}$) | Net growth rate ($d^{-1}$) | $R^2$ |
|---|---|---|---|---|---|
| CCS | 4 | -0.21 | 0.10 | 0 | 0.02 |
| CCS | 11 | 0.86 | 0.51* | 0.35 | 0.44 |
| CCS | 15 | 0.36 | 0.60* | -0.36 | 0.49 |
| CCS | 20 | -0.39 | 0.74* | 0 | 0.48 |
| CCS | 25 | 1.23 | 1.32** | -0.09 | 0.71 |
| CS2 | 9 | 0.41 | 0.30 | 0.11 | 0.20 |
| J2 | 27 | 0.29 | 0.23** | 0.06 | 0.67 |

Intrinsic (gross) growth rates were variable during spring at CCS (0.0-1.2 $d^{-1}$) with an initial increase on the 11th April (0.86 $d^{-1}$), declining on the 15th April (0.36 $d^{-1}$) and finally peaking again on the 25th April (1.2 $d^{-1}$). Grazing rates of microzooplankton (≤63 µm; due to mesh screening) showed a positive trend throughout spring at CCS, ranging from 0.1 to 1.3 $d^{-1}$ (Table 3.5). The percentage of calcite production consumed in the Celtic Sea ranged from 59 to >100%, with the lowest seen on the 11th April and the highest on the 15th April. Results were not statistically different (F-test) between *E. huxleyi* and total coccolithophores for either intrinsic growth ($p = 0.21$) or mortality ($p = 0.46$) rates, likely due to *E. huxleyi* dominating cell abundances (Table 3.3). The dilution experiment from the 27th April at J2 (*E. huxleyi* bloom) displayed an intrinsic growth rate of 0.29 $d^{-1}$ and a grazing coefficient of 0.23 $d^{-1}$ (Table 3.5), demonstrating high (79%) microzooplankton grazing mortality during this coccolithophore bloom event.

**Table 3.6.** Abundance and net growth rates of microzooplankton (ciliates and dinoflagellates) from dilution experiments conducted at CCS, CS2 and J2. Not determined (ND).

| Site | Date | Experiment time | Microzooplankton (T0) | Ciliates | | Dinoflagellates | |
|---|---|---|---|---|---|---|---|
| | | | Cells ($L^{-1}$) | Cells ($L^{-1}$) | Growth rate ($d^{-1}$) | Cells ($L^{1}$) | Growth rate ($d^{-1}$) |
| CCS | 04 April | T0 | 1610(±335) | 1060 (±320) | -0.35(±0.32) | 550 (±100) | 0.88(±0.59) |
| | | T24 | | 750 (±640) | | 1330 (±860) | |
| | 11 April | T0 | 850(±355) | 470 (±230) | 0.04(±0.03) | 380 (±270) | -0.34(±0.31) |
| | | T24 | | 490 (±220) | | 270 (±160) | |
| | 15 April | T0 | 800(±255) | 300 (±110) | ND | 500 (±230) | ND |
| | | T24 | | ND | | ND | |
| | 25 April | T0 | 280(±160) | 140 (±160) | 1.6(±2.1) | 140 (±0) | 1.7(±0.71) |
| | | T24 | | 690 (±460) | | 770 (±320) | |
| CS2 | 09 April | T0 | 190(±120) | 60 (±80) | 1.58(±2.35) | 130 (±90) | 1.35(±1) |
| | | T24 | | 290 (±190) | | 500 (±130) | |
| J2 | 27 April | T0 | 460(±58) | 150 (±50) | 0.9(±0.4) | 310 (±30) | 0.95(±0.29) |
| | | T24 | | 370 (±110) | | 800 (±230) | |

Microzooplankton abundances (dinoflagellates and ciliates) were determined for all T0 experiments (apart from 20 April) whilst T24 abundances were determined for all aside from experiments conducted on 15 and 20 April (Table 3.6). Abundances of microzooplankton at T0 in the CCS declined from 1610 (± 335) to 280 (± 160) cells L-1 and were 190 (± 120) and 460 (± 58) cells L-1 at the shelf edge and station J2 respectively (Table 3.6). Ciliates and dinoflagellates represented on average 44 (± 13) and 56 (± 13)% of the total abundance in the dilution experiments. The growth rates of ciliates in experiments varied between -0.35 and 1.60 d-1, showing higher values later in April (Table 6). The same trend is observed for dinoflagellates, with growth rates between -0.34 to 1.70 d-1.

## 3.5 Discussion

### 3.5.1 Coccolithophores during spring in the Celtic Sea

Coccolithophores were present at all of the sites sampled within the Celtic Sea during spring. By assuming a chlorophyll-*a* content of 0.34 pg cell$^{-1}$ (the average content for *E. huxleyi*) (Daniels et al., 2014) coccolithophores generally displayed very low estimated contributions to total chlorophyll-*a* (≤2.4%) along with PP (≤1.3%) (Table 3.2). The exception to this pattern was station J2 (18.8% and 30.6% contribution to chlorophyll-*a* and PP respectively), which was the site of an *E. huxleyi* bloom (i.e. cell numbers >1000 mL$^{-1}$) on April 27th, although this date also had low integrated chlorophyll-*a* (45.2 mg m$^{-2}$). This may be due to the relatively low chlorophyll-*a* content of *E. huxleyi* cells (0.2-0.34 pg cell$^{-1}$; Daniels et al., 2014; Paasche, 2002). The cruise average PP contribution of coccolithophores (4.1%) agrees well with the low contribution of coccolithophores to PP reported for the north-west European shelf during June 2011 (<3%; Poulton et al., 2014) and with estimates from other marine environments (see Poulton et al., 2007). This highlights that the biogeochemical importance of coccolithophores during non-bloom conditions does not relate to their organic carbon production (PP), but rather to their inorganic carbon production (CP).

Integrated CP at CCS and CS2 (0.4-1.5 mmol C m$^{-2}$ d$^{-1}$) was similar to other Celtic sea sites sampled in summer 2011 (0.7-1.2 mmol C m$^{-2}$ d$^{-1}$; Poulton et al., 2014) suggesting similar spring to summer calcification rates. Aside from the coccolithophore bloom on the 27th April at J2, measured ratios of CP to PP (0.01-0.09; Table 2) were also similar to other studies of coccolithophores during non-bloom conditions in shelf regions (0.01-0.11; Poulton et al., 2013, 2014). Within the Iceland Basin in summer these ratios were higher (0.10-0.14; Poulton et al., 2010) suggesting that in open ocean regions CP may represent

a greater proportion of fixed carbon than during non-coccolithophore bloom conditions in shelf regions. This is not the case during blooms, such as the one observed at J2 (ratio; 0.46), where CP often represents a significant proportion of fixed carbon (~30-40%; Poulton et al., 2007, 2013). The cruise average integrated CP for April 2015 (1.9 ± 3.3 mmol C $m^{-2}$ $d^{-1}$, excluding the J2 coccolithophore bloom) was similar to the cruise average for a 2011 study around the NW European shelf in summer (2.6 mmol C $m^{-2}$ $d^{-1}$; Poulton et al., 2014), and slightly lower than in non-bloom conditions in the Iceland Basin (3.6 mmol C $m^{-2}d^{-1}$). Our observed lower rate is likely due to the higher cell numbers (100-870 cells $mL^{-1}$) observed in the Iceland Basin (Poulton et al., 2010) than in the Celtic Sea in spring (6.3-134.5 cells $mL^{-1}$).

Integrated CP on the 27th April (240 mmol C $m^{-2}$ $d^{-1}$) was much greater than observed in other *E. huxleyi* blooms, such as the Iceland Basin (9.5 mmol C $m^{-2}$ $d^{-1}$), Patagonian Shelf (4 mmol C $m^{-2}$ $d^{-1}$), or North Sea (11.5 mmol C $m^{-2}$ $d^{-1}$) (Holligan et al., 1993; Marañón and González, 1997; Poulton et al., 2013). The bloom observed by Poulton et al. (2013) on the Patagonian shelf had lower CP despite high cell numbers (up to 2000 cells $mL^{-1}$) due to dominance of the bloom by the low cellular calcite-containing morphotypes (morphotype B/C) of *E. huxleyi* (Poulton et al., 2013), whereas morphotype A dominated in the Celtic Sea in April 2015. The A morphotype of *E. huxleyi* has ~50% more coccolith calcite relative to the B/C morphotype (Poulton et al., 2011, 2010), which may have led to the higher CP observed. This is further supported from cell normalised calcification (cell-CF) rates observed on the Patagonian shelf (0.07-0.65 pmol C $cell^{-1}$ $d^{-1}$) (Poulton et al., 2013) compared to J2 (3 ± 1 pmol C $cell^{-1}$ $d^{-1}$).

Our observations of coccolithophores during spring suggest at the CCS they occupied a primary biogeochemical role in CP, with only small contributions to phytoplankton biomass (chlorophyll-*a*) or PP. The CP of coccolithophore communities can be impacted by the rate at which the populations grow, as well as the composition of the coccolithophore community (Daniels et al., 2016).

### 3.5.2 Coccolithophore growth rates in the Celtic Sea

Net growth rates for coccolithophores based on cell abundances between subsequent site visits during our study (0.04-0.25 $d^{-1}$) were very similar to net growth rates observed from our 24-hour incubation experiments (0.04-0.31 $d^{-1}$) (Table 4). These results compare well to incubation experiments previously conducted on the north-west European shelf (0.2-0.4 $d^{-1}$; Poulton et al., 2014), and net growth rates during a spring bloom in the North Atlantic (0.05-0.13 $d^{-1}$; Daniels et al., 2015). These studies, and our results, also support the observation that coccolithophore populations begin to increase during the spring bloom (Schiebel et al., 2011).

Different species of coccolithophores have been observed to have different net growth rates in culture (Daniels et al., 2014; Gibbs et al., 2013) and natural communities (Daniels et al., 2015, 2016). The net growth rates calculated between site visits for the dominant species in our study (*E. huxleyi* and *C. caudatus*) also differed, with ranges of -0.08 to 0.23 $d^{-1}$ and 0.03 to 0.55 $d^{-1}$, respectively. Not only the range, but also the timing of maximum growth differed. The maximum net growth period observed for *E. huxleyi* was between 6$^{th}$ - 11$^{th}$ April (0.23 $d^{-1}$) and 11$^{th}$ – 15$^{th}$ (0.22$d^{-1}$), whereas for *C. caudatus* it was 4$^{th}$ - 6$^{th}$ April (0.55 $d^{-1}$). A possible explanation for this temporal separation may be that *C. caudatus* is more adapted to the high nutrient-high mixing conditions observed at the beginning of April, a similar high nutrient-low light environment to where it is found in the Arctic Ocean (see Daniels et al., 2016). In contrast, *E. huxleyi* is better adapted to the low nutrient-highly stratified (high light) conditions seen towards late April (Table 3.1), possibly due to *E. huxleyi*'s ability to utilise different sources of nitrogen and a high affinity for phosphate uptake via alkaline phosphatase (Benner and Passow, 2010; Paasche, 2002). Species-specific growth rates during the incubation experiments were highly variable for *E. huxleyi* (0.21 - 0.59 $d^{-1}$) and *C. caudatus* (-0.79 - -2.29 $d^{-1}$) (Fig. 3.4). The only noticeable trend being that *E. huxleyi* always showed positive growth, whilst *C. caudatus* often displayed negative growth rates. It is also possible that *C. caudatus* responds negatively to the artificial environment in incubation experiments, which may also explain why it has yet to be maintained in laboratory culture.

Different species of coccolithophores contain different amounts of calcite, based on the number of coccoliths, the calcite content of individual coccoliths and cell size (Daniels et al., 2016; Young and Ziveri, 2000), and the rates of growth (Daniels et al., 2014; Sheward et al., 2017). The amount of cellular calcite within an *E. huxleyi* cell is approximately 0.52 pmol (Poulton et al., 2010; Daniels et al., 2014), whereas for *C.* caudatus it is estimated at ~0.09 pmol $cell^{-1}$ (Daniels et al., 2016). Hence, even when *C. caudatus* displayed a higher growth rate than *E. huxleyi* it is unlikely to be the dominant calcifier due to its lower cellular calcite quota and cell abundances than *E. huxleyi* (after Daniels et al., 2014). To determine CP per species it is possible to multiply growth rate, species specific calcite content and species specific abundances (Daniels et al., 2014, 2016). Aside from where negative net growth rates were observed, *C. caudatus* showed a $CP_{sp}$ range of 0.05 to 0.27 pmol C $mL^{-1}d^{-1}$, whilst for *E. huxleyi* this range was 1.34 to 3.80 pmol C $mL^{-1}d^{-1}$. However, the decline observed in cell-CF throughout April is likely due to "other" species, such as the larger, and more heavily calcified *Coronosphaera mediterranea* (~9 pmol C $cell^{-1}$ estimated from cell calcite and number of coccoliths per cell; Young and Ziveri, 2000) becoming less abundant (7% contribution to coccolithophore abundance on 4$^{th}$ April and <1% from 20$^{th}$ April onwards).

Rates of coccolithophore calcification can be impacted by many environmental variables, for example within culture experiments *E. huxleyi* calcification has been shown to increase with increasing nutrient and light stress (Paasche, 2002), particularly under phosphorus limitation (Dyhrman et al., 2006). During nutrient replete conditions, *E. huxleyi* cells have a single layer of coccoliths, whilst during nutrient depletion this is seen to increase to multiple layers (Paasche, 2002; Gibbs et al., 2013). However, nitrate and phosphate concentrations were low on 27th April (0.6 and 0.1 µM, respectively), possibly leading to the high rates of calcification. *E. huxleyi* cells sampled from this bloom also displayed multiple layers of coccoliths (see Supplementary Figure 3.1) and a coccolith: cell ratio from SEM images was estimated as ~25 loose coccoliths cell$^{-1}$, further supporting this hypothesis. Detached coccolith:cell ratios have also been used to determine the 'phase' (early, intermediate or late) of coccolithophore blooms, with the ratio increasing over time as the production of coccoliths exceeds rates of cellular division (Poulton et al., 2013). The ratio from the J2 bloom (25 loose coccoliths cell$^{-1}$) suggests sampling activities occurred during the intermediate phase, which appears to be the point of highest calcite production (Poulton et al., 2013). Bloom stage is also likely to be influenced by changing environmental variables, and thus we may have sampled during the time of peak calcite production. This excess calcification is likely the reason for the high cell-CF values observed at station J2.

Additional information about growth dynamics can be gained by comparing net and potential gross growth rates. Intrinsic (gross) growth rates, measured from dilution experiments displayed higher values (0.36-1.23 d$^{-1}$) (Table 5) which are close to reported estimates for cultured species (0.6-2.8 d$^{-1}$; Paasche, 2002). By assuming a maximum growth rate of *E. huxleyi* of 1.6 d$^{-1}$, based on cultures growing in optimum temperature, light and nutrient conditions (Paasche, 2002) we can calculate a growth potential ($u/u_{max}$ *100) for the coccolithophores at CCS. The average growth efficiency was ~30% (range: 10-53%) throughout April at CCS, which is very similar to that reported for the Iceland Basin in non-bloom (coccolithophore) conditions (~33%, range 15-54%; Poulton et al., 2010). This suggests that other factors, such as grazers, may be regulating coccolithophore populations in the Celtic Sea.

### 3.5.3 Top-down control of coccolithophore populations

Grazing on coccolithophores has previously been demonstrated in laboratory settings (e.g. Hansen et al., 1996; Harvey et al., 2015) and bloom communities in the field (e.g. Archer et al., 2001; Fileman et al., 2002; Holligan et al., 1993; Olson and Strom, 2002), but rarely within non-coccolithophore bloom communities. Moreover, many of the open-ocean mortality rates have been estimated using pigment markers (e.g. Fileman et al.,

2002), flow cytometry (e.g. Archer et al., 2001), and size fractionated chlorophyll (e.g. Olson and Strom, 2002) rather than by direct coccolithophore enumeration by microscopy. In this study, microzooplankton grazing on coccolithophores ranged from 0.10 to 1.32 $d^{-1}$, which represented a daily consumption of from 59 to >100% of daily calcite production. These values are similar to the range observed from dilution experiments conducted at coastal Atlantic sites for total phytoplankton (35.5 -100%) and the global average (65%) of microzooplankton-mediated phytoplankton losses (Schmoker et al., 2013). This suggests a strong top-down control in non-bloom conditions on coccolithophore populations.

Non-significant grazing rates based on the dilution regression was observed at CCS on the 4th April, which was likely to be due to the low coccolithophore cell numbers (at $T_0$, 100%: 14 cells $mL^{-1}$; 20%: 4 cells $mL^{-1}$) encountered (see Supplementary Figure 3.2). We therefore suggest that this experiment was not able to detect coccolithophore growth or grazing dynamics due to low prey abundances. On the 25th April an “L” shaped curve was seen, suggesting saturated feeding by microzooplankton (Calbet and Saiz, 2013) towards the end of the spring bloom. A polynomial regression was a better fit to the data from 25$^{th}$ April rather than a linear one ($R^2$ = 0.84 and 0.71 respectively), further supporting a conclusion of a saturated grazer community. This result could also be caused due to alleviation of nutrient limitation via dilution. Hence, the rates observed on this date may be overestimated, though the low net growth rate calculated (-0.09$d^{-1}$) is lower than the net growth rate incubation observed on this date (0.07$d^{-1}$), suggesting it may be due to biological differences.

By removing predators over 63 µm in size we are potentially relieving microzooplankton from (meso-zooplankton) grazer control, which would lead to a change in trophic dynamics of the plankton community (Calbet and Saiz, 2013), and potential overestimation of grazing rates in our experiments. A comparison of net growth rates calculated from dilution experiments and net growth rates from incubation experiments (without a pre-treatment of a 63 µm filter) (Table 3.3,3. 5) shows some differences later in April. These differences imply an increasing importance of complex trophic interactions as the spring bloom progressed (see also Giering et al., 2018), as well as the potential to overestimate grazing rates during late April. Indeed, the biomass of meso-zooplankton (>63 - 500 µm) increased from 1.2 to 1.8 g DW $m^{-2}$ from early to late April (Giering et al., 2018), along with an increasing growth rate, and declining T0 abundance of microzooplankton during late April experiments (Table 6). The trophic positioning of mesozooplankton based on biovolume spectra also displayed an increase from 2.4 – 4.3 from early to late April (Giering et al., 2018). Although it appears we did induce a trophic cascade, and thus the estimates of grazing from the mid to end of April may be overestimated. However, grazing rates on coccolithophores (1.32 $d^{-1}$), were still observed

to be very high. Suggesting even if we corrected for these trophic interactions the grazing rate is still substantial.

The contrast between constant positive accumulation of coccolithophores from subsequent site visits at CCS (Table 3.3) and the negative rates observed in dilution experiments (Table 3.5) brings into question the role of mesozooplankton for coccolithophore populations. The observed negative rates from dilution experiments could be due to the release of grazing pressure on microzooplankton seen and higher mortality rates. However, it raises the possibility that the presence of mesozooplankton could lead to net accumulation of coccolithophores via a trophic cascade (Calbet and Saiz, 2013). Indeed, mesocosm experiments with copepods added displayed an increase in autotrophic nanoflagellate communities (Pree et al., 2016b; Zöllner et al., 2009) supporting this hypothesis. Although, with no mesozooplankton data from station J2 to compare we can only speculate on this result. A greater understanding of trophic dynamics within *E. huxleyi* blooms will allow us to test this hypothesis.

Cellular levels of calcite content (i.e. 'calcification state') of *E. huxleyi* cells has been demonstrated to offer no additional protection against microzooplankton grazing in culture experiments (Harvey et al., 2015). In fact, Harvey et al. (2015) observed ingestion rates ~20% higher for calcified *E. huxleyi* cells compared with non-calcified ('naked') cells, although variability in ingestion rates was more strongly linked to the use of different strains. The growth rate of the dinoflagellate prey was also shown to be reduced by ingestion of calcified cells, and was hypothesised to be due to inhibition of food vacuole digestion of the calcite (Harvey et al., 2015). These observations suggest that, particularly for *E. huxleyi*, calcification does not directly provide protection against instantaneous microzooplankton grazing rates, and rather slows the growth rate of the microzooplankton and hence limits their population development (Harvey et al., 2015). During the J2 *E. huxleyi* bloom, growth rates of microzooplankton (0.9 and 0.95 $d^{-1}$ for ciliates and dinoflagellates respectively) compared to CCS on a similar date (1.6 and 1.7 $d^{-1}$) (Table 3.6) provides limited support to the suggestion of negative effects of calcite ingestion on microzooplankton grazers. However, these were not the lowest microzooplankton growth rates observed in the Celtic Sea (Table 3.6), potentially suggesting that other factors (e.g. prey quantity, environmental conditions) may be involved.

The dilution experiment conducted during the *E. huxleyi* bloom at J2 found that a high proportion (~80%) of daily calcite production (0.29 $d^{-1}$) was grazed (0.23 $d^{-1}$) (Table 3.5). The grazing values from J2 in the Celtic Sea in April are higher than other studies during coccolithophore blooms in the Bering Sea ($\mu$, 0.67 $d^{-1}$; g, 0.14 $d^{-1}$; Olson and Strom, 2002) and the North Sea ($\mu$, 0.69 $d^{-1}$; g, 0.36 $d^{-1}$; Archer et al., 2001), representing losses of 22 and 52% of daily growth, respectively. Both studies observed higher intrinsic growth rates,

possibly suggesting these experiments were conducted in an earlier bloom stage to those experienced at J2. Within the Bering Sea bloom, Olsen and Strom (2002) measured growth and grazing rates using less than 10 µm chlorophyll-*a* (62 ± 21% of total chlorophyll-*a*). This may have led to an underestimation of rates, particularly as *E. huxleyi* blooms have been shown to contain significant chlorophyll-*a* contributions from phytoplankton other than *E. huxleyi* (Poulton et al., 2013; this study). High grazing on *E. huxleyi* has also been observed within the North Atlantic ($\mu$, 0.38 $d^{-1}$, g, 0.74 $d^{-1}$; (Holligan et al., 1993), suggesting during periods of *E. huxleyi* blooms microzooplankton can be major agents of mortality. Although large (potentially dsDNA viruses) were detected, viral mortality was not quantified in this *E. huxleyi* bloom. We believe viral mortality to be similar in all dilutions given the size of the virus (~180nm; Bratbak et al., 1993) and filter size used (0.2 µm).

Both ciliates and dinoflagellates have been observed to graze coccolithophores in culture experiments (Evans and Wilson, 2008; Hansen et al., 1996; Harvey et al., 2015; Kolb and Strom, 2013) suggesting both groups could be responsible for the coccolithophore mortality seen within our study. During *E. huxleyi* blooms ciliates can be a major component of microzooplankton communities (11-51% *Strombidium ovale*; (Archer et al., 2001). However, heterotrophic dinoflagellates can also dominate the microzooplankton biomass within *E. huxleyi* blooms (63% by Gymnodiniales; (Fileman et al., 2002). Throughout an *E. huxleyi* bloom in the Bering Sea, a higher biomass of the large ciliate *Laboea* and the dinoflagellates *Protoperidinium* and *Gyrodinium* were associated with bloom stations (Olson and Strom, 2002). These studies suggest a possible role of microzooplankton composition for *E.* huxleyi populations. A greater understanding of microzooplankton community structure, and the impact of different predators on coccolithophores will help us improve our understanding of coccolithophore bloom dynamics.

We have presented here one of the first set of measurements of microzooplankton grazing (≤63 µm) on coccolithophore populations based on actual cell counts rather than pigment analysis in both coccolithophore bloom and non-bloom conditions. These results indicate that microzooplankton significantly graze coccolithophore populations in shelf seas and exert a strong top-down effect. The results also question whether calcification is an effective grazer deterrent (e.g. Young, 1994; Monteiro et al., 2016), especially in *E. huxleyi* and microzooplankton dominated communities. This study focused on a shelf sea environment in spring, while better understanding of the impact of microzooplankton grazers on coccolithophores requires more measurements from open ocean communities, across seasonal and spatial gradients as well as a direct analysis of grazing rates on coccolithophores by different types of predators.

## 3.6 Conclusions

Low contributions (<2-3%) of coccolithophores towards autotrophic biomass (chlorophyll-a) and primary production during spring in the Celtic Sea implies that coccolithophores have only a minor role in ecosystem dynamics at this time of the year. Rather, the key role for coccolithophores in shelf sea biogeochemistry and carbon cycling is through the production of calcite. Growth rates of coccolithophores varied throughout spring, concurrently with the dynamics of the phytoplankton spring bloom, with generally positive growth rates, particularly for the cosmopolitan *E. huxleyi*. Grazing rates by microzooplankton on coccolithophores were shown to be high (>60% daily calcite production), suggesting a strong top-down control on coccolithophore populations. This calcite will enter microzooplankton food vacuoles, with pH values during digestion of ~3-5 pH units to ensure the enzymes associated with protist digestion working optimally (Gonzalez et al., 1993; Nagata and Kirchman, 1992). Much of the calcite produced in the euphotic zone could therefore undergo rapid dissolution in microzooplankton food vacuoles, with the resulting carbon respired or excreted. However, calcite could also buffer the pH of the vacuoles and slow the digestion (dissolution) process (Harvey et al., 2015). In this case, microzooplankton growth may be negatively impacted (Harvey et al., 2015), and a portion of the ingested material may be excreted and exported to depth. Clearly, a greater understanding of the pathways for the fate of coccolithophore calcite is required to better understand coccolithophore biogeochemistry and their influence on oceanic $CO_2$ fluxes.

# Chapter 4: Chewing on chalk: Is there a role for coccolithophore calcification in protection from microzooplankton grazing?

This chapter is in preparation for publication as: Chewing on chalk: Is there a role for coccolithophore calcification in protection from microzooplankton grazing? Kyle M.J. Mayers[1], Alex J. Poulton[2], Kay Bidle[3], Brittany Schieler[3], Sarah L.C. Giering[4], Seona R. Wells[5], Glen A. Tarran[6], Dan Mayor[4], Thais Bittar[7], Sean R. Anderson[7], Elizabeth L. Harvey[7].

[1] Ocean & Earth Sciences, University of Southampton, Southampton, UK

[2] The Lyell Centre, Heriot-Watt University, Edinburgh, UK

[3] Marine & Coastal Sciences, Rutgers University, New Brunswick, NJ, USA

[4] Ocean Biogeochemistry and Ecosystems, National Oceanography Centre, Southampton, UK

[5] University of Aberdeen, Aberdeen, UK

[6] Plymouth Marine Laboratory, Plymouth, UK

[7] Skidaway Institute of Oceanography at University of Georgia, Savannah, GA, USA

KMJM conducted dilution experiments during the 2017 mesocosm experiment, from the Celtic Sea cruise, also conducted all data analysis, and wrote the manuscript.
BS, GAT and TB provided flow cytometry data, ELH conducted experiments and provided data from 2016 mesocosm experiment. SLCG and SRW conducted dilution experiments during Celtic Sea cruise with some assistance from KMJM. KB, BS,TB, SRA and ELH were involved in the 2017 Mesocosm experiments.

AJP and ELH provided feedback on the manuscript.

## 4.1 Abstract

The species *Emiliania huxleyi* is considered the most cosmopolitan and numerically dominant coccolithophore in the modern ocean. This species is biogeochemically important as it is able to form extensive blooms at temperate latitudes, contributes to the production of the gas dimethylsulphide and enhances carbon export through the production and deep-sea flux of calcium carbonate plates ('coccoliths'). One hypothesis for the evolution and function of these coccoliths is as protection against ingestion by microzooplankton (<200 µm) grazers. Here, we analyse data from 53 dilution experiments from the coastal North Atlantic oceanic region, where grazing and growth rates for *E. huxleyi* have been measured, and compare them to similar rates for other phytoplankton groups within the same assemblage. The median of grazing to growth ratios for *E. huxleyi* (0.63 ± 0.47) was not significantly (Kolmogorov-Smirnov *p* value = 0.37) different from nanoeukaryotes (0.89 ± 0.43) or picoeukaryotes (0.52 ± 0.32), but was significantly higher than for *Synechococcus* spp. (0.33 ± 0.33). This demonstrates that ~60% of coccolithophore production was grazed by microzooplankton. The relative proportion of *E.huxleyi* biomass to the phytoplankton community appeared to show no relationship with community grazing rate. This data suggest that coccoliths do not provide *E. huxleyi* with efficient protection against microzooplankton ingestion rates, and that they are grazed at similar rates to other phytoplankton groups. This has significant implications for the population dynamics of *E. huxleyi*, and possible bloom formation mechanisms, along with the fate of grazed calcite within the upper euphotic layers of the ocean.

## 4.2 Introduction

Coccolithophores are single celled eukaryotic phytoplankton, which are unique in that they produce an exoskeleton composed of calcium carbonate plates, known as coccoliths. Coccolithophores play important roles in the marine carbon cycle through the production and export of these coccoliths, with their formation altering the air-sea flux of $CO_2$ and they may also act as ballast material for sinking organic matter (Bach et al., 2016; Klaas and Archer, 2002).

One of the most prevalent coccolithophore species is *Emiliania huxleyi*, which is present in almost all oceanic regions and is able to form extensive blooms in shelf regions. This species can be responsible for up to 40% of carbon production (Poulton et al., 2007; Mayers et al., 2018) and are strong producers of the osmolyte dimethylsulfoniopropionate (DMSP), which cleaves to produce the gas dimethyl sulphide (DMS) the main natural source of atmospheric sulphur (Malin et al., 1993).

Despite their ecological importance, a clear evolutionary and ecological mechanism for coccolith formation is still not yet fully resolved. Many theories have been suggested (see Monteiro et al., 2016 for a recent review), including concentrating light, as an energy 'dump', buoyancy control, protection against viral and bacterial attack, and as a defence mechanism against microzooplankton grazers. Microzooplankton are small grazers (20 - 200 µm) which are responsible for consuming an average of ~64% of primary production in the oceans each day (Calbet and Landry, 2004; Schmoker et al., 2013). They primarily consist of dinoflagellates and ciliates.

Within the laboratory, experimental data have shown no evidence that calcification in *E.huxleyi* provides protection against ingestion by heterotrophic dinoflagellates (Harvey et al., 2015; Strom et al., 2017). However, Harvey et al. (2015) showed that calcified *E.huxleyi* could slow the growth rate of the predator, possibly due to the presence of a calcite shell. Previously, there has been some evidence that during *E. huxleyi* blooms there appears to be a depression in the overall community level grazing rates (measured as chlorophyll-*a* rather than *E. huxleyi* cells) in the Bering and Celtic Seas (Fileman et al., 2002; Olson and Strom, 2002). For field experiments, there is limited evidence that *E.huxleyi* is selectively grazed on, with one experiment demonstrating this for the North Atlantic (Holligan et al., 1993), and high grazing rates observed in non-bloom conditions on the north-west European shelf (Mayers et al., 2018; Chapter 3).

Prey selectivity within plankton communities can be estimated using the Chesson-Manly selection index (Manly, 1974; Chesson, 1978, 1983). This index measures if there is an imbalance between the proportion of prey in the predator's diet and the proportion of the same prey within the environment. Selectivity within phytoplankton could be based on factors such as prey size, motility, nutritional value or chemical cues (Verity, 1988; Muller and Schlegel, 1999). This index has been used in marine planktonic communities to investigate prey selectivity of copepods (Nejstgaard et al., 1997) and microzooplankton (both ciliates and dinoflagellates) (Evans and Wilson, 2008; Loder et al., 2011). Other measures of prey selectivity include Strauss's linear index (Strauss, 1979), which compares observed vs expected frequencies in the diet compared with environmental proportions. This method has previously been applied to coral communities (Bonaldo and Hay, 2014) but not to those of phytoplankton. However, we consider both methodologies within this study to attempt to elucidate possible microzooplankton prey selectivity.

In this study, a meta-analysis was conducted of dilution experiments primarily performed during mesocosm experiments in Bergen, Norway and from a cruise on the north-west European Shelf (Celtic Sea) during spring 2015 (see Mayers et al., 2018; Chapter 3). The main aim was to investigate whether there are statistically different grazing rates on coccolithophores relative to other phytoplankton groups from the same community,

including the similarly sized (2-20 µm), but non calcified nano-eukaryotes (including haptophytes, cryptophytes, chlorophytes). Secondly, the data were examined to observe if there was a decline in predator growth rate with high *E. huxleyi* relative abundance in the environment. These results provide information how microzooplankton may regulate *E.huxleyi* population dynamics, the fate of coccolithophore calcium carbonate, and the possible evolutionary role of calcification.

## 4.3 Materials and methods

The majority of the data used in this study (*n* = 48) are from experiments conducted with mesocosms in 2016 and 2017, whilst a smaller sub-set (*n* = 5) are from experiments conducted during a cruise to the UK Shelf Sea (Celtic Sea).

### 4.3.1 Mesocosm set-up

Mesocosm experiments were conducted at the Espegrend Marine Biological Field Station in Raunefjorden near Bergen, Norway (60°22.1'N, 5°28.1'E). In 2016, 9 floating KOSMOS (Kiel Off-Shore Mesocosms for future Ocean Simulations; Riebesell et al., 2013), 4 with altered $CO_2$ concentrations, were set up and monitored for 50 days. In 2017, 12 bags were filled from the surrounding fjord, with 4 experimental treatments (3 bags each). These treatments were; replete inorganic nutrients (16 µM and 1 µM of nitrate and phosphate added respectively), shaded (nutrients as in the replete bags but with a shaded screen placed on day 10 of the experiment to reduce surface Photosynthetically Active Radiation (PAR) to 1%), low phosphorus (same nitrate as replete bags and minor phosphorus addition to a 60:1 N:P ratio), and ambient which had no nutrient manipulation. Following nutrient additions to the relevant bags, all 12 bags were bubbled with ambient air for two days before air pumps were removed. Experiments to estimate phytoplankton growth and microzooplankton grazing rates were conducted every two days for 18 days in both 2016 and 2017.

### 4.3.2 Dilution experiments

Phytoplankton growth and microzooplankton grazing rates were estimated using the dilution method (Landry et al., 1995; Landry and Hassett, 1982). A slightly modified version of this method was used, with only one low dilution level (20%) and an undiluted treatment used (Morison and Menden-Deuer, 2017, 2015). Rates calculated using this method are considered accurate but conservative compared with those using multiple dilution levels and a linear regression, furthermore any nonlinear responses in grazing rates have been shown to not bias the reliability of the rate estimates (Morison and

Menden-Deuer, 2017). All dilution experiments conducted in 2016 and 2017 had the same experimental set-up.

In 2016, experiments were conducted during days 19 to 31 of the experiment. Water was collected using a depth integrated water sampler (IWS, HYDRO-BIOS, Kiel). During 2017, water was collected from ~1 m depth using a 10 L Niskin bottle, and equal volumes of water were pooled from the triplicate mesocosm bags. During both years, larger mesozooplankton were removed from the collected seawater by screening all water through 200 µm Nitex mesh into clean carboys. The collected water was then shaded with black plastic and returned to shore. Mixing of the dilutions and partitioning into incubation bottles occurred in a temperature-controlled room, set to ambient water temperature (± 1$^{o}$C). Grazer-free diluent (FSW) was prepared by gravity-filtering whole seawater (WSW) through a 0.45 µm inline filter (PALL Acropak™ Supor® membrane capsule) into a clean carboy, to ensure passage of viruses. To the grazer-free diluent, WSW was added at a proportion of 20%. The 20% dilution and 100% WSW treatments were prepared in single carboys and then siphoned into triplicate 1.2 L Nalgene™ incubation bottles. To control for nutrient limitation, additional triplicate bottles of 100% WSW were incubated with added nutrients (10 µM nitrate and 1 µM phosphate to ensure replete conditions). The 1.2 L incubation bottles were incubated for 24 h in an outdoor tank maintained at *in-situ* surface temperatures through a flow-through system of ambient seawater. Bottles were allowed to freely float around and the seawater inflow caused gentle agitation throughout the 24 h period. A screen was used to mimic light conditions at ~1 m depth, this was verified using a HOBO data logger (Onset).

Dilution experiments conducted on board the RRS Discovery within the Celtic Sea were set up as described in Mayers et al. (2018; Chapter 3). Briefly, seawater samples were collected from 5 to 10 m and filtered through a 63 µm mesh into 10 L clean carboys. We made FSW by gravity filtering water through a 0.2 µm cartridge filter (PALL Acropak™ Supor® membrane capsule). Sequential dilutions were set up of 100, 70, 40 and 20% WSW, samples were gently agitated prior to sampling to ensure they were well mixed. For these experiments, nutrients were not added as nutrient levels remained replete through most of the sampling period (see Mayers et al., 2018; Chapter 3). For each experiment, twelve 3 L glass jars were filled with seawater dilutions (triplicates of each dilution) and incubated for 24 h in a controlled temperature refrigeration container with artificial lighting provided by LED panels (Powerpax, UK) and neutral density filters (Lee Filters™, UK) to replicate the daily light regime at the collection depth.

### 4.3.3 Chlorophyll-*a* and phytoplankton population counts

For the mesocosms, water for the measurement of chlorophyll-*a* concentration (150 mL) was filtered under low vacuum pressure through Whatman GF/F filters (effective pore size 0.7 µm) and then extracted in vials containing 6 mL of 95% ethanol, at room temperature in the dark for 12 to 15 h. All chlorophyll readings were conducted on a Turner TD700 fluorometer (Jespersen and Christoffersen 1987, Graff and Rynearson, 2011). Ethanol blanks were included, and all samples were corrected for phaeophytin using a drop of 10% hydrochloric acid and then reading the sample again.

For experiments conducted in the Celtic Sea, samples for chlorophyll-*a* concentration, flow cytometry, and coccolithophore enumeration were taken at T0 and after 24 hours (T24). Water for chlorophyll-*a* (200-250 mL) was gently filtered onto Whatman GF/F filtersand extracted in 6 to 10 mL 90% acetone (HPLC grade, Sigma-Aldrich, UK) at 4$^{o}$C for 18 to 24 h (Poulton et al., 2014). Chlorophyll readings were taken on a Turner Designs Trilogy fluorometer using a non-acidification method and calibrated with a solid standard and pure chlorophyll-*a* standard (Sigma-Aldrich, UK).

Samples for phytoplankton biomass via flow cytometry were treated differently between mesocosm experiments in 2016 and 2017. In 2016, samples were enumerated using a BD Accuri™ flow cytometer with a C6 auto-sampler, and data were analysed using the BD Accuri™ C6 software. Water samples for each bottle at T24, and in triplicate from T0 were pre-filtered through a 45 µm mesh and run for 6 to 7 min at a low flow rate (35 µL min$^{-1}$). Events that triggered the forward scatter threshold value were recorded. The sample introduction probe was washed and samples agitated between each sample run. All events with red autofluoresence (692 nm) above 3,000 (the background level of fluorescent particles present in de-ionised water and sheath fluid) were considered phytoplankton. Nanoeukaryotes (>2 µm) and picoeukaryotes (<2 µm) were determined based on their forward scatter signal relative to 3 µm calibration beads. *Synechococcus* was defined as events that fell as picoeukaryotes but displayed orange fluorescence (585 nm). *Emiliania huxleyi* was determined as events that fell into nanuoeukaryotes but displayed an elevated side scatter (SSC) due to the presence of calcium carbonate coccoliths (Fig 4.1). Sphero™ rainbow calibration beads (3 µm, 8-peak) were run as daily quality control.

In 2017, phytoplankton were enumerated on samples fixed in <1% glutaraldehyde (final concentration). For each bottle at T24, and in triplicate from T0, 5 mL of sample was taken and screened through a 40 µm mesh (to remove larger organisms and particles) into a cryovial, and preserved in glutaraldehyde. Then, 250 µL of this preserved sample was added to a 96-well plate and analysed on a Guava EasyCyte HT (Millipore) flow

cytometer. Samples were differentiated into 4 groups; picoeukaryotes, nanoeukaryotes, *E.huxleyi*, and *Synechococcus* based on forward and side scatter (for size, and calcification), chlorophyll-*a* fluoresence and orange fluoresence for *Synechococcus*. Example flow cytometry plots are shown in Fig 4.1.

For the research cruise, samples for flow cytometry were collected in clean 250 mL polycarbonate bottles and analysed using a Becton-Dickinson FACSort instrument (Tarran et al., 2006). Samples for coccolithophore enumeration were sampled as described in Poulton et al. (2010) and Mayers et al. (2018; Chapter 3). Briefly, 250 mL of water from T0 and T24 of dilution experiments was gently filtered onto 0.8 µm cellulose nitrate filters. Permanent slides of the filters were prepared by mounting the filters using low viscosity Norland Optical adhesive 074. Samples were analysed under cross-polarized light using an Olympus BX51 (x1000 oil immersion). Either 300 individual cells, or 300 fields of view (whichever was reached first) were counted, with a minimum of 50 fields of view. Cell numbers were calculated based on the area of the filter examined, cells counted and volume filtered. Full coccospheres (including *E. huxleyi*) were identified following the taxonomy of Frada et al. (2010).

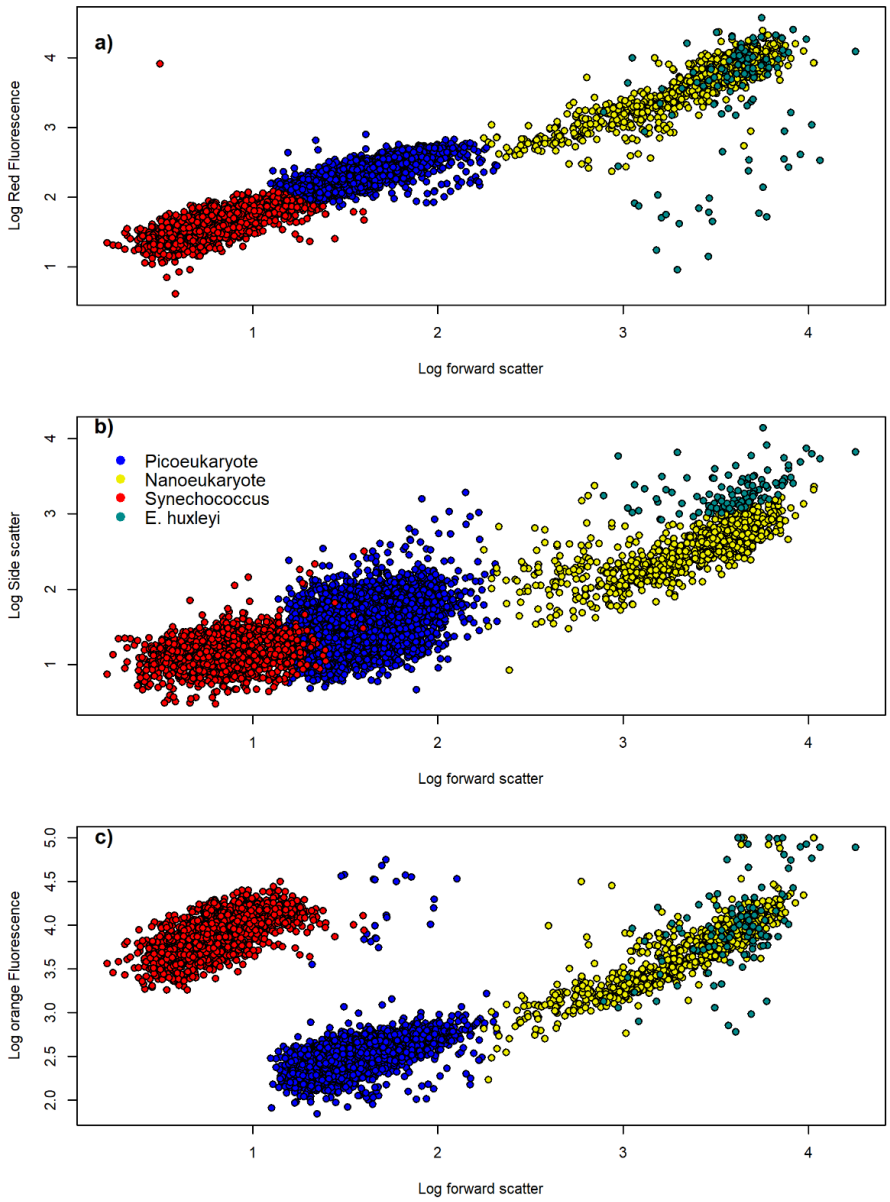


**Figure 4.1.** Flow cytometry plot showing individual events against log forward scatter and log red fluorescence (a), log forward scatter against log side scatter (b), and log forward scatter against log orange fluorescence (c).

For studies conducted during mesocosm experiments, the apparent growth rates (*k*, $d^{-1}$) were calculated using the equation:

$$k = 1/t \ln(C_t - C_o) \qquad \text{(Equation 1)}$$

where t = incubation time in days, $C_t$ and $C_o$ are the final and initial concentrations of chlorophyll-*a* or cell counts, respectively.

Grazing and growth rates were calculated as in Morison and Menden-Deuer (2017). Grazing (*g*, $d^{-1}$) rates were calculated as:

$$g = (k_d - k_{1+N}) / (1 - x) \qquad \text{(Equation 2)}$$

where, $k_d$ is the average growth rate in the diluted (20% WSW) treatment, and $x$ is the fraction of WSW, and $k_{1+N}$ is the growth rate in 100% WSW with added nutrients (i.e. the growth rate in the absence of nutrient-limited mortality). Once grazing rates were calculated, the intrinsic growth rate ($\mu$) is calculated with $k_1$, the growth rate without nutrients added (the estimated true net growth rate) as:

$$\mu = g + k_1 \qquad \text{(Equation 3)}$$

For Celtic Sea samples, growth rates were calculated as in equation 3. Changes in coccolithophore cell numbers, measured by cross-polarized light microscopy (see Section 2.2) were used to calculate apparent growth rates, assuming:

$$NGR = k - cg = \frac{1}{t} LN \left(\frac{Pt}{Po}\right) \qquad \text{(Equation 4)}$$

where P0 and Pt are the initial and final cell numbers, $k$ is the intrinsic growth rate of coccolithophores (Y-intercept), $g$ is the coefficient of grazing mortality (the slope of the linear regression) and $c$ is the dilution factor (1, 0.7, 0.4, and 0.2) (Landry and Hassett, 1982; Landry et al., 1995). There was no significant difference of intrinsic growth or grazing rates when using the two or four-point method (F-test = 0.93 and 0.99, respectively).

### 4.3.4 Data processing and statistical analysis

Our data set consists of 530 rate measurements of different phytoplankton groups. Similar to previous studies that compared a compilation of microzooplankton grazing rates (Calbet and Landry, 2004; Schmoker et al., 2013), negative grazing rates were adjusted to 0.00 $d^{-1}$ ($n$ = 54) and negative growth rates to 0.01 $d^{-1}$ ($n$ = 48) to avoid dividing by negative numbers and skewing the data towards zero. Grazing to growth rate ratios ($g$:$\mu$) were calculated as a proxy for the fraction of production consumed for each phytoplankton group. The $g$:$\mu$ ratios were arctangent transformed, which reduces the impact of large ratios on averages and makes the data more normally distributed (as in Calbet and Landry, 2004). The arctangent medians and median absolute deviations were then converted back to percent consumed using the tangent function. To test for differences between growth and grazing rates, and in $g$:$\mu$ ratios between different phytoplankton groups, pairwise two-sided Kolmogorov-Smirnov tests were conducted using R (v. 3.3.2) (R Core Team, 2015).

Although this paper has experiments conducted under a variety of different environmental parameters and manipulations, using a like for like comparison where possible, I reduced

the influence of potential biases due to environmental differences. Cell abundances from flow cytometry and microscopy counts (for *E. huxleyi* on the shelf sea) were converted to biomass using literature values for organic carbon (Tarran et al., 2006): for *Synechococcus* (8.58 fmol C cell$^{-1}$), picoeukaryotes (36.67 fmol C cell$^{-1}$) and nanoeukaryotes (0.76 pmol C cell$^{-1}$). A conversion factor for the organic component of *E.huxleyi* was used (0.68 pmol C cell$^{-1}$) (Harvey et al., 2015), assuming microzooplankton are not able to assimilate the inorganic carbon (calcite) fraction.

The Chesson-Manly selection index (Manly, 1974; Chesson, 1978, 1983) relates the proportion of a food group grazed to the proportion of that food group in the environment (community). It was calculated as:

$$\alpha 1 = \frac{ri \,/\, pi}{\sum_{i=1}^{n} ri \,/\, pi} \qquad \text{(Equation 5)}$$

Where *ri* is the relative abundance of food in the diet (determined as *g*:*μ* ratio) and *pi* is the relative abundance of food in the environment. The α is a function of the forage ratio (*ri / pi)*. Strauss's Linear index (Li) is also a food selectivity index, however does not factor in the rest of the community (Strauss, 1979), it is calculated as:

$$Li = ri - pi \qquad \text{(Equation 6)}$$

To test for significant differences between values of Chesson-Manly and Strauss-Linear indices, two-sided Kolmogorov-Smirnov were calculated as above.

## 4.4 Results

### 4.4.1 Phytoplankton community grazing impact

Using chlorophyll-*a* as a measure of community-level change, microzooplankton grazing rates ranged from 0.0 to 0.80 d$^{-1}$, whereas growth rates ranged from 0.01 to 0.82 d$^{-1}$ (Fig 4.2a). Grazing rates were found to be higher than growth rates in only 15% of experiments, and all the events occurred during the 2016 mesocosm experiment (except for one result in 2017). Interestingly, there was no significant relationship between the grazing rate derived from chlorophyll-*a* measurements and the proportion of *E. huxleyi* biomass found in the population ($R^2$ = < 0.001; Fig 4.2b), suggesting that *E. huxleyi* relative abundance does not negatively affect community level grazing rates. This lack of a relationship is also observed between grazing rates on different phytoplankton groups and proportion of *E. huxleyi* in the population (Supplementary Figure 4.1).

### 4.4.2 Phytoplankton group specific growth and mortality rates

Growth and grazing rates on different phytoplankton groups were much more variable than for chlorophyll-*a* (Fig 3a). Though there was a generally positive relationship between growth and mortality rates for all the phytoplankton groups (linear equation, y = 0.04 + 0.67x, $p < 0.001$, $n = 192$). The highest observed rates were generally seen for nanoeukaryotes (>3 $d^{-1}$), *E. huxleyi* and picoeukaryotes (2-3 $d^{-1}$). A large majority of paired rate measurements ($n = 159$) cluster within the less than 1 $d^{-1}$ range in the bottom left of the plot (Fig. 4.3a).

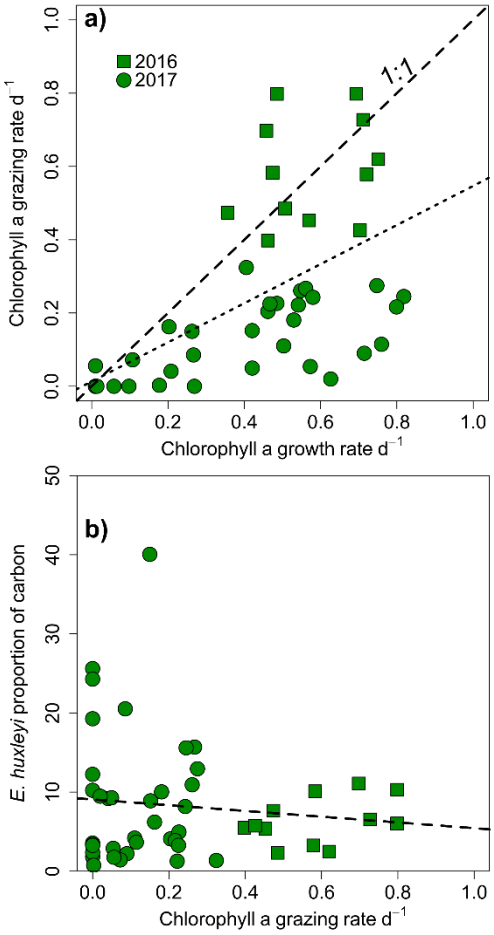

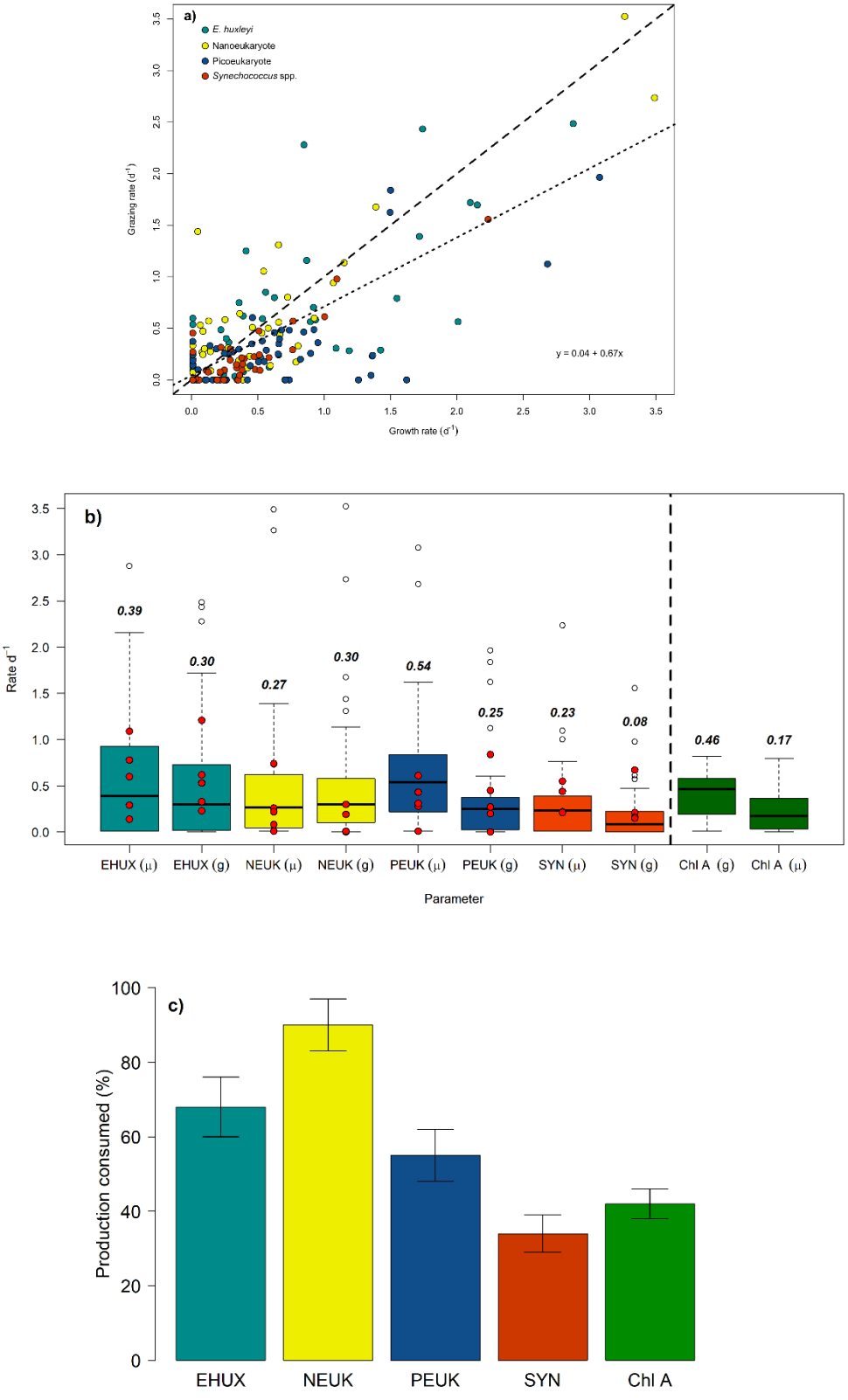


**Figure 4.3:** Growth and grazing rates ($d^{-1}$) from all mesocosm experiments (3a), dashed line is the 1:1 line, dotted line is the linear regression between growth and grazing rates, box plots of growth and mortality rates ($d^{-1}$) (3b), the red dots overlaid are samples from the Celtic Sea, bold and italicised text represents median values. White points represent

outliers of the data set. Average proportion of daily production consumed (%) of each phytoplankton group (3c), error bars represent standard errors of the data set (*n* = 48 for all phytoplankton groups). EHUX = *E. huxleyi*, NEUK = nanoeukaryote, PEUK = picoeukaryote, SYN = *Synechococcus* spp and Chl A = chlorophyll a

Due to the large spread of observed rate measurements, we present these as box and whisker plots of median and quartile ranges (Fig. 3b), with the overlaid red dots samples from the cruise during spring in the Celtic Sea. The cruise data overlay generally quite well with the observed mesocosm data, suggesting that mesocosms are representative of growth and mortality dynamics occurring within the natural environment. The largest median growth rates were observed for picoeukaryotes (0.54 $d^{-1}$), chlorophyll-*a* (0.46 $d^{-1}$) and *E. huxleyi* (0.39 $d^{-1}$), whilst the lowest were for *Synechococcus* (0.23 $d^{-1}$) and nanoeukaryotes (0.27 $d^{-1}$). In terms of grazing rates, the largest estimated means were for nanoeukaryotes and *E. huxleyi* (0.3 $d^{-1}$ for both), closely followed by picoeukaryotes (0.25 $d^{-1}$). The lowest rates were again observed for *Synechococcus* (0.08 $d^{-1}$). Chlorophyll-*a* growth and grazing rates were similar to those for the main phytoplankton groups (0.46 $d^{-1}$ and 0.17 $d^{-1}$).

Using a two-sided Kolmogorov-Smirnov (K-S) test, we tested for nonparametric differences in the distributions of growth and grazing rates between different groups. For growth rates, significant differences were only found between *E. huxleyi* and *Synechococcus* ($p$ = 0.01), and between picoeukaryotes and *Synechococcus* ($p$ = 0.001). For grazing rates, all groups displayed significant differences ($p$ = <0.02), except for between nano- and pico-eukaryotes ($p$ = 0.1), and *E. huxleyi* and nanoeukaryotes ($p$ = 0.85).

The average amount of production consumed (estimated from the average $g:\mu$ ratios) was highest for nanoeukaryotes (90 ± 7%), followed by *E. huxleyi* (68 ± 8%) (Fig 4.3c). The lowest values were reported for *Synechococcus* (34 ± 5%) and chlorophyll-*a* (42 ± 4%), with picoeukaryote consumption slightly higher (55 ± 7%). By transforming $g:\mu$ ratios into their arctangent values we can reduce the impact of large ratios (Fig. 4.4). The median $g:\mu$ (± median absolute deviation) is highest for nanoeukaryotes (0.89 ± 0.43), showing that almost 100% of daily production is consumed by microzooplankton grazers on this phytoplankton group. For *E. huxleyi*, the median ratio is slightly lower (0.63 ± 0.47), but still suggests that ~60% of daily production is consumed. For picoeukaryotes, the median ratio (0.52 ± 0.32) suggests ~50% daily production is consumed. The lowest observed median ratio (0.33 ± 0.33) is for *Synechococcus*, closely followed by chlorophyll-*a* (0.39 ± 0.19).

A two-sided K-S test displayed significant differences for *g:μ* ratios between *E. huxleyi* and *Synechococcus* ($p$ = 0.01), and *E. huxleyi* and chlorophyll-*a* ($p$ = 0.005) (Table 4.1). Nanoeukaryotes were significantly different ($p$ = 0.02 - < 0.001) from all phytoplankton groups except for *E. huxleyi* ($p$ = 0.37). Picoeukaryotes were not significantly different from *Synechococcus* spp. ($p$ = 0.06). These results suggest that there is no statistically significant difference in the proportion consumed between *E. huxleyi* and the similarly sized nanoeukaryote or picoeukaryote populations, and that differences are mainly between chlorophyll-*a* and *Synechococcus* spp.

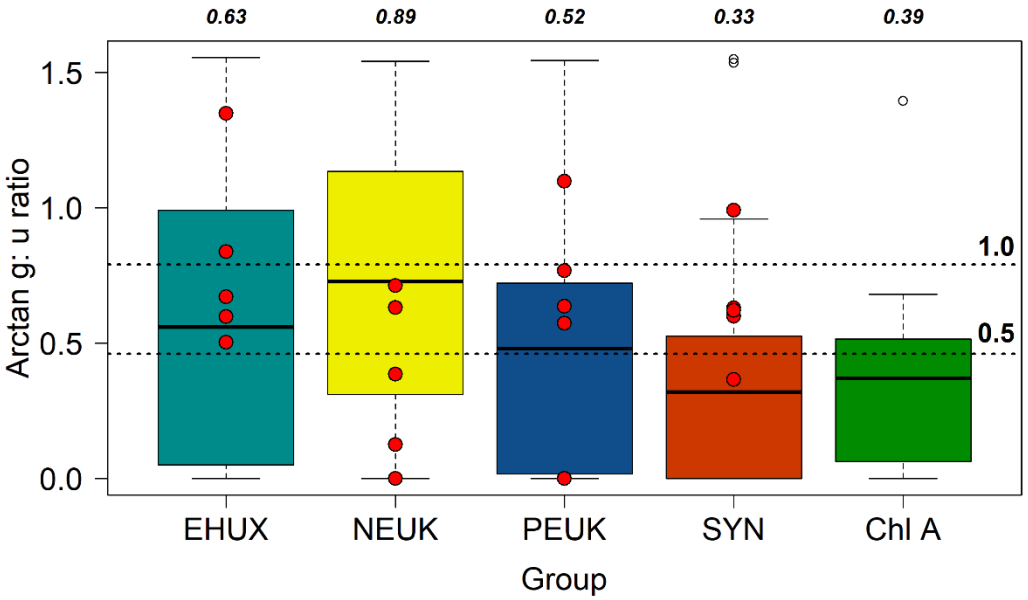


**Figure 4.4.** Box plots of arctangent *g*:μ ratios of the different phytoplankton groups. Red points are samples from the Celtic Sea. White points represent outliers of the data set. Dashed lines labelled as 1.0 and 0.5 represent 100 and 50% of daily growth consumed by grazers, respectively. Bold italicised values are median values converted back from arctangent values using the tangent($x$) function.

**Table 4.1:** *p*-values from a two-sided Kolmogorov-Smirnov test of *g:μ* ratios between different phytoplankton groups. Bold values indicate significant differences ($p < 0.05$).

| | *E. huxleyi* | NEUK | PEUK | SYN | Chlorophyll-*a* |
|---|---|---|---|---|---|
| *E. huxleyi* | - | 0.37 | 0.37 | **0.01** | **0.005** |
| NEUK | | - | **0.02** | **< 0.001** | **< 0.001** |
| PEUK | | | - | 0.16 | 0.06 |
| SYN | | | | - | 0.37 |
| Chlorophyll-*a* | | | | | - |

### 4.4.3 Selective grazing

To gain a better understanding on whether a particular phytoplankton group is grazed preferentially, we can use one of two indices: the Chesson-Manly (CM) or Strauss Linear (Li) index. Both of these relate the proportion of a food group grazed, to the proportion of that food group observed in the environment (community). The CM index assumes neutral grazing is 1/*n* (Manly, 1974; Chesson, 1978, 1983), where *n* is the number of food groups present (which in our case is 4), whilst the Li index assumes neutral grazing is equal to zero (Strauss, 1979).

The median values for the different phytoplankton groups using the CM index are highest for nanoeukaryotes (0.3), lowest for *Synechococcus* (0.13), and similar for *E. huxleyi* and picoeukaryotes (0.25 and 0.24 respectively) (Fig. 4.5). These results suggest that nanoeukaryotes are preferentially selected for, whilst *Synechococcus* is selected against by microzooplankton grazers. For *E. huxleyi* and picoeukaryotes, Fig 4.5 suggests that the grazing rates observed are density-dependent.

The difference between CM indices, using a two-sided K-S test, were only significant between *Synechococcus* and all other phytoplankton groups ($p = <0.01$) (Table 4.2). The overlaid points from the Celtic Sea cruise fall in the upper and lower ranges for *Synechococcus* and nanoeukaryotes, respectively. The Li indices displayed a median indicating neutral grazing for *Synechococcus* (-0.2), slightly selective grazing on nanoeukaryotes (2.0), and slight grazing avoidance in *E. huxleyi* and picoeukaryotes (-1.3 and -1.8 respectively) (Figure 4.6). These results were significantly different between all groups (K-S test, $p < 0.05$), aside from *E. huxleyi* and picoeukaryotes (K-S test, $p = 0.83$; see Table 4.3).

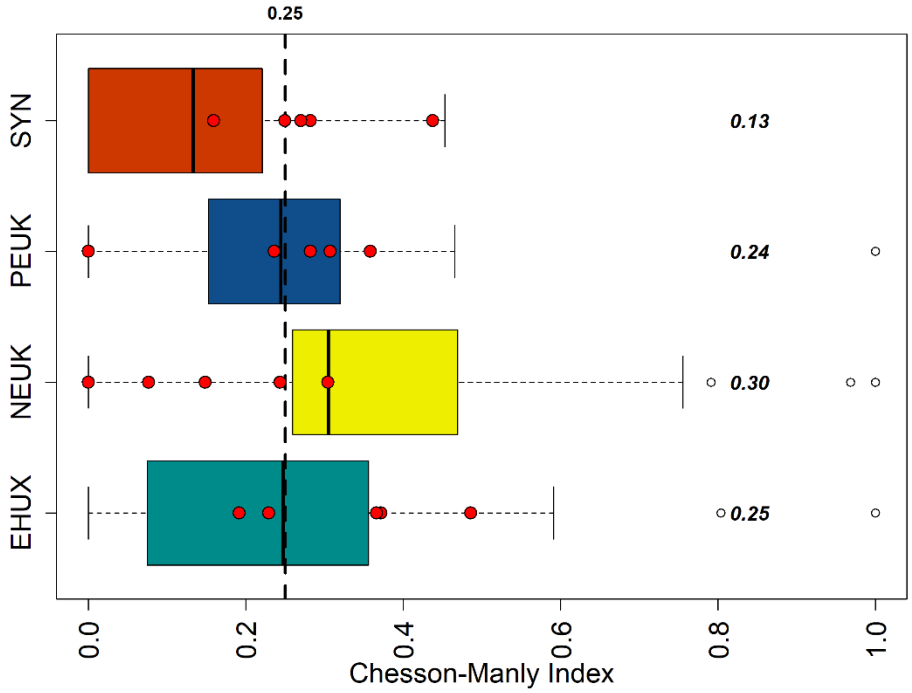


**Figure 4.5.** Box plots of the Chesson-Manly (C-M) index for preferential grazing. Dashed vertical line is the 0.25 value, which is the line of "neutral grazing preference" (Manly, 1974). Red points are from the Celtic Sea cruise in 2015. White data points represent outliers of the entire data set. Values in bold italics are the median values for each group from mesocosm data

**Table 4.2**: *p*-values from a two-sided Kolmogorov-Smirnov test of Chesson-Manly index values between different phytoplankton groups. Bold values indicate significant differences ($p < 0.05$).

| | *E. huxleyi* | NanoEUK | PicoEUK | *Synechococcus* |
|---|---|---|---|---|
| *E. huxleyi* | - | 0.08 | 0.82 | **0.01** |
| NanoEUK | | - | 0.05 | **< 0.001** |
| PicoEUK | | | - | **0.003** |
| *Synechococcus* | | | | - |

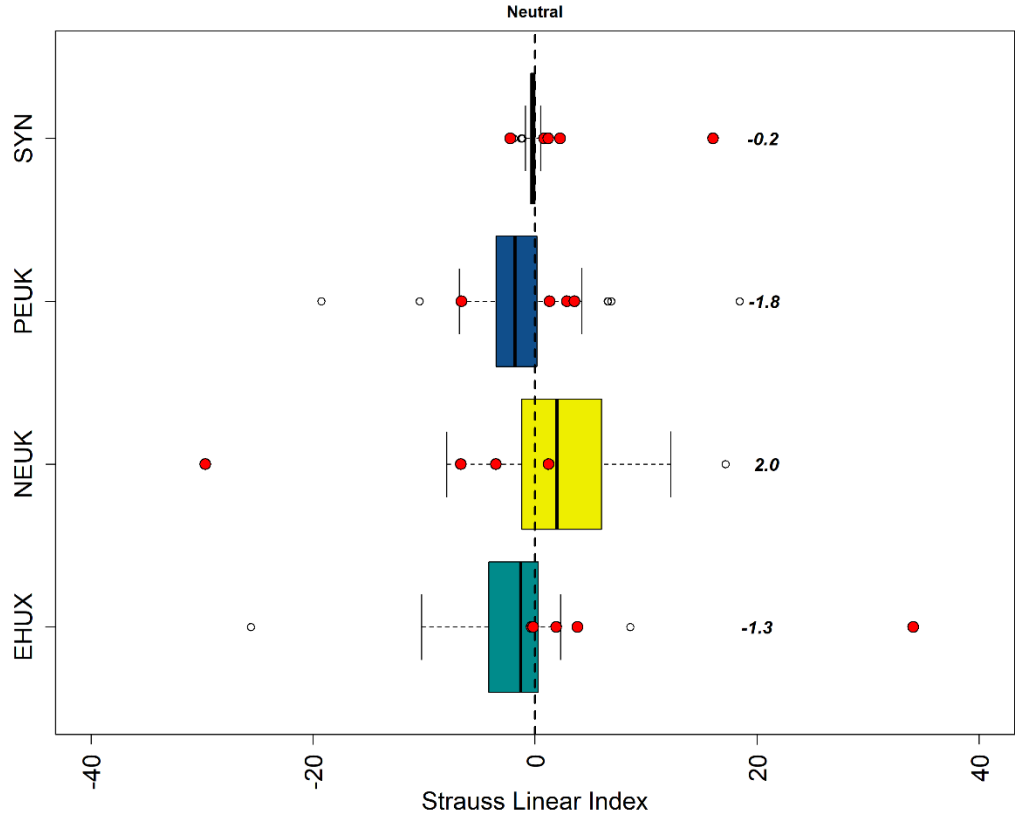


**Figure 4.6.** Box plots of Strauss-Linear index for grazing selectivity. Dashed vertical line is at 0, the value for netural grazing selection. Red points are from the Celtic Sea cruise in 2015. White points represent outliers of the entire data set. Values in bold italics are the median values for each group from mesocosm data.

**Table 4.3**: *p*-values from a two-sided Kolmogorov-Smirnov test of Strauss Linear index values between different phytoplankton groups. Bold values indicate significant differences ($p < 0.05$).

| | *E. huxleyi* | NanoEUK | PicoEUK | *Synechococcus* |
|---|---|---|---|---|
| *E. huxleyi* | - | **< 0.001** | 0.825 | **< 0.001** |
| NanoEUK | | - | **< 0.001** | **< 0.001** |
| PicoEUK | | | - | **< 0.001** |
| *Synechococcus* | | | | - |

## 4.5 Discussion

### *4.5.1* Grazing control of *Emiliania huxleyi*

There have been a variety of hypotheses put forth for the mechanisms that promoted the evolution of coccolith formation (Young, 1994), with protection from predation being a prominent suggestion (Monteiro et al., 2016). While this has been investigated in several laboratory experiments, it has yet to be explored extensively in field populations. Given that our data suggest that the presence of *E. huxleyi* does not significantly affect the ability of microzooplankton to graze (Fig. 4.2b), and that microzooplankton do not preferentially graze other similar sized-species over *E. huxleyi* (Fig. 4.5; Table 4.2), we suggest that calcification in this coccolithophore species does not act as a mechanism to protect against microzooplankton ingestion.

Previous field experiments have observed decreased grazing pressure within *E. huxleyi* bloom areas, compared to regions outside of the bloom (Fileman et al., 2002; Olson and Strom, 2002). In a previous mesocosm experiment, the grazing rate on chlorophyll-*a* was much lower during the peak of *E. huxleyi* biomass ($g$ = 0.18 – 0.23 $d^{-1}$), compared to periods before this (0.37 – 0.45 $d^{-1}$) (Nejstgaard et al., 1997). This was not observed during *E. huxleyi* blooms within the North or Celtic sea (Archer et al., 2001; Mayers et al., 2018) or within our meta-analysis (Fig. 4.2b). Rather, while we do not see many cases where grazing rates are higher than growth rates (at a community level) it is observed that grazing rates are not influenced by the proportion of the community that is *E. huxleyi*.

One possible explanation for this is that grazers are readily consuming *E. huxleyi* the same as other small algae. In laboratory experiments, calcified *E. huxleyi* cells are readily consumed (e.g., Hansen et al., 1996; Harvey et al., 2015; Strom et al., 2017), although consequences to grazer fitness (reduced growth rates) have been observed (Harvey et al., 2015). However, even during *E. huxleyi* blooms, calcified cells typically make up only 30 to 40% of the phytoplankton carbon biomass (Mayers et al., 2018; Poulton et al., 2007, 2013), whilst other nano-eukaroyte sized phytoplankton are also present (Holligan et al., 1993; Malin et al., 1993; Poulton et al., 2013), suggesting there may be other prey sources available. Hence, microzooplankton grazers may be preferentially consuming similar-sized phytoplankton groups, such as nano- and picoeukaryotes, in bloom conditions.

The linear regression of all phytoplankton group specific growth and mortality rates showed the equation y = 0.04 + 0.67x, which is very similar to the equation from 788 paired rate estimates of phytoplankton growth and grazing across the global ocean (y = -.041 + 0.67x; Calbet and Landry, 2004). This, along with the overlaid data points

shown from field sites in the Celtic Sea suggest our data on different phytoplankton groups are representative of natural populations, even though it was conducted in mesocosm enclosures.

In marine phytoplankton, maximum gross growth rates tend to decline with increasing cell volume (Edwards et al., 2012); a trend seen in our data with pico-eukaryotes showing the highest intrinsic growth rates, followed by *E. huxleyi* and nano-eukaryotes. However, the cyanobacteria *Synechococcus* displayed the lowest growth rates, despite having the smallest cell size (< 1 µm). Comparisons of the net (growth – mortality) growth rates calculated from dilution experiments, and net growth rates calculated from T0 measurements between experiments showed the best agreement with *E. huxleyi* and pico-eukaryotes ($p$ = 0.84 and 0.43 respectively using a two-sided K-S test). In contrast, nano-eukaryotes and *Synechococcus* were found to be significantly different ($p$ = 0.01 and 0.04 respectively using a two sided K-S test). Hence, other mortality factors than microzooplankton grazing may have affected the observed growth rates. In the 2017 mesocosm, nano-eukaryotes bloomed in six of the bags and a viral lysis-mediated crash was observed (data not shown). This would have had the impact of lowering intrinsic growth rates during those dates, but due to the filter size used to produce diluent (0.45 µm), estimated grazing rates would be unaffected. The main grazers of *Synechoccocus* may also be heterotrophic nanoflagellates (HNFs) (Caron et al., 1999), so the dynamics measured in our data may be due to a different grazer population, especially given that HNFs and ciliates can display different dynamics in dilution experiments (Agis et al., 2007).

Similar to growth rates, microzooplankton grazing rates measured from dilution experiments show a mild positive relationship ($r$ = 0.27, $p$ = <0.001) with cell size (Chen and Liu, 2010). This fits with our data, with similar grazing rates between *E. huxleyi* and nano-eukaryotes, followed by slightly lower rates for pico-eukaryotes and the lowest rates for *Synechococcus*. In further support of these results, the C-M index showed there was a slight selection for nano-eukaryotes and selection against *Synechococcus* sp., whilst selection appeared neutral for *E. huxleyi* and pico-eukaryotes (Fig. 4.5). Active avoidance by microzooplankton has been observed for *Synechoccocus* in previous field experiments (Teixeira and Figueiras, 2009), which may have led to the lower results observed in our data. Possible explanations for this are that a lower digestibility of *Synechococcus* spp, particularly when compared to heterotrophic bacteria, or a limiting quantity of a particular compound within these cyanobacteria (Caron et al., 1991). For this data set, it is suggested that microzooplankton grazing was primarily driven by cell-size selectivity. This has also been observed in microzooplankton feeding on calcified vs. non-calcified *E.*

*huxleyi*, with higher grazing rates on calcified cells suggested to be due to their slightly larger cell size (Hansen et al., 1996; Kolb and Strom, 2013).

Our datasets are only for the coccolithophore *E. huxleyi*, and within the coastal North Atlantic oceanic region (Norway, NW European Shelf). Different coccolithophore species display variable growth rates and calcification rates in mixed communities (Daniels et al., 2016, 2015, 2014; Mayers et al., 2018), and it is likely there are also differences in grazing rates (Mayers, pers obs.). Along with different species, consideration of growth and grazing rates within different oceanic regions is also an important consideration, and these are both particular areas for further study.

The significant differences observed between grazing rates based on chlorophyll-*a* and nano-eukaryotes is surprising, given that they represented the dominant fraction of chlorophyll-*a* (>58% of total was in the 3 – 10 µm) within the 2017 experiments (data not shown). As chlorophyll-*a* is a measure of the whole autotrophic plankton community it may be that the reduced changes could be due to other components of the plankton community we have not considered. Examples include autotrophic dinoflagellates, and mixotrophic dinoflagellates and/or ciliates, which can possess chlorophyll-*a* (Stoecker et al., 2017).

### 4.5.2 Biogeochemical implications

The rates presented in this study have implications for the flow of carbon through the marine food web as well as in terms of understanding of *E. huxleyi* population dynamics. The observed median *g:u* for *E huxleyi* (0.68) is very close to the global average of microzooplankton-mediated phytoplankton losses (65 - 67%) (Calbet and Landry, 2004; Schmoker et al., 2013). This suggests, when representing a microzooplankton grazing loss term in coccolithophore biogeochemical or population models, it is suitable to use the phytoplankton average mortality rate. However, it should be noted that the interquartile ranges for coccolithophore microzooplankton-mediated mortality losses are quite large, suggesting there may be other factors to take into consideration (e.g., viral mortality).

Our results suggest strong microzooplankton control on *E. huxleyi* populations, which brings into question the role of trophic cascades in biomass accumulation and population growth of *E. huxleyi*. Mesocosm experiments with added copepods have seen an increase in autotrophic nano-flagellate biomass (Pree et al., 2016b; Zöllner et al., 2009), which could include *E. huxleyi* and implies that mesozooplankton may release *E. huxleyi* populations from microzooplankton predation control (i.e. via a trophic cascade). Indeed, such dynamics were inferred during spring at a shelf sea site (Mayers et al., 2018; Chapter 3), where dilution experiments using <63 µm filtered water displayed high grazing

rates whereas constant net accumulation of *E. huxleyi* was seen between subsequent site visits over a monthly period.

The species *E. huxleyi* has a high level of genetic plasticity (Read et al., 2013), and different grazing rates have been observed on different strains of *E. huxleyi* (both diploid and haploid) in culture (Harvey et al., 2015; Kolb and Strom, 2013; Strom et al., 2017). The osmolyte DMSP, which is produced by *E. huxleyi*, may also deter grazing and favour the growth of low-producing DMSP strains (Archer et al., 2001). Conversely, it has also been observed that the cleavage product of DMSP, dimethylsulphide (DMS) can attract potential microzooplankton predators (Seymour, 2010). In laboratory studies, a link between cellular DMSP-content and grazing pressure was not found for different *E. huxleyi* strains (Harvey et al., 2015; Strom et al., 2017), however Strom et al. (2017) did observe higher grazing rates on strains associated with high hydrogen peroxide content. Clearly, there is a complex interaction between infochemicals, *E. huxleyi* strains and grazers within the environment. More research should focus on disentangling these interactions, and how they might influence the flow of material from prey to predators.

The fate of the calcite produced by *E huxleyi* and then grazed by microzooplankton is currently a black box in terms of the marine carbon cycle. If we assume a global ocean calcification rate of 1.6 Gt C $yr^{-1}$, then less than 40% is believed to be exported from the upper ocean and only ~9% is believed to be preserved in the sediments (Berelson et al., 2007; Balch, 2018). Whilst dissolution can occur below the lysocline, and in micro-zones of bacteria oxidation, there is the possibility that dissolution of calcite can also occur in the guts of microzooplankton. The gut pH of microzooplankton food vacuoles is assumed to be ~ 3 to 5 pH units to ensure enzymes associated with protist digestion work optimally (Gonzalez et al., 1993; Nagata and Kirchman, 1992). Therefore, the high microzooplankton grazing on *E huxleyi* observed would lead to a high proportion of produced calcite entering these food vacuoles with the strong possibility of its dissolution. However, whether the calcite affects the pH and therefore the ability of microzooplankton to digest food particles is currently unknown; this could affect the trophic transfer of material through the lower levels of the marine food web. Further consideration of the fate of this material is important for biogeochemical models of carbon fluxes in the oceans, as a greater understanding of potential calcite dissolution will reduce the influence of calcite as a ballasting material for marine particles.

### 4.5.3 Future work

The analysis of variations in growth and grazing rates on phytoplankton groups can provide information on how the phytoplankton communities are impacted by *E. huxleyi* abundance, however it does not provide details on the microzooplankton population

response. By directly observing changes in microzooplankton growth rates and biomass (e.g., through FlowCam) we can analyse if the proportion of *E. huxleyi* in the community has a negative impact on their growth. An analysis of microzooplankton growth rates during an *E. huxleyi* bloom (Mayers et al., 2018) showed slightly lower, but non-significant values than at a non-*E. huxleyi* bloom site on the NW European Shelf (0.93 and 1.65 $d^{-1}$, respectively), however this was linked to a possible trophic cascade effect rather than the presence of calcite.

Another aspect of our data we can investigate further is the forward vs side scatter plots of *E huxleyi* populations identified on the flow cytometer. Although there appears to be no selection on *E. huxleyi* per se, there exists natural variability within the population in terms of calcite content (Poulton et al., 2010, 2011). By analysing if there is a shift in the flow cytometry 'clouds' over the course of a grazing experiment, we can examine if the degree of cellular calcification has an impact on grazing rates.

The application of techniques to measure the pH change within the food vacuole of microzooplankton would allow observation of whether calcified coccolithophores can lead to a reduction in pH, and subsequent growth rate reduction, as implied in Harvey et al., 2015. A pH sensitive dye was microinjected into the gut of the copepod *Calanus helgolandicus*, and displayed that a slightly higher pH was observed when copepods were feeding on *E. huxleyi*, the diatom *Thalassiosira weissflogii* and the dinoflagellate *Procentrum micans* compared with other prey (Pond et al., 1995). This may not be appropriate for microzooplankton, due to their small size, so perhaps the application of fluorescent acidic probes (e.g. lysotracker-green), which have been applied to determine feeding in nanoflagellate communities (Sintes and del Giorgio, 2010), could be utilised to trace changes in pH over time when fed a diet of calcified cells.

## 4.6 Conclusion

This study has shown that grazing on the cosmopolitan coccolithophore *E. huxleyi* is not significantly different from similar-sized, but non-calcified, phytoplankton groups (pico- and nanoeukaryotes). I have also displayed evidence that higher proportions of *E. huxleyi* in the community do not lead to reduced microzooplankton grazing pressure, through negative impacts. However, in periods of exceptionally high (i.e. bloom) coccolithophore concentrations this effect may be observed. Questions still exist regarding the ultimate reason for coccolithophore calcification; however, we believe this study provides evidence that in field populations of *E. huxleyi*, it is not a grazing deterrent, or effective protection against microzooplankton-mediated mortality, supporting the lab results of Harvey et al., 2015. The same may not be applicable to other coccolithophore species (e.g., Young et

al., 2009), though studies using similar direct measures of grazing rates on coccolithophores do currently not exist to the best of our knowledge.

# Chapter 5: General Synthesis

The work presented in this thesis aimed to analyse cross-shelf and seasonal gradients in coccolithophore populations, how populations during spring (April) may be controlled by microzooplankton grazing, and finally whether or not calcification appears to play a protective function against microzooplankton ingestion. The individual hypotheses were:

1. A relationship between nutrients and irradiance and coccolithophore biogeography will be observed across seasonal and spatial scales, within Shelf Sea environments (Chapter 2).
2. Microzooplankton grazing exerts little control on coccolithophore communities due to the protection conferred by calcification (Chapter 3).
3. Coccolithophores will display low growth rates during the spring bloom, as other phytoplankton dominate the community (Chapter 3).
4. Coccolithophores, such as *E. huxleyi*, due to their possession of a coccosphere are grazed at significantly lower rates by microzooplankton than similar-sized phytoplankton groups (Chapter 4).
5. Greater proportions of *E. huxleyi* in the environment will cause a reduction in community grazing rate, due to the negative impact of calcite on microzooplankton growth rates (Chapter 4).

In this chapter, a summary of the three data chapters is presented, including an attempt to appreciate rates of coccolithophore dissolution within microzooplankton food vacuoles, a key gap in our understanding of the fate of coccolithophore organic and inorganic carbon flow. Finally, the wider implications, limitations of this study and future directions are discussed.

## 5.1 Summary

Chapter 2: Spatial and seasonal differences were observed in coccolithophore populations across the north-west European shelf. Contrary to a recent analysis conducted in the open-ocean of the Atlantic Ocean (Poulton et al., 2017a) no difference was observed vertically, aside from during July at the Central Celtic Sea. The common coccolithophore *Emiliania huxleyi* in summer showed highest proportions in areas where intermittent nutrient supply was common (e.g. internal tidal mixing, riverine input), suggesting this may be an important factor for its dominance during summer months, when *E. huxleyi* shows its highest abundance (e.g., Iglesias-Rodriguez et al., 2002; Tyrrell and Merico, 2009; Widdicombe et al., 2010). The intermittent nutrient input into the euphotic layer could be a mechanism leading to the success of this species and its bloom formation. A redundancy analysis of the dataset showed the two main axes represent

changes in cross-shelf parameters (RDA1), and changes across seasons (RDA2), with different coccolithophore species displaying different scores with each of these. The major variables, which altered across the shelf and seasons, were light and nutrients supporting hypothesis 1, that light and nutrients are controlling coccolithophore biogeography across the Celtic Sea shelf.

Chapter 3: During April, as the spring phytoplankton bloom developed, I observed an increasing abundance of coccolithophores throughout the month. These results are consistent with the previous field observations (Barber and Hiscock, 2006; Hopkins et al., 2015), where coccolithophores begin to increase at the same time as other phytoplankton, rather than there being a succession of species as proposed by Margalef (Margalef, 1997), thus rejecting hypothesis 3. The coccolithophore community became increasingly dominated by *E. huxleyi* throughout April, representing almost 70% of coccolithophore numbers by the end of the month.

It was also observed that microzooplankton exerted strong control over coccolithophore populations, with grazing estimated to remove >59% of daily production during April. Consistent with this is a recent modelling study of coccolithophore populations in the Southern Ocean Great calcite belt (Nissen et al., 2018) which showed in population models that top-down grazing pressure was an important factor representing coccolithophore population dynamics within this region. I therefore reject hypothesis 2, that microzooplankton grazing exerts little control over coccolithophore communities. I also observed that during an April *E. huxleyi* bloom, there was a high rate of microzooplankton grazing (~79% daily calcite production) as well as high rates of calcification (6,000 μmol C $m^{-3}$ $d^{-1}$). The fate of the produced calcite is unclear, as the pH of a food vacuole in microzooplankton is low (pH 3-5), so it may be that a large amount of grazed coccolithophore calcite undergoes dissolution in the upper ocean layers.

Chapter 4: Finally, the relationship between *E. huxleyi* and microzooplankton grazers was examined from a large dataset of dilution experiments to measure phytoplankton growth and grazing rates ($n$ = 48). I found no evidence that when proportions of *E. huxleyi* in the community were high there was a negative impact on microzooplankton grazing rates, due to a reduction in fitness of the grazer, as suggested in Harvey et al. (2015), and thus reject hypothesis 5. I also show that there was no significant difference in grazing rates on *E. huxleyi* or similar sized (0.2-20 μm) phytoplankton such as nano- and picoeukaryotes, therefore rejecting hypothesis 4. Using prey selection indexes, I find that ingestion rates on *E. huxleyi* are likely related to its proportion in the community (i.e. are density-dependent), rather than due to active avoidance and/or selection by microzooplankton predators. This suggests that for *E. huxleyi*, calcification likely does not act as a direct predator defence mechanism and may have another ecological role (e.g., protection

against digestion; see Section 5.2.1). It remains to be seen if this hypothesis holds true for other coccolithophore species.

## 5.2 Alternative measures of mortality and dissolution

### 5.2.1 Lipid biomarkers

Lipids are important components of the organic biomass of *E. huxleyi*, being major constituents of the cell membrane, organelles within the cell (including chloroplasts), and playing roles as essential signalling molecules (Vardi et al., 2009). Specific lipids have been identified as biomarkers for viral infection in the *E. huxleyi* – EhV model (Hunter et al., 2015), as well as for oxidative stress in diatoms (Collins et al., 2016). Using a lipid dataset collected from *E. huxleyi* grazing experiments conducted with *Oxyrrhis marina* (Harvey et al., 2015) I attempted to analyse relationships between grazers and calcified and non-calcified *E. huxleyi* strains (see Figure 5.1).

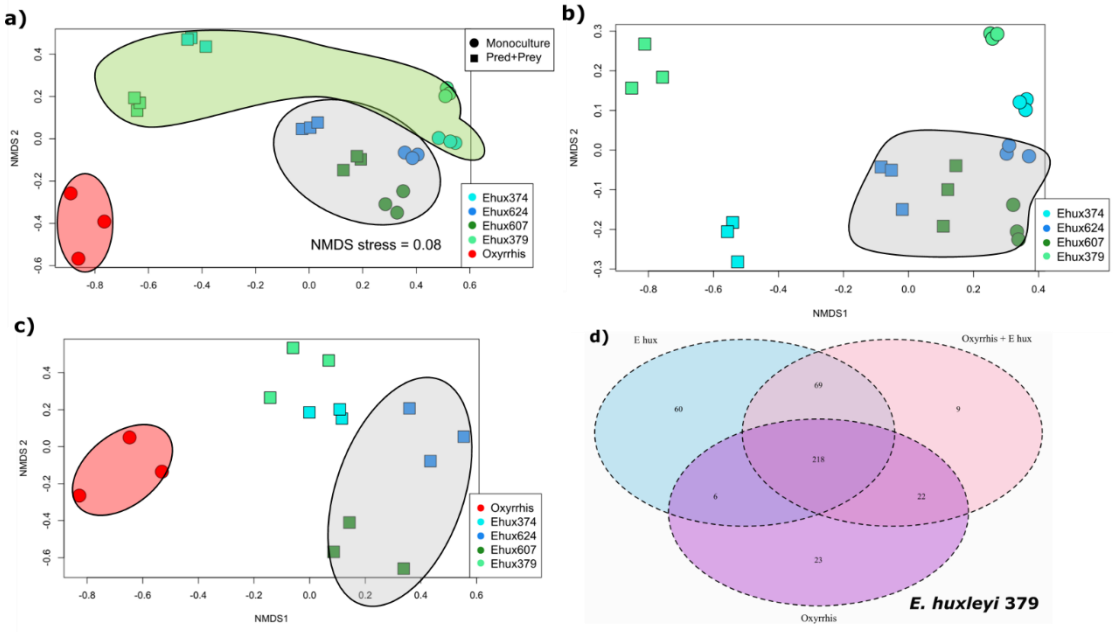


**Figure 5.1.** Non-metric Multi-Dimensional (nMDS) plots of lipid profiles from *E. huxleyi* and *Oxyrrhis marina* grazing experiments; a) includes all lipids (calcified strains = 624 and 607, naked strains = 374, 379), b) and c) are lipids defined as "*E. huxleyi* & *O. marina* specific" respectively (see text). Grey circles represent calcified strains, red circles are *O. marina* and green are non-calcified strains d) Venn diagram of lipids identified in *E. huxleyi* strain 379 and *O. marina* and together. Raw data courtesy of Elizabeth Harvey (Skidaway Institute for Oceanography at Univ. of Georgia, USA) and K Mayers; all data analysis by K Mayers.

In these results, there is a clear separation of *E. huxleyi* and *O. marina* in terms of lipid profiles, and between different *E. huxleyi* strains when grown alone (monoculture) and with *O. marina* (Pred+prey) (Fig. 5.1a). Interestingly, the differences in lipid profiles, as represented by nMDS distance, when *E. huxleyi* is cultured with a grazer, relative to being in monoculture alone is greater for naked strains (374 and 379) than for calcified strains (624 and 607). This is also observed if *O. marina* lipids are averaged and removed from the *E. huxleyi* samples to generate an "*E. huxleyi* specific" lipidome (Fig. 5.1b). If the same is done, but all of the *E. huxleyi* (monoculture) lipids are averaged, and removed from the samples containing *O. marina*, an assumed *O. marina* specific lipidome can be generated (Fig 5.1c). The naked strains cluster closer together in this analysis as well.

A hypothesis I provide for this low variability in the calcified lipidomes is that the calcite may play a role in protecting the organic cell from dissolution within the food vacuole of *O. marina*. We must take into account several assumptions for this explanation. Firstly, it has to be assumed that the ingested cells were not excreted, as ingestion rates were measured by continuous cell counts, and these rates would have been altered if full cells were also egested (Harvey et al., 2015). To satisfy this assumption, I made a rough calculation of the proportion of *E. huxleyi* cells which would theoretically be grazed throughout the experiment, using T0 cell counts of predator and prey and the measured ingestion rates (cell$^{-1}$ predator$^{-1}$ d$^{-1}$) over 48 hours (Harvey et al., 2015). For the non-calcified strains, 90 – 135% of cells would be ingested, whereas for the calcified strains, only 29% would be ingested for strain 607 but 107% for 624. Although, a low number of strain 607 would therefore have been exposed to the food vacuole, the clustering on the NMDS plot of both 607 and 624 (Fig 5.1b), with the latter being heavily ingested, supports our conclusion that calcite protects the organic cell from dissolution.

Though little is known regarding the gut transit times of microzooplankton, estimates from changes in chlorophyll auto-fluorescence in ciliates range from ~75 minutes to 5 hours (Dolan and Simek, 1997; First et al., 2012). In *O. marina* feeding on the chlorophyte *Dunaliella* sp., the digestion time was estimated to be of the order of 12 to 24 hours (Opik and Flynn, 1989), and almost 5 hours particle$^{-1}$ when feeding on *Chlorella* (Hammer et al., 2001). The lipid experiments by Harvey et al. (2015) were carried out for 48 hours, so if efficient digestion was occurring, I assume grazed *E. huxleyi* would have been sufficiently digested. The low rate of change in the (ingested) calcified *E. huxleyi* lipidomes (see Fig. 5c) suggests many lipids are not being broken down or being altered in the same way as in the naked populations. From Harvey et al. (2015) it is known that this is not due to differences in ingestion rates (strains 607 and 624 showed the highest and lowest ingestion rates respectively), however the growth rate of *O. marina* was significantly lower when fed these strains, supporting the hypothesis that *O. marina* is unable to utilise the *E.*

*huxleyi* organic lipids. The clustering of naked *E. huxleyi* strains in the presence of a grazer may suggest *O. marina* is able to assimilate these lipids, which may be undergoing trophic upgrading (enhancing the biochemical quality of prey lipids), which is observed in this species when grown on the chlorophyte *Dunaliella* sp. (Klein Breteler et al., 1999).

Finally, I was interested to potentially identify a biomarker lipid for *E. huxleyi* grazed (ingested) by *O. marina* within the dataset; I compared the lipids only identified in all triplicate experiments between all four *E. huxleyi* strains and looked for lipids which were only present when predator and prey were cultured together (Fig. 5.1d). Two potential biomarkers were identified; the first is a triacylglycerol (TAG) (TAG 60:14) found in all four strains only when exposed to a grazer. TAGs have previously been shown in phytoplankton to be produced in response to stressors (including viral infection and nutrient limitation) (Hunter et al., 2018; Malitsky et al., 2016). The other potential biomarker is a phospholipid known as phosphatidylglycerol (PG) (PG 48:1), which is observed in all triplicates for the three strains, and in duplicate for one strain (*E. huxleyi* 624).

The data set presented here also highlights how lipidomics can be used to investigate predator-prey dynamics with microzooplankton grazers, and may provide new insights into the fate of organic material being ingested by these predators. My preliminary analysis only examined un-oxidised lipids, and it is likely oxidised lipids also play a role, especially if stress-related TAGs were observed. Analysis of field data sets where *E. huxleyi* is known to be present, and grazed upon, will help to confirm the applicability of our biomarkers.

### 5.2.2 Gross and net calcification rates

The dilution experiment provides estimates of intrinsic growth (i.e. growth in the absence of mortality) and grazing rates (Landry and Hassett, 1982), therefore the intrinsic growth rates estimated during April (Chapter 2) can be used to calculate a theoretical calcite production, and compared with the rates measured by $^{14}$C-incorporation at the same time. Differences in these rate measurements could indicate a decoupling of growth and calcification, or dissolution during the experiment. It can also provide information on whether rates observed are net (production and loss) or gross (production only) rate measurements during these experiments.

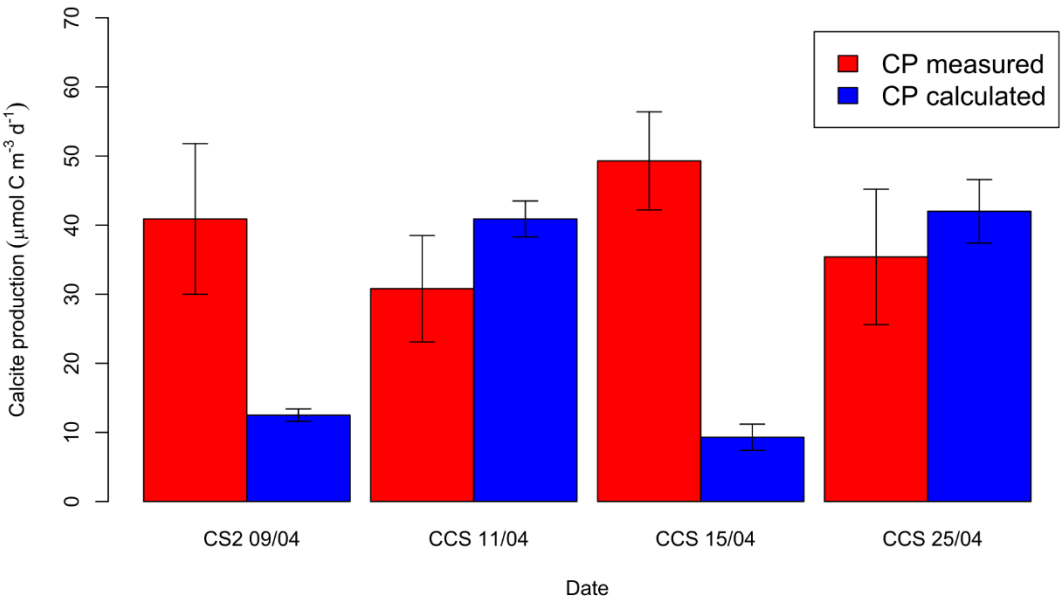


**Figure 5.2**. Calcite production (CP) measured during 24-hour incubation experiments, and a theoretical CP calculated using intrinsic growth rates from parallel dilution experiments. Error bars show standard errors (*n* = 3).

I estimated CP using the coccolithophore abundances at T24 of dilution experiments of different coccolithophore species, assumed the same intrinsic growth rate estimated from dilution experiments for all species, and used species-specific CP (Daniels et al., 2014, 2016, Young & Ziveri, 2000). In all cases, the calculated CP is lower than or similar to the measured CP rate (Figure 5.2). For two of the dates (CS2 on 9$^{th}$ and CCS on 15$^{th}$ April), the calculated CP rates appear to be large underestimates.

Hence, I suggest that CP measurements by the Micro-Diffusion Technique (Balch et al., 2000; Mayers et al., 2018; Chapter 3) are likely to be gross uptake rates of $^{14}C$ into inorganic carbon, rather than net; as it would be expected that our calculated rates would be higher in all instances if this was the case. This also provides extra evidence that calcification may protect the organic cell against dissolution by microzooplankton guts, similar to the lipid profiles (Fig. 5.1) - if labelled $^{14}C$-calcite underwent dissolution in the food vacuole, then it would be released in a dissolved form ($^{14}CO_2$) via respiration or excretion, resulting in this fraction being lost from our measurements of inorganic particulate $^{14}C$-uptake. Alternatively, it may suggest dissolution of calcite (coccoliths) which is re-assimilated into particulate matter, or excretion of coccoliths in dinoflagellate “mini-pellets” (Gowing and Silver, 1985), or excretion and incorporated into the lorica of tintinnids (Winter et al., 1986). However, with each of these alternative processes, the short-time frame (24 h) and small volumes (~ 75 mL) of the measurements makes these unlikely or relatively rare occurrences as the abundance of microzooplankton would have been low.

Factors that likely influenced the calculations could include differing rates of intrinsic growth for different species (Daniels et al., 2014, 2016). The earlier dates in April were associated with more heavily calcified species of coccolithophore (see Chapters 2 and 3), such as *Coccolithus pelagicus* and *Coronasphaera mediterranea*, which may have had a greater impact on community calcification rates than calculated here. The volume used for CP measurements (~75 mL) could also have underestimated grazing dynamics due to possible bottle effects on grazers, providing another reason why I believe the rate measurements were gross rather than net production. There is a difficulty in estimating accurate rates for the larger species, as their abundances were not particularly high (low statistical confidence in cell counts) and when diluted may be overlooked or missed. A suggestion for future dilution experiments would be to sample a larger volume of water (e.g. 1 L) to allow statistically significant quantification of intrinsic growth and mortality rates of rarer coccolithophore species.

Exceptionally high calcite production (CP) was measured during the J2 *E. huxleyi* bloom in April (6,000 µmol C $m^{-3}$ $d^{-1}$, Chapter 2). By dividing CP by the number of cells (2,688 $mL^{-1}$) I calculated a cell-specific calcification rate of 2.2 pmol C $cell^{-1}$ $d^{-1}$ (after Poulton et al., 2010), and correcting for day length and assuming calcification only in the light (~14 hours in April) gives a value of 0.16 pmol C $cell^{-1}$ $h^{-1}$. The type A overcalcified morphotype observed within this bloom (see Chapter 3) has a coccolith calcite value of 0.046 pmol C (i.e. a distal shield length 3.5 µm, *ks* value of 0.04; following Poulton et al., 2011 and Young & Ziveri, 2000), which equates to ~3.3 coccoliths $cell^{-1}$ $h^{-1}$. This is well within observed coccolith production rates in field (Poulton et al., 2010, 2013; Charalampopoulou et al., 2016) and laboratory (Balch et al., 1996) studies, showing our observed rates are physiologically possible.

Using the intrinsic growth rate, calculated from the dilution experiment conducted on this date (0.29 $d^{-1}$), and a cell calcite of 0.92 pmol C $cell^{-1}$ (assuming 20 coccoliths $cell^{-1}$ (see SEM image in Chapter 3) and 0.046 pmol C $coccolith^{-1}$), as well as the cell abundances, I calculate a calcite production of ~717 µmol C $m^{-3}$ $d^{-1}$. This calculated rate is only ~12% of the measured rate, suggesting that only a small proportion of the *E. huxleyi* population was actively producing coccoliths to form a new coccosphere. The majority of the population was therefore producing coccoliths that were not being used for new cell formation (and likely forming multiple layers on the coccosphere; Gibbs et al., 2013; Sheward et al., 2017). In low phosphorus conditions, *E. huxleyi* cells in culture have been shown to pause in the G1 phase of the cell cycle, where they continue to calcifiy without dividing (Müller et al., 2008), which is most likely occurring at this stage of the J2 bloom.

If ~80% of CP is being grazed by microzooplankton (Mayers et al., 2018, Chapter 3), this means ~1,200 µmol C $m^{-3}$ $d^{-1}$ of CP is not being grazed. As the amount of CP being

grazed, is higher than the amount being actively produced by dividing cells, this means that the grazers are consuming at least some of the non-dividing part of the community. In this situation, of high losses and low new cell production, a rapid crash of the bloom population is likely if the grazed material is completely removed (e.g. through dissolution) from the environment. This loss of material through dissolution in microzooplankton vacuoles would lead to respiration of the material and enhanced $CO_2$ fluxes from the bloom community. Time-series measurements of CP rates and standing stocks of calcite through the bloom, as well as microzooplankton grazing and carbonate chemistry data, would be needed to examine further the fate of the non-dividing and dividing portions of the bloom coccolithophore community (and its calcite).

## 5.3 Wider implications

Through cell counts at L4 (Widdicombe et al., 2010), the continuous plankton recorder in the north Atlantic (Rivero-Calle et al., 2015), and as prymnesiophyte pigment markers in Bermuda (Krumhardt et al., 2016), it has been suggested that coccolithophores are increasing in abundance in these temperate regions. This is suggested to be due to enhanced $CO_2$ benefiting coccolithophore growth rate. Compared to other phytoplankton groups, coccolithophore photosynthesis is carbon-limited (Rost et al., 2003), and lab experiments display a hyperbolic increase in coccolithophore growth rates with $pCO_2$ (Rivero-Calle et al., 2015). Coccolithophores, particularly *E. huxleyi*, also appear to be expanding their range polewards (Smyth et al., 2004; Winter et al., 2013), particularly in the Arctic, where increasing *E. huxleyi* abundance is believed to be due to enhanced intrusion of Atlantic water masses (Neukermans et al., 2018).

This enhancement of coccolithophores could increase or decrease air-sea $CO_2$ fluxes, partly depending on how much calcite is exported to depth (Balch, 2018). However, depending on the fate of calcite grazed by microzooplankton, this may also lead to enhanced $CO_2$ being retained in the upper ocean due to the dissolution within food vacuoles and subsequent respiration. This would reduce the calcite exported to depth, and available to function as a ballast for marine particles (Klaas and Archer, 2002; Balch et al., 2016). This would reduce the strength of the biological carbon pump. Along with this, enhanced warming could lead to higher microzooplankton grazing rates (Caron and Hutchins, 2013; Chen et al., 2012) in regions where coccolithophores are found. By enhancing dissolution and retention of $CO_2$ in the upper water column, this results in more $CO_2$ available for the ocean to atmosphere flux. A greater understanding of calcite fate is therefore needed to resolve this question.

This thesis raises questions regarding the evolution and ecological role of calcification within coccolithophores. Support for a protective function comes from geological evidence, with coccolithophores appearing at the same time as armoured dinoflagellates (~252 Ma) (MacRae et al., 1996). In addition, once the calcification trait has evolved in coccolithophores, it has almost always been subsequently retained, suggesting it provides a constitutive benefit to the organism (Monteiro et al., 2016). There has been only one known example of secondary loss of calcification in the Isochrysidaceae family (Bendif et al., 2013). However, my data does not currently support a role in *E. huxleyi* as a defence mechanism against microzooplankton grazers. More evidence is required to test the theory that calcification acts as a population level defence, by indirectly impacting microzooplankton by enhancing energy use needed to digest calcite (Harvey et al., 2015; Monteiro et al., 2016), particularly in bloom scenarios when coccolithophore biomass is highest. However, given that calcification is retained, even in non-bloom populations (i.e. the majority of the year in temperate regions), this points to another evolutionary adaptation. It is also unlikely, given the wide range of coccolithophore morphologies observed (Young et al., 2003) that the function of coccoliths is the same across this entire group of organisms, and indeed, modelling work provides evidence for differential roles across biogeographical ranges (Monteiro et al., 2016). For instance enhanced light uptake and protection against viral and bacterial attack are suggested as possible mechanisms through ecosystem modelling.

## 5.4 Limitations and future directions

Examining coccolithophore populations from coastal regions to the shelf edge provide an understanding of what variables could be driving population changes within these regions. However, coccolithophores are also abundant off-shelf, including in bloom populations and open-ocean regions. Further work should use cross-shelf, in combination with off-shelf populations to provide details on possible connectivity between open ocean and shelf populations, as well as how biogeography shifts with changing depth and light environments.

My research has shown strong microzooplankton grazing on non-bloom coccolithophore populations, and some evidence in *E. huxleyi* bloom populations, although only from one experiment. This contrasts with previous work which has measured reduced grazing rates within *E. huxleyi* bloom regions, compared to outside them (Fileman et al., 2002; Olson and Strom, 2002). These differences may be due to the composition of microzooplankton populations, or different stages of the bloom. It could also be due to the fact these studies used chlorophyll-*a* and pigment biomarkers rather than direct enumeration of coccolithophores through microscopy, which could lead to an underestimation of grazing

rates as these markers are not coccolithophore specific (Mayers et al., 2018). An ideal study would be able to track a developing bloom population from pre-bloom to the post-bloom decline phase measuring coccolithophore growth and grazing rates, and how they vary throughout the bloom cycle. This has been conducted in a mesocosm experiment before, using cell counts (Nejstgaard et al., 1997), however experiments were conducted approximately every five days, during which time phytoplankton and microzooplankton communities can shift dramatically. The possible use of biomarkers for mortality processes (e.g. viral glycosphinolipids (Hunter et al., 2015)) could also help to track progression of other mortality processes.

A greater consideration of the direct effects of coccolithophore calcification on microzooplankton populations is needed. In a similar manner to Harvey et al. (2015), however, rather than using naked and calcified versions of the same coccolithophore species, advantage could be taken of the wide range of currently cultured coccolithophores. The experiments could use gradients in coccolithophore cell-size, calcite content and even motility to observe how these traits impact ingestion rates, and the growth rates of microzooplankton predators. Many grazing experiments on *E. huxleyi* have also considered only heterotrophic dinoflagellates (Hansen et al., 1996; Harvey et al., 2015; Strom et al., 2017), however ciliates are known to be significant contributors to biomass during *E. huxleyi* blooms (Fileman et al., 2002; Olson and Strom, 2002), suggesting they could be significant grazers of coccolithophores. To our knowledge, only one study has used ciliates for *E. huxleyi* grazing experiments, and this was conducted using only non-calcifying strains (Strom and Bright, 2009).

Finally, to gain a greater understanding of the fate of fixed carbon into calcite by coccolithophores is an important gap in our understanding. In the past, $^{14}C$ uptake experiments have been incorporated into dilution experiments (Gutiérrez-Rodríguez et al., 2011; Latasa et al., 2005), to estimate carbon flow through different phytoplankton groups. It could be possible to utilise the micro-diffusion technique (MDT) (Balch et al., 2000) to measure uptake of organic and inorganic carbon in dilution experiments. As these experiments measure net (i.e. production and loss) fixation, we can use the same reduction in grazing rate with dilution to see how the loss of inorganic and organic carbon changes, using the assumption that growth (and here, calcification) rate is unaffected by dilution. Alongside this, larger volumes of filtered water would allow us to track growth and mortality rates of different coccolithophore taxa through microscopic enumeration. One of the major issues encountered when attempting to consider individual taxa (except *E. huxleyi*) was a low abundance, particularly at the lowest dilutions. A larger volume would allow us to consider species-specific growth and grazing rates, providing information on the pathways of calcite production by different species.

This thesis, and these experiments, provide a greater understanding of the role of coccolithophores in ecological settings, as well as biogeochemical cycles. Examining how coccolithophores, and coccolithophore population dynamics respond to future ocean scenarios (e.g. warmer waters, enhanced stratification and a decreasing ocean pH (Bopp et al., 2001; Gruber, 2011) will allow us to predict how these organisms may change into the future.

# Chapter 6: Supplementary information

## 6.1 Supplementary data for Chapter 3

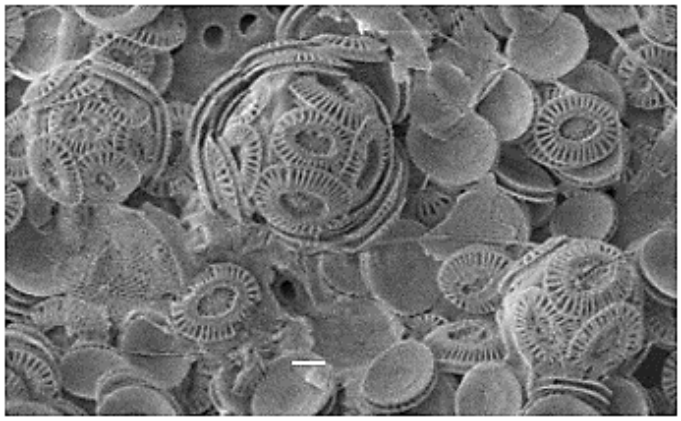

**Supplementary Figure 3.1:** Scanning electron microscopy image of *E. huxleyi* cells from J2 on 27 April. Scale bar is 1 µm.

**Supplementary Figure 3.2:** Plots of coccolithophore cell numbers ($mL^{-1}$) from dilution experiments conducted at the CCS, CS2 and J2 sites.

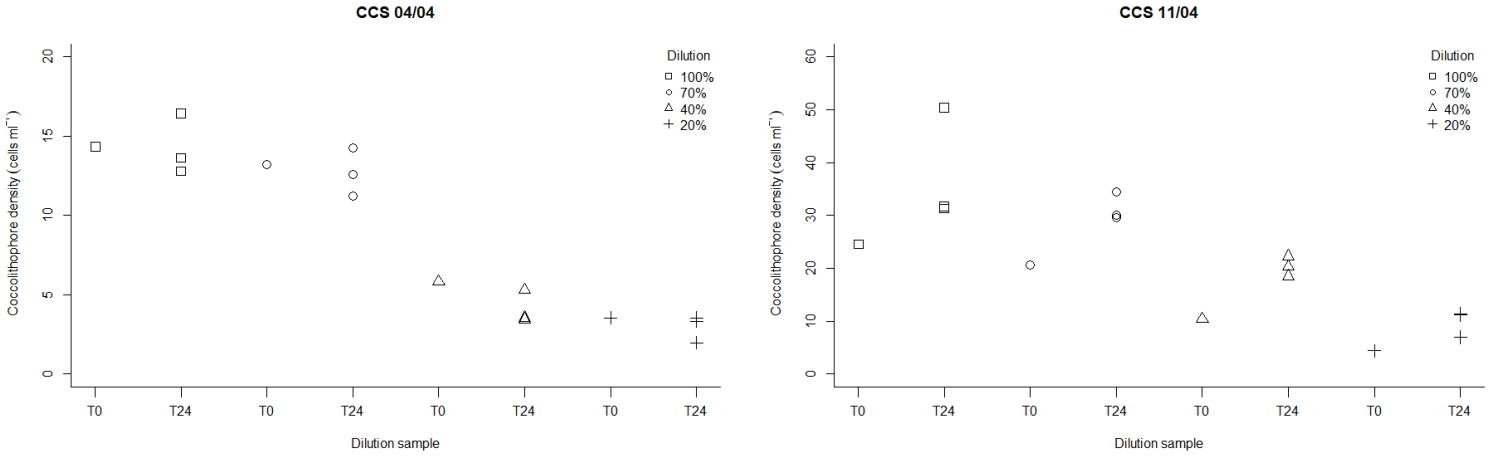

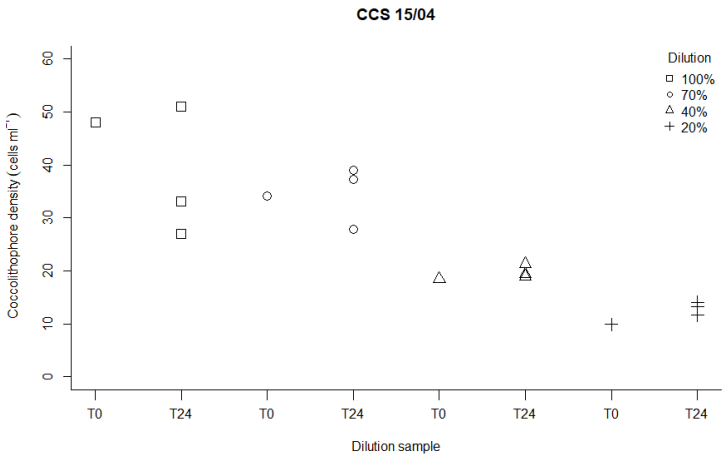
CCS 15/04
Coccolithophore density (cells ml⁻¹)
0
10
20
30
40
50
60
T0
T24
T0
T24
T0
T24
T0
T24
Dilution sample
Dilution
100%
70%
40%
20%

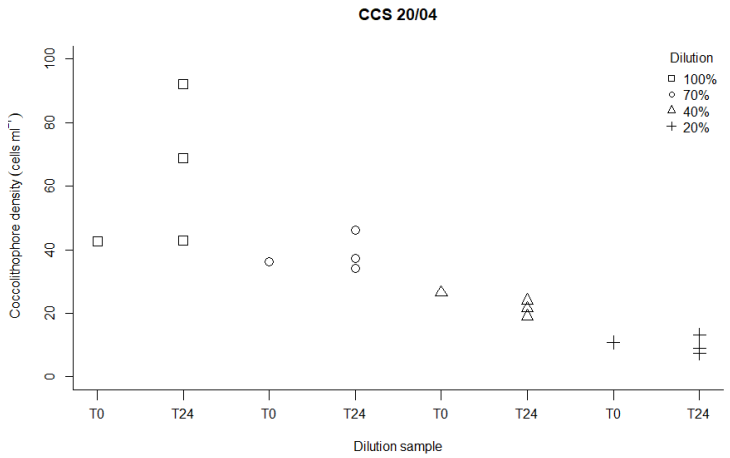
CCS 20/04
Coccolithophore density (cells ml⁻¹)
0
20
40
60
80
100
T0
T24
T0
T24
T0
T24
T0
T24
Dilution sample
Dilution
100%
70%
40%
20%

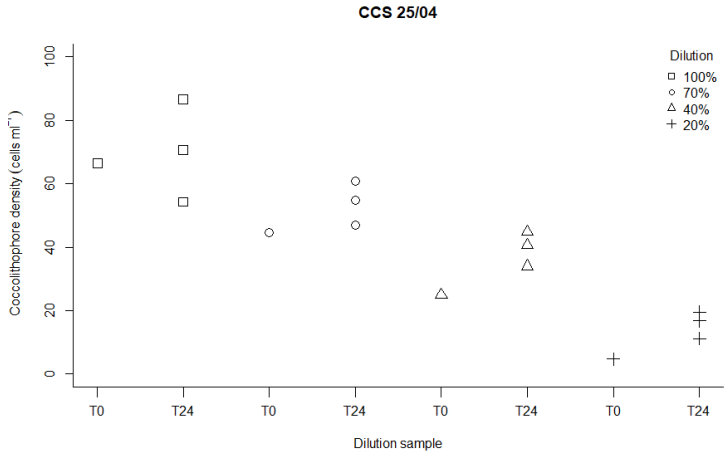
CCS 25/04
Coccolithophore density (cells ml⁻¹)
0
20
40
60
80
100
T0
T24
T0
T24
T0
T24
T0
T24
Dilution sample
Dilution
100%
70%
40%
20%

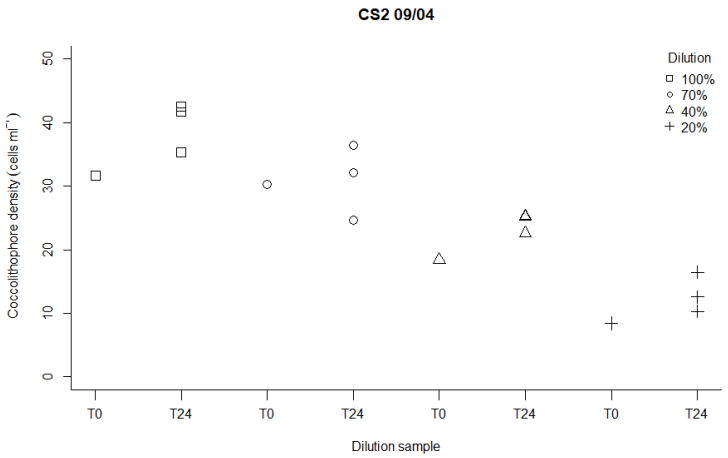
CS2 09/04
Coccolithophore density (cells ml⁻¹)
0
10
20
30
40
50
T0
T24
T0
T24
T0
T24
T0
T24
Dilution sample
Dilution
100%
70%
40%
20%

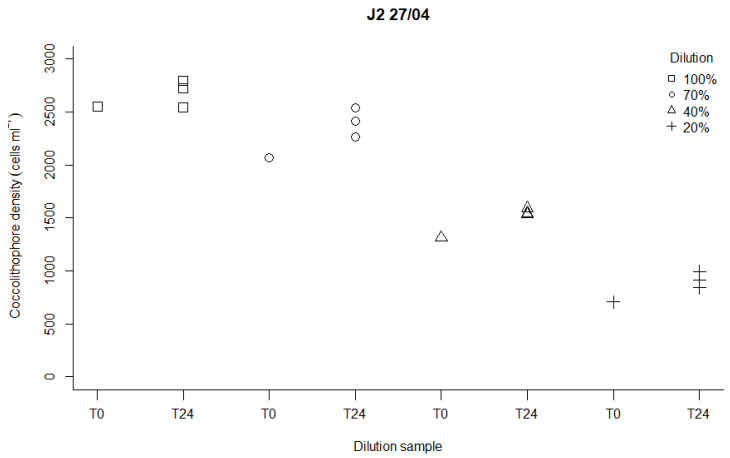
J2 27/04
Coccolithophore density (cells ml⁻¹)
0
500
1000
1500
2000
2500
3000
T0
T24
T0
T24
T0
T24
T0
T24
Dilution sample
Dilution
100%
70%
40%
20%

## 6.2 Supplementary data for Chapter 4

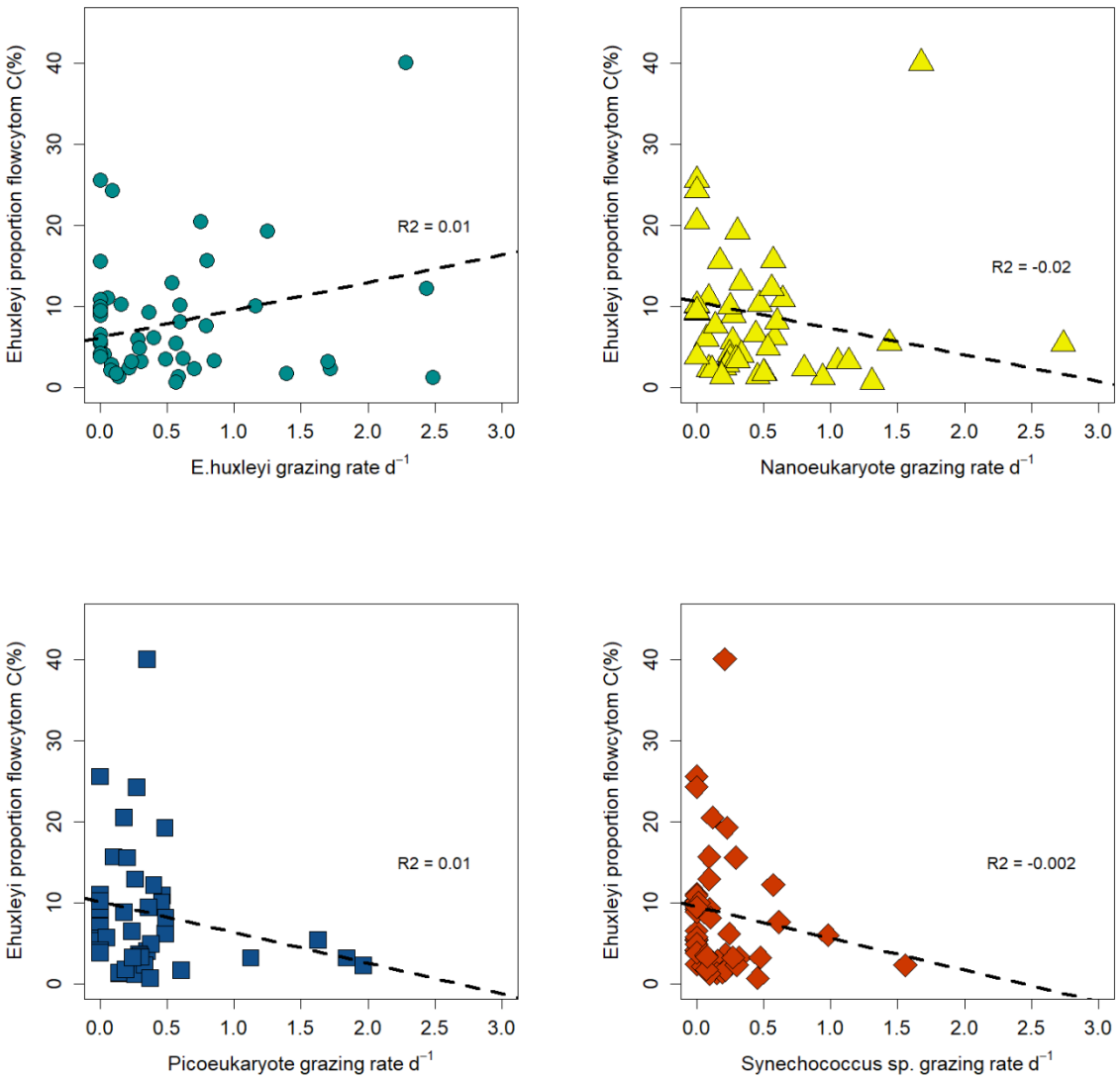


**Supplementary figure 4.1.** Plots of grazing rate for different phytoplankton groups against the proportion of *E. huxleyi* within the community. Dashed lines represent linear regression, none of which were significantly different from zero ($R^2$ = <0.01).

## 6.3 Supplementary data for General Synthesis chapter

### 6.3.1 Lipid data methods

Culturing of *E. huxleyi* strains and grazing experiments were conducted as in Harvey et al., 2015. Briefly, four strains of *E. huxleyi*, two calcified (607 and 624), and two non-calcified (373, 379) were grown in 0.2-µm filtered autoclaved seawater (FSW), enriched with f/2 –Si media. The predatory dinoflagellate, *O. marina* (LB1974) was cultured in FSW only, with *Isochrysis galbana* (CCMP1323) used to rear predators prior to experiments. All cultures were maintained on a 12:12 light:dark cycle at 18°C, salinity of ~30 and light intensity of 85 – 100 µmol photon $m^{-2}$ $s^{-1}$. Cultures were not axenic. Phytoplankton cultures were transferred every 7-10 days to maintain exponential growth. The grazer was fed twice weekly with *I. galbana* at a concentration of 50,000 cells $mL^{-1}$.

Grazing experiments were conducted over 48 hours at a prey concentration of ~80,000 cells $mL^{-1}$ (~1080 ng C $mL^{-1}$) and a predator concentration of 200 cells $mL^{-1}$ (prey:predator ratio of 400:1) in triplicate. Seawater, predator- and prey-only controls were also measured. Organisms were first combined in 2 L cultures at the appropriate concentrations, mixed gently and then triplicate aliquots were poured gently into 250 mL clear polycarbonate bottles. Sample bottles were incubated on a plankton wheel (rotation 1 rpm) and maintained on a 12:12 light:dark cycle at 18°C with a light intensity of ~30 µmol photon $m^{-2}$ $s^{-1}$.

At T48, samples were removed from incubation, gently mixed, and 40-mL was filtered onto combusted (450°C, 24h) glass fiber filters, which were immediately frozen in liquid nitrogen and stored at -80°C until extraction.

Total lipid extracts were prepared using a modified Bligh & Dyer extraction (Bligh and Dyer, 1959, Popendorf et al., 2013) with addition of an internal DNP-PE standard (C16:0/C16:0 2,4-dinitrophenylphosphatidylethanolamine, Avanti Polar Lipids Inc). Filters were placed into 12 mL glass centrifuge tubes and 0.8 mL phosphate buffered saline (PBS; Fisher Scientific, pH 7.4), 2 mL methanol (Optima™ LC/MS Grade, Fisher Scientific) and 1 mL dichloromethane (DCM; GC Resolv™ Fisher Scientific) were added along with 20 µL of DNP-PE standard (0.5 $mgmL^{-1}$ in methanol). The tubes were capped and vortexed for 5-10 seconds. Samples were placed into an ultrasonic water bath for 10 minutes to disrupt cells. A further 1 mL PBS and 1 mL DCM were added and spun in a centrifuge at 1600 rpm for 5 minutes. The lower organic phase was transferred using a combusted glass pipette into a 2 mL HPLC vial. Samples were capped with argon to limit oxidation and sample degradation before being stored at -80°C prior to analysis, allowing samples to be stable for up to several years (Popendorf et al., 2013).

Lipid extracts were subjected to lipid analysis by reverse-phase high performance liquid chromatography mass spectrometry (HPLC-MS) on an Exactive Plus Orbitrap mass spectrometer (Thermo Scientific) connected to an Agilent 1200 chromatography system. Chromatography and mass spectrometry conditions were as described by Hunter et al 2015. For analysis, 20 μL (from 2,000 μL total) of total lipid extract was injected into the HPLC-MS. The R packages, xcms, CAMERA and LOBSTAHS were then used to identify and annotate lipidome components from the MS data (Collins et al., 2016). The R package IPO was used to optimise the settings for xcms, and a 2.5 ppm mass uncertainty tolerance was used to generate database matches in LOBSTAHS. For this analysis, we removed oxidised lipids (~30% total lipidome) from the results; we also excluded compounds with an odd total number of acyl-carbon atoms, as nonacetogenic fatty acid synthesis is confined to bacteria and archaea (Pearson, 2014). Where the assignment of a compound was unclear (e.g. due to isomers), manual identification to the most likely compound was carried out.

Data analysis and plotting was carried out in R (version 3.3.2) (R Core Team, 2015). Un-oxidised lipids were normalised to each sample and a dissimilarity matrix was produced using the vegan package. A non-metric multidimensional scaling analysis was used to examine differences between predator and prey samples, and samples containing both predator and prey. For "*E. huxleyi* / *O. marina* specific lipidomes" the average lipids of all prey-only or predator only samples was subtracted from all other samples. To look for biomarkers within the database we produced Venn diagrams using the R package VennDiagram. We used a stringent cut-off that lipids had to be present in all triplicates before plotting.

# Chapter 7: Bibliography

Agis, M., Granda, A., Dolan, J.R., 2007. A cautionary note: Examples of possible microbial community dynamics in dilution grazing experiments. J. Exp. Mar. Bio. Ecol. 341, 176–183. doi:10.1016/j.jembe.2006.09.002

Anderson, R., Jürgens, K., Hansen, P.J., 2017. Mixotrophic Phytoflagellate Bacterivory Field Measurements Strongly Biased by Standard Approaches: A Case Study. Front. Microbiol. 8, 1–12. doi:10.3389/fmicb.2017.01398

Anderson, S.R., Menden-Deuer, S., 2016. Growth, Grazing and Starvation Survival in Three Heterotrophic Dinoflagellate Species. J. Eukaryot. Microbiol. 0, 1–13. doi:10.1111/jeu.12353

Archer, S.D., Widdicombe, C.E., Tarran, G.A., Rees, A.P., Burkill, P.H., 2001. Production and turnover of particulate dimethylsulphoniopropionate during a coccolithophore bloom in the northern North Sea. Aquat. Microb. Ecol. 24, 225–241. doi:10.3354/ame024225

Armbrecht, L.H., Eriksen, R., Leventer, A.M.Y., Armand, L.K., 2017. First observations of living sea-ice diatom agglomeration to tintinnid loricae in East. J. Plankton Res. 0, 1–8. doi:10.1093/plankt/fbx036

Bach, L.T., Larsen, A., Hildebrandt, N., Schulz, K.G., Riebesell, U., 2016. Influence of plankton community structure on the sinking velocity of marine aggregates. Global Biogeochem. Cycles 30, 1145–1165. doi:10.1002/2015GB005324.

Bach, L.T., Riebesell, U., Gutowska, M.A., Federwisch, L., Schulz, K.G., 2015. A unifying concept of coccolithophore sensitivity to changing carbonate chemistry embedded in an ecological framework. Prog. Oceanogr. 135, 125–138. doi:10.1016/j.pocean.2015.04.012

Balch, W.M., 2018. The Ecology, Biogeochemistry, and Optical Properties of Coccolithophores. Ann. Rev. Mar. Sci. 10, 71–98. doi:10.1146/annurev-marine-121916-063319

Balch, W.M., Bates, N.R., Lam, P.J., Twining, B.S., Rosengard, S.Z., Bowler, B.C., Drapeau, D.T., Garley, R., Lubelczyk, L.C., Mitchell, C., Rauschenberg, S., 2016. Factors regulating the Great Calcite Belt in the Southern Ocean and its biogeochemical significance. Global Biogeochem. Cycles 30. doi:10.1002/2014GB004832.

Balch, W.M., Drapeau, D.T., Bowler, B. C., Lyczskowski, E. R., Lubelczyk, L. C., Painter, S.C., Poulton, A. J., 2014. Surface biological, chemical and optical properties of the Patagonian Shelf coccolithophore bloom, the brightest waters of the Great Calcite Belt, Limnol. Oceanogr., 59, 1715-1732. doi: https://doi.org/10.4319/lo.2014.59.5.1715, 2014.

Balch, W.M., Drapeau, D.T., Bowler, B.C., Booth, E.S., Windecker, L.A., Ashe, A., 2008. Space-time variability of carbon standing stocks and fixation rates in the Gulf of Maine, along the GNATS transect between Portland, ME, USA, and Yarmouth, Nova Scotia, Canada. J. Plankton Res. 30, 119–139. doi:10.1093/plankt/fbm097

Balch, W. M., Gordon, H. R., Bowler, B. C., Drapeau, D. T., Booth, E. S., 2005. Calcium carbonate measurements in the surface global ocean based on Moderate-Resolution Imaging Spectroradiometer data, J. Geophys. Res.-Oceans, 110, C07001, doi: https://doi.org/10.1029/2004JC002560, 2005

Balch, W.M., 2004. Re-evaluation of the physiological ecology of coccolithophores. In: Coccolithophores from molecular processes to global impact, Thierstein, H.R. and Young, J.R. (Eds.), Springer, Berlin, 165-190.

Balch, W.M., Drapeau, D.T., Fritz, J.J., 2000. Monsoonal forcing of calcification in the Arabian Sea. Deep. Res. Part II Top. Stud. Oceanogr. 47, 1301–1337. doi:10.1016/S0967-0645(99)00145-9

Balch, W.M., Fritz, J., Fernandez, E., 1996. Decoupling of calcification and photosynthesis in the coccolithophore *Emiliania huxleyi* under steady-state light-limited growth. Mar. Ecol. Prog. Ser. 142, 87–97. doi:10.3354/meps142087

Balch, W.M., Holligan, P.M., Ackleson, S.G., Voss, K.J., 1991. Biological and optical properties of mesoscale coccolithophore blooms in the Gulf of Maine. Limnol. Oceanogr. 36, 629–643. doi:10.4319/lo.1991.36.4.0629

Barber, R. T., Hiscock, M. R., 2006. A rising tide lifts all phytoplankton: Growth response of other phytoplankton taxa in diatom-dominated blooms. Global Biogeochem. Cy., 20, GB4S03, https://doi.org/10.1029/2006GB002726

Bendif, E. M., Probert, I., Schroeder, D. C., de Vargas, C., 2013. On the description of *Tisochrysis lutea* gen. nov. sp. nov. and *Isochrysis nuda* sp. nov. in the Isochrysidales, and the transfer of *Dicrateria* to the Prymnesiales (Haptophyta). J. Appl. Phycol, 25, 1763-1776.

Benner, I., Passow, U., 2010. Utilization of organic nutrients by coccolithophores. Mar.

Ecol. Prog. Ser. 404, 21–29. doi:10.3354/meps08474

Berelson, W. M., Balch, W. M., Najjar, R., Feely, R. A., Sabine, C., Lee, K., 2007. Relating estimates of $CaCO_3$ production, export, and dissolution in the water column to measurements of $CaCO_3$ rain into sediment traps and dissolution on the sea floor: A revised global carbonate budget. Global Biogeochem. Cy., 21, 1.

Berge, T., Hansen, P.J., Moestrup, Ø., 2008. Feeding mechanism, prey specificity and growth in light and dark of the plastidic dinoflagellate *Karlodinium armiger*. Aquat. Microb. Ecol. 50, 279–288. doi:10.3354/ame01165

Berge, T., Poulsen, L.K., Moldrup, M., Daugbjerg, N., Juel Hansen, P., 2012. Marine microalgae attack and feed on metazoans. ISME J. 6, 1926–1936. doi:10.1038/ismej.2012.29

Billard, C., 1994. Life cycles, in Green, J. C. and Leadbeater, B. S. C. (eds) The Haptophyte Algae. Clarendon Press, Oxford, Systematics Association Special Volume, No. 51, 167-186.

Birchill, A.J., A. Milne, E. M. S. Woodward, A. L. Annett, W. Giebert, S. Ussher, P. J. Worsfold, D. Rusiecka, E. P. Achterberg, C. Harris, M. Gledhill & M. C. Lohan, 2017. Seasonal iron depletion in temperate shelf seas. Geophys. Res. Lett, 44, 17, 8987-8996.

Bligh EG, J, D.W., 1959. A rapid method of total lipid extraction and purification. Can. J. Biochem. Physiol. 37, 911–917. doi:dx.doi.org/10,1139/cjm2014-0700

Bonaldo, Roberta M., Hay, Mark E., 2014. Seaweed-coral Interactions: Variance in Seaweed Allelopathy, Coral Susceptibility, and Potential Effects on Coral Resilience. PLoS One, 9 (1), e85786. doi: 10.1371/journal.pone.0085786

Bopp, L., Monfray, P., Aumont, O., Dufresne, J.-L., Le Treut, H., Madec, G., Terray, L., Orr, J.C., 2001. Potential impact of climate change on marine export production. Global Biogeochem. Cycles 15, 81–99. doi:10.1029/1999GB001256

Bown, P. R. 1998. Calcareous nanofossil biostratigraphy. Chapman & Hall, p.315.

Boyd, P.W., Trull, T.W., 2007. Understanding the export of biogenic particles in oceanic waters: Is there consensus? Prog. Oceanogr. 72, 276–312. doi:10.1016/j.pocean.2006.10.007

Boye, M., Adjou, M.A., Dulaquais, G., Tréguer, P., 2017. Trace metal limitations (Co, Zn) increase PIC/POC ratio in coccolithophore *Emiliania huxleyi*. Mar. Chem. 192, 22–

31. doi:10.1016/j.marchem.2017.03.006

Brand, L.E., Sunda, W.G., Guillard, R.R.L., 1983. Limitation of marine phytoplankton reproductive rates by zinc, manganese, and iron. Limnol. Oceanogr. 28, 1182–1198. doi:10.4319/lo.1983.28.6.1182

Bratbak, G., Egge, J.K., Heldal, M., 1993. Viral mortality of the marine alga *Emiliania huxleyi* ( Haptophyceae ) and termination of algal blooms. Mar. Ecol. Prog. Ser. 93, 39–48.

Breckels, Mark N., Roberts, Emily C., Archer, Stephen D., Malin, Gill., Steinke, M., 2011. The role of dissolved infochemicals in mediating predator – prey interactions in the heterotrophic dinoflagellate *Oxyrrhis marina*. J. Plankton Res. 33 (4), 629 – 639.

Broecker, W. S., Clark, E., 2009. Ratio of coccolith $CaCO_3$ to foraminifera $CaCO_3$ in late holocene deep sea sediments, Paleoceanography, 24. doi: 10.1029/2009PA001731

Brussaard, C., Kempers, R., Kop, A., Riegman, R., Heldal, M., 1996. Virus-like particles in a summer bloom of *Emiliania huxleyi* in the North Sea. Aquat. Microb. Ecol. 10, 105–113. doi:10.3354/ame010105

Buitenhuis, E., van Bleijswijk, J., Bakker, D., Veldhuis, M., 1996. Trends in inorganic and organic carbon in a bloom of *Emiliania huxleyi* in the North Sea. Mar. Ecol. Prog. Ser. 143, 271–282. doi:10.3354/meps143271

Burkill, Peter H., Archer, Stephen D., Robinson, Carol., Nightingale, Philip D., Groom, Stephen B., Tarran, Glen A., Zubkov, Mikhail V., 2002. Dimethyl sulphide biogeochemistry within a coccolithophore bloom (DISCO): an overview. Deep Sea Res. Part II Top. Stud. Oceanogr. 49, 2863 – 2885.

Calbet, A., 2001. Mesozooplankton grazing effect on primary production : A global comparative analysis in marine ecosystems. Limnol. Oceanogr. 46, 51–57. doi:10.4319/lo.2001.46.7.1824

Calbet, A., Landry, M.R., 2004. Phytoplankton growth, microzooplankton grazing, and carbon cycling in marine systems. Limnol. Oceanogr. 49, 51–57. doi:10.4319/lo.2004.49.1.0051

Calbet, A., Saiz, E., 2013. Effects of trophic cascades in dilution grazing experiments: From artificial saturated feeding responses to positive slopes. J. Plankton Res. 35, 1183–1191. doi:10.1093/plankt/fbt067

Campbell, L., Nolla, H. A., Vaulot, D., 1994. The importance of *Prochlorococcus* to

community structure in the central Pacific Ocean. Limnol. Oceanogr. 39, 954-961.

Caron, D.A., Hutchins, D.A., 2013. The effects of changing climate on microzooplankton grazing and community structure: drivers, predictions and knowledge gaps. J. Plankton Res. 35, 235–252. doi:10.1093/plankt/fbs091

Caron, D.A., Peele, E.R., Lim, E.L., Dennett, M.R., 1999. Picoplankton and nanoplankton and their trophic coupling in surface waters of the Sargasso Sea south of Bermuda. Limnol. Oceanogr. 44, 259–272. doi:10.4319/lo.1999.44.2.0259

Caron, D. A., Lim, E. L., Miceli, G., Waterbury, J. B., Valois, F.W., 1991. Grazing and utilization of chroococcoid cyanobacteria and heterotrophic bacteria by protozoa in laboratory cultures and a coastal plankton community. Mar. Ecol. Prog. Ser. 76, 205-217.

Cerino, F., Malinverno, E., Fornasaro, D., Kralj, M., Cabrini, M., 2017. Coccolithophore diversity and dynamics at a coastal site in the Gulf of Trieste (northern Adriatic Sea). Estuar. Coast. Shelf Sci. 196, 331–345. doi:10.1016/j.ecss.2017.07.013

Charalampopoulou, A., Poulton, A.J., Bakker, D.C.E., Lucas, M.I., Stinchcombe, M.C., Tyrrell, T., 2016. Environmental drivers of coccolithophore abundance and calcification across Drake Passage (Southern Ocean). Biogeosciences 13, 5917–5935. doi:10.5194/bg-13-5917-2016

Charalampopoulou, A., Poulton, A.J., Tyrrell, T., Lucas, M.I., 2011. Irradiance and pH affect coccolithophore community composition on a transect between the North Sea and the Arctic Ocean. Mar. Ecol. Prog. Ser. 431, 25–43. doi:10.3354/meps09140

Chen, B., Landry, M.R., Huang, B., Liu, H., 2012. Does warming enhance the effect of microzooplankton grazing on marine phytoplankton in the ocean? Limnol. Oceanogr. 57, 519–526. doi:10.4319/lo.2012.57.2.0519

Chen, B., Liu, H., 2010. Relationships between phytoplankton growth and cell size in surface oceans: Interactive effects of temperature, nutrients, and grazing. Limnol. Oceanogr. 55, 965–972. doi:10.4319/lo.2010.55.3.0965

Chesson, J., 1978. Measuring preference in the selective predation. Ecology, 59, 211-215.

Chesson, J. 1983. The estimation and analysis of preference and its relationship to foraging models. Ecology, 64, 1297 – 1304.

Chisholm, S., Olson, R., Zettler, E., Goericke, R., Waterbury, J., Welschmeyer, N., 1988.

A novel free-living prochlorophyte abundant in the oceanic euphotic zone. Nature, 334, 340-343.

Christaki, U., Jacquet, S., Dolan, J.R., Vaulot, D., Rassoulzadegan, F., 1999. Growth and grazing on *Prochlorococcus* and *Synechococcus* by two marine ciliates. Limnol. Oceanogr. 44, 52–61.

Collins, J.R., Edwards, B.R., Fredricks, H.F., Van Mooy, B.A.S., 2016. LOBSTAHS: An Adduct-Based Lipidomics Strategy for Discovery and Identification of Oxidative Stress Biomarkers. Anal. Chem. 88, 7154–7162. doi:10.1021/acs.analchem.6b01260

Coolen, M.J.L., 2011. 7000 years of *Emiliania huxleyi* viruses in the Black Sea. Science. 333 (6041), 451–2. doi:10.1126/science.1200072

Cros, L., Estrada M. 2013. Holo-heterococcolithophore life cycles: ecological implications. Mar. Ecol. Prog. Ser. 492, 57-68.

D'Amario, B., Ziveri, P., Grelaud, M., Oviedo, A., Kralj, M., 2017. Coccolithophore haploid and diploid distribution patterns in the Mediterranean Sea: can a haplo-diploid life cycle be advantageous under climate change? J. Plankton Res. 0, 1–14. doi:10.1093/plankt/fbx044

Daniels, C.J., Poulton, A.J., Esposito, M., Paulsen, M.L., Bellerby, R., St John, M., Martin, A.P., 2015. Phytoplankton dynamics in contrasting early stage North Atlantic spring blooms: Composition, succession, and potential drivers. Biogeosciences 12, 2395–2409. doi:10.5194/bg-12-2395-2015

Daniels, C.J., Poulton, A.J., Young, J.R., Esposito, M., Humphreys, M.P., Ribas-Ribas, M., Tynan, E., Tyrrell, T., 2016. Species-specific calcite production reveals *Coccolithus pelagicus* as the key calcifier in the Arctic Ocean. Mar. Ecol. Prog. Ser. 555, 29–47. doi:10.3354/meps11820

Daniels, C.J., Sheward, R.M., Poulton, A.J., 2014. Biogeochemical implications of comparative growth rates of *Emiliania huxleyi* and *Coccolithus* species. Biogeosciences 11, 6915–6925. doi:10.5194/bg-11-6915-2014

De Vargas C., Aubry, M-P, Probert, I., Young, J. R. 2007. Origin and evolution of coccolithophores: from coastal hunters to oceanic farmers. In Falkowski, P. G., Knoll, A. H. (Eds) The Evolution of Aquatic Photoautotrophs, New York: Academic, 251-85.

Dolan, J.R., Gallegos, C.L., Moigis, A., 2000. Dilution effects on microzooplankton in dilution grazing experiments. Mar. Ecol. Prog. Ser. 200, 127–139. doi:10.3354/meps200127

Dolan, J.R., Mckeon, K., 2005. The reliability of grazing rate estimates from dilution experiments: Have we over-estimated rates of organic carbon consumption by microzooplankton? Ocean Sci. 1, 1–7. doi:10.5194/os-1-1-2005

Dolan, J.R., Simek, K., 1997. Processing of ingested matter in *Strombidium sulcatum*, a marine ciliate (Oligotrichida). Limnol. Oceanogr. 42, 393–397.

Dugdale, R.C., Wilkerson, F.P., Minas, H.J., 1995. The role of a silcate pump in driving new production. Deep. Res. I 42, 697–719.

Durak, G.M., Taylor, A.R., Walker, C.E., Probert, I., de Vargas, C., Audic, S., Schroeder, D., Brownlee, C., Wheeler, G.L., 2016. A role for diatom-like silicon transporters in calcifying coccolithophores. Nat. Commun. 7. doi:10.1038/ncomms10543

Dyhrman, S.T., Haley, S.T., Birkeland, S.R., Wurch, L.L., Cipriano, M.J., Andrew, G., Mcarthur, A.G., 2006. Long Serial Analysis of Gene Expression for Gene Discovery and Transcriptome Profiling in the Widespread Marine Coccolithophore *Emiliania huxleyi*. Appl. Environ. Microbiol. 72, 252–260. doi:10.1128/AEM.72.1.252

Dyhrman, S.T., Palenik, B., 2003. Characterization of ectoenzyme activity and phosphate-regulated proteins in the coccolithophorid *Emiliania huxleyi*. J. Plankton Res. 25, 1215–1225. doi:10.1093/plankt/fbg086

Edwards, K.F., Thomas, M.K., Klausmeier, C.A., Litchman, E., 2012. Allometric scaling and taxonomic variation in nutrient utilization traits and maximum growth rate of phytoplankton. Limnol. Oceanogr. 57, 554–566. doi:10.4319/lo.2012.57.2.0554

Egge, J. K., Aksnes, D. L. 1992. Silicate as regulating nutrient in phytoplankton competition. Mar. Ecol. Prog. Ser. 83, 281-289.

Egge, J. K., Heimdal, B. R. 1994. Blooms of phytoplakton including *Emiliania huxleyi* (Haptophyta). Effects of nutrient supply in different N:P ratios. Sarsia, 79, 333-348.

Estep, K. W., MacIntyre, F. 1989. Taxonomy, life cycle, distribution and dasmotrophy of *Chrysochromulina*: a theory accounting for scales, haptonema, muciferous bodies and toxicity. Mar. Ecol. Prog. Ser. 57, 11-21. doi: 10.3354/meps057011

Evans, C., Archer, S.D., Jacquet, S., Wilson, W.H., 2003. Direct estimates of the contribution of viral lysis and microzooplankton grazing to the decline of a *Micromonas* spp. population. Aquat. Microb. Ecol. 30, 207–219. doi:10.3354/ame030207

Evans, C., Wilson, W.H., 2008. Preferential grazing of *Oxyrrhis marina* on virus-infected

*Emiliania huxleyi*. Limnol. Oceanogr. 53, 2035–2040.

Falkowski, P. G. and Raven, J.A. 2007. Aquatic photosynthesis, Princeton University Press.

Feng, Y., Roleda, M. Y., Armstrong, E., Boyd, P. W., Hurd, C. L. 2016. Environmental controls on the growth, photosynthetic and calcification rates of a Southern Hemisphere strain of the coccolithophore *Emiliania huxleyi*. Limnol. Oceanogr. doi: 10.1002/lno.10442.

Fileman, E., Smith, T., Harris, R., 2007. Grazing by *Calanus helgolandicus and Para-Pseudocalanus* spp. on phytoplankton and protozooplankton during the spring bloom in the Celtic Sea. J. Exp. Mar. Bio. Ecol. 348, 70–84. doi:10.1016/j.jembe.2007.04.003

Fileman, E.S., Cummings, D.G., Llewellyn, C. a., 2002. Microplankton community structure and the impact of microzooplankton grazing during an Emiliania huxleyi bloom, off the Devon coast. J. Mar. Biol. Assoc. UK 82, 359–368. doi:10.1017/S0025315402005593

Finkel, Z. V., Beardall, J., Flynn, K.J., Quigg, A., Rees, T.A. V., Raven, J.A., 2010. Phytoplankton in a changing world: Cell size and elemental stoichiometry. J. Plankton Res. 32, 119–137. doi:10.1093/plankt/fbp098

First, M.R., Park, N.Y., Berrang, M.E., Meinersmann, R.J., Bernhard, J.M., Gast, R.J., Hollibaugh, J.T., 2012. Ciliate ingestion and digestion: Flow cytometric Measurements and Regrowth of a Digestion-Resistant *Campylobacter jejuni*. J. Eukaryot. Microbiol. 59, 12–19. doi:10.1111/j.1550-7408.2011.00589.x

Frada, M. J., Young, J. R., Cachao, M., Lino, S., Martins, A., Narciso, A. Probert, I., and de Vargas, C. 2010. A guide to extant coccolithophores (Calcihaptophycidae, Haptophyta) using light microscopy. J. Nannoplankton Res., 31, 2, 58-112.

Frada, M.J., Bidle, K.D., Probert, I., de Vargas, C., 2012. In situ survey of life cycle phases of the coccolithophore *Emiliania huxleyi* (Haptophyta). Environ. Microbiol. 14, 1558–1569. doi:10.1111/j.1462-2920.2012.02745.x

Franzè, G., Lavrentyev, P.J., 2014. Microzooplankton growth rates examined across a temperature gradient in the Barents Sea. PLoS One 9, e86429. doi:10.1371/journal.pone.0086429

Friedrichs, L., Hörnig, M., Schulze, L., Bertram, A., Jansen, S., Hamm, C., 2013. Size and biomechanic properties of diatom frustules influence food uptake by copepods. Mar.

Ecol. Prog. Ser. 481, 41–51. doi:10.3354/meps10227

Geisen, M., Young, J. R., Probert, I. Saez, A. G., Baumann, K. H., Sprengel, C., Bollmann, J., Cros, L. 2004. Species level variation in Coccolithophores. In Thierstein, H. R. and Young, J. R. (eds), Coccolithophores From Molecular Processes to Global Impact. Springer, London, 327-366.

Gibbs, S.J., Bown, P.R., Ridgwell, A., Young, J.R., Poulton, A.J., O'Dea, S.A., 2016. Ocean warming, not acidification, controlled coccolithophore response during past greenhouse climate change. Geology 44, 59–62. doi:10.1130/G37273.1

Gibbs, S.J., Poulton, A.J., Bown, P.R., Daniels, C.J., Hopkins, J., Young, J.R., Jones, H.L., Thiemann, G.J., O'Dea, S.A., Newsam, C., 2013. Species-specific growth response of coccolithophores to Palaeocene–Eocene environmental change. Nat. Geosci. 6, 218–222. doi:10.1038/ngeo1719

Giering, S. L. C. Wells, S. R., Mayers, K. M. J., Schuster, H., Cornwell, L., Fileman, E, Atkinson, A., Cook, K. B., Preece, C., Mayor, D. J. 2017. Trophic position of shelf sea zooplankton communities vary in space and time: insights from stable isotope and biovolume spectra analyses. Prog. Oceanogr. doi: 10.1016/j.pocean.2018.03.012

Gifford, D.J., 1988. Impact of grazing by microzooplankton in the Northwest Arm of Halifax Harbour, Nova Scotia. Mar. Ecol. Prog. Ser. 47, 249–258. doi:10.3354/meps047249

Gifford, D. J., Dagg, M. J. 1988. Feeding of the estuarine copepod, *Acartia tonsa* Dana: carnivory vs. herbivory in natrual microplankton assemblages. Bull. Mar. Sci. 43, 458-468.

Gifford, D.J., 1985. Laboratory culture of marine planktonic oligotrichs (Ciliophora, Oligotrichida). Mar. Ecol. Prog. Ser. 23, 257–267. doi:10.3354/meps023257

Gonzalez, J.M., Sherr, B.F., Sherr, E.B., 1993. Digestive enzyme activity as a quantitative measure of protistan grazing: the acid lysozyme assay for bacterivory. Mar. Ecol. Prog. Ser. 100, 197–206. doi:10.3354/meps100197

Gowing, M.M., Silver, M.W., 1985. Minipellets: A new and abundant size class of marine fecal pellets. J. Mar. Res. 43, 395–418. doi:10.1357/002224085788438676

Graff, J. R. Rynearson, T. A. 2011. Extraction method influences the recovery of phytoplankton pigments from natural assemblages. Limnol. Oceanogr. Methods, 9, 129-139.

Gruber, N., 2011. Warming up, turning sour, losing breath: ocean biogeochemistry under

global change. Philos. Trans. R. Soc. A 369, 1980–1996. doi:10.1098/rsta.2011.0003

Guillard, R. R. L., Kilham, P. 1977. The ecology of marine planktonic diatoms. In Werner, D. (Ed) The biology of diatoms. Blackwell, London, 372-469.

Gutiérrez-Rodríguez, A., Latasa, M., Agustí, S., Duarte, C.M., 2011. Distribution and contribution of major phytoplankton groups to carbon cycling across contrasting conditions of the subtropical northeast Atlantic Ocean. Deep. Res. Part I Oceanogr. Res. Pap. 58, 1115–1129. doi:10.1016/j.dsr.2011.08.003

Haddock, S.H.D., Moline, M.A., Case, J.F., 2010. Bioluminescence in the sea., Annual review of marine science. doi:10.1146/annurev-marine-120308-081028

Haidar, A.T., Thierstein, H.R., 2001. Coccolithophore dynamics off Bermuda (N. Atlantic). Deep. Res. Part II Top. Stud. Oceanogr. 48, 1925–1956. doi:10.1016/S0967-0645(00)00169-7

Hajdu, S., Larsson, U. Moestrup, Ø., 1996. Seasonal dynamics of *Chrysochromulina* species (Prymnesiophyceae) in a coastal area and a nutrient-enriched inlet of the Northern Baltic Proper. Bot. Mar. 39, 281-295.

Hamm, C.E., Merkel, R., Springer, O., Jurkojc, P., Maiert, C., Prechtelt, K., Smetacek, V., 2003. Architecture and material properties of diatom shells provide effective mechanical protection. Nature 421, 841–843. doi:10.1038/nature01416

Hammer, A., Grüttner, C., Schumann, R., 2001. New biocompatible tracer particles: Use for estimation of microzooplankton grazing, digestion, and growth rates. Aquat. Microb. Ecol. 24, 153–161. doi:10.3354/ame024153

Hansen, F.C., Witte, H.J., Passarge, J., 1996. Grazing in the heterotrophic dinoflagellate *Oxyrrhis marina*: size selectivity and preference for calcified *Emiliania huxleyi* cells. Aquat. Microb. Ecol. 10, 307–313. doi:10.3354/ame010307

Harris, R.P., 1994. Zooplankton grazing on the coccolithophore *Emiliania huxleyi* and its role in inorganic carbon flux. Mar. Biol. 119, 431–439. doi:10.1007/BF00347540

Harvey, E.L., Bidle, K.D., Johnson, M.D., 2015. Consequences of strain variability and calcification in *Emiliania huxleyi* on microzooplankton grazing. J. Plankton Res. 37, 1137–1148. doi:10.1093/plankt/fbv081

Henson, S. A., Sanders, R., Madsen, E. 2012. Global patterns in efficiency of particulate organic carbon export and transfer to the deep ocean. Glob. Biogeochem. Cycles. 26: GB1028. doi: 10.1029/2011GB004099

Hickman, A.E., Holligan, P.M., Moore, C.M., Sharples, J., Krivtsov, V., Palmer, M.R., 2009. Distribution and chromatic adaptation of phytoplankton within a shelf sea thermocline. Limnol. Oceanogr. 54, 525–536. doi:10.4319/lo.2009.54.2.0525

Holligan, P., Viollier, M., Harbour, D., Camus, P., Champagne-Philippe, M., 1983. Satellie and ship studies of coccolithophore production along a continental shelf edge. Lett. to Nat. 304, 339–342. doi:10.1038/304339a0

Holligan, P.M., Fernández, E., Aiken, J., Balch, W.M., Boyd, P., Burkill, P.H., Finch, M., Groom, S.B., Malin, G., Muller, K., Purdie, D. a., Robinson, C., Trees, C.C., Turner, S.M., van der Wal, P., 1993. A biogeochemical study of the coccolithophore, *Emiliania huxleyi*, in the North Atlantic. Global Biogeochem. Cycles 7, 879–900. doi:10.1029/93GB01731

Hopkins, J., Henson, S.A., Painter, S.C., Tyrrell, T., Poulton, A.J., 2015. Phenological characteristics of global coccolithophore blooms. Global Biogeochem. Cycles 29, 239–253. doi:10.1002/2014GB004919.Received

Horner, R.A., Garrison, D.L., Plumley, F.G., 1997. Harmful algal blooms and red tide problems on the U.S. west coast. Limnol. Oceanogr. 42, 1076–1088.

Houdan, A., Probert, I., Zatylny, C., Veron, B., Billard, C., 2006. Ecology of oceanic coccolithophores. I. Nutritional preferences of the two stages in the life cycle of *Coccolithus braarudii* and *Calcidiscus leptoporus*. Aquat. Microb. Ecol. 44, 291–301. doi:10.3354/ame044291

Humphreys, M., Moore, M. 2015. RRS Discovery cruise DY033, Cruise Rep.1, pp. 37. Natl. Oceanogr. Centr. Southampton, Southampton, U. K. (Available at https://www.bodc.ac.uk/resources/inventories/cruise_inventory/report/15014/)

Humphreys, M. P., Achterberg, E. P., Chowdhury, M. Z. H., Griffiths, A. M., Hartman, S. E., Hopkins, J. E., Hull, T., Kivimae, C., Smilenova, A., Wihsgott, J., Woodward, E. M. S., Moore, C. M. 2017. Mechanisms for nutrient-conserving carbon pump in a seasonally stratified, temperate continental shelf sea. Prog. Oceanogr. in press.

Hunter, J.E., Brandsma, J., Dymond, M.K., Koster, G., Moore, C.M., Postle, A.D., Mills, R.A., Attard, G.S., 2018. Lipidomics of *Thalassiosira pseudonana* under Phosphorus Stress Reveal Underlying Phospholipid Substitution Dynamics and Novel Diglycosylceramide Substitutes. Appl. Environ. Microbiol. 84, 1–17. doi:https://doi.org/10.1128/AEM.02034-17.

Hunter, J.E., Frada, M.J., Fredricks, H.F., Vardi, A., Van Mooy, B.A.S., 2015. Targeted

and untargeted lipidomics of *Emiliania huxleyi* viral infection and life cycle phases highlights molecular biomarkers of infection, susceptibility, and ploidy. Front. Mar. Sci. 2, 81. doi:10.3389/fmars.2015.00081

Hydes, D. M., Aoyama, A., Aminot, A., Bakker, K., Becker, S., Coverly, S., Daniels, A., Dickson, A., Grosson, O., Kerouel, R., 2010. Determination of dissolved nutrients (N, P, Si) in seawater with high precision and inter.comparability using gas segmented continuous flow analysers, The GO-SHIP Repeat Hydrography Manual: A collection of export reports and guidelines; IOCCP report No. 14, ICPO publication series No. 134, version 1.

Iglesias-Rodriguez, M.D., Brown, C.W., Doney, S.C., Kleypas, J.A., Kolber, D., Kolber, Z., Hayes, P.K., Falkowski, P.G., 2002. Representing key phytoplankton functional groups in ocean carbon cycle models: Coccolithophorids. Global Biogeochem. Cycles 16, 47-1-47–20. doi:10.1029/2001GB001454

Iglesias-Rodriguez, M.D., Halloran, P.R., Rickaby, R.E.M., Hall, I.R., Colmenero-Hidalgo, E., Gittins, J.R., Green, D.R.H., Tyrrell, T., Gibbs, S.J., von Dassow, P., Rehm, E., Armbrust, E. V, Boessenkool, K.P., 2008. Phytoplankton calcification in a high-CO2 world. Science. 320, 336–340. doi:10.1126/science.1154122

Ishizaka, J., Harada, K., Ishikawa, K., Kiyosawa, H., Furusawa, H., Watanabe, Y., Ishida, H., Suzuki, K., Handa, N., Takahashi, M. 1997. Size and taxonomic plankton community structure and carbon flow at the equator, 175$^{o}$E during 1990-1994. Deep Sea Res. II, 44, 1927-1949.

Jakobsen, H.H., Hansen, P.J., 1997. Prey size selection, grazing and growth response of the small heterotrophic dinoflagellate *Gymnodinium* sp. and the ciliate *Balanion comatum* - A comparative study. Mar. Ecol. Prog. Ser. 158, 75–86. doi:10.3354/meps158075

Jaya, B.N., Hoffmann, R., Kirchlechner, C., Dehm, G., Scheu, C., Langer, G., 2016. Coccospheres confer mechanical protection: New evidence for an old hypothesis. Acta Biomater. 42, 258–264. doi:10.1016/j.actbio.2016.07.036

Jeong, H.J., Du Yoo, Y., Kim, J.S., Seong, K.A., Kang, N.S., Kim, T.H., 2010. Growth, feeding and ecological roles of the mixotrophic and heterotrophic dinoflagellates in marine planktonic food webs. Ocean Sci. J. 45, 65–91. doi:10.1007/s12601-010-0007-2

Jespersen, A. M. Christoffersen, K. 1987. Measurements of chlorophyll-*a* from phytoplankton using ethanol as extraction solvent. Arch. Hydrobiol. 109. 445-454.

Jiao, N., Herndl, G.J., Hansell, D.A., Benner, R., Kattner, G., Wilhelm, S.W., Kirchman, D.L., Weinbauer, M.G., Luo, T., Chen, F., Azam, F., 2010. Carbon Storage in the Global Ocean. Nat. Rev. Microbiol. 8, 593–599. doi:10.1038/nrmicro2386

Jickells, T.D., Liss, P.S., Broadgate, W., Turner, S., Kettle, A.J., Read, J., Baker, J., Cardenas, L.M., Carse, F., Hamren-Larssen, M., Spokes, L., Steinke, M., Thompson, A., Watson, A., Archer, S.D., Bellergy, R.G.J., Law, C.S., Nightingale, P.D., Liddicoat, M.I., Widdicombe, C.E., Bowie, A., Gilpin, L.C., Moncoiffe, G., Savidge, G., Preston, T., Hadziabdic, P., Frost, T., Upstill-Goddard, R., Pedros-Alio, C., Simo, R., Jackson, A., Allen, A., DeGrandpre, M.D., 2008. A Lagrangian biogeochemical study of an eddy in the Northeast Atlantic. Prog. Oceanogr. 76, 266 – 398.

Karatsolis, B.T., Triantaphyllou, M. V., Dimiza, M.D., Malinverno, E., Lagaria, A., Mara, P., Archontikis, O., Psarra, S., 2016. Coccolithophore assemblage response to Black Sea Water inflow into the North Aegean Sea (NE Mediterranean). Cont. Shelf Res. 149, 138–150. doi:10.1016/j.csr.2016.12.005

Kawachi, M., Inouye, I., Maeda, O., Chihara, M. 1991. The haptonema as a food-capturing device: Observations on *Chrysochromulina hirta* (Prymnesiophyceaea). J. Phycol. 30, 563-573.

Klaas, C., Archer, D.E., 2002. Association of sinking organic matter with various types of mineral ballast in the deep sea: Implications for the rain ratio. Global Biogeochem. Cycles 16, 1–14. doi:10.1029/2001GB001765

Klein Breteler, W.C.M., Koski, M., Rampen, S., 2004. Role of essential lipids in copepod nutrition: No evidence for trophic upgrading of food quality by a marine ciliate. Mar. Ecol. Prog. Ser. 274, 199–208. doi:10.3354/meps274199

Klein Breteler, W.C.M., Schogt, N., Baas, M., Schouten, S., Kraay, G.W., 1999. Trophic upgrading of food quality by protozoans enhancing copepod growth: Role of essential lipids. Mar. Biol. 135, 191–198. doi:10.1007/s002270050616

Kolb, A., Strom, S., 2013. An inducible antipredatory defense in haploid cells of the marine microalga *Emiliania huxleyi* ( Prymnesiophyceae ). Limnol. Oceanogr. 58, 932–944. doi:10.4319/lo.2013.58.3.0932

Krueger-Hadfield, S. a., Balestreri, C., Schroeder, J., Highfield, a., Helaouët, P., Allum, J., Moate, R., Lohbeck, K.T., Miller, P.I., Riebesell, U., Reusch, T.B.H., Rickaby, R.E.M., Young, J., Hallegraeff, G., Brownlee, C., Schroeder, D.C., 2014. Genotyping an *Emiliania huxleyi* (Prymnesiophyceae) bloom event in the North Sea reveals evidence of asexual reproduction. Biogeosciences Discuss. 11, 4359–4408.

doi:10.5194/bgd-11-4359-2014

Krumhardt, K.M., Lovenduski, N.S., Freeman, N.M., Bates, N.R., 2016. Apparent increase in coccolithophore abundance in the subtropical North Atlantic from 1990 to 2014. Biogeosciences 13, 1163–1177. doi:10.5194/bg-13-1163-2016

Krumhardt, K.M., Lovenduski, N.S., Iglesias-rodriguez, M.D., Kleypas, J.A., 2017. Coccolithophore growth and calcification in a changing ocean. Prog. Oceanogr. doi:10.1016/j.pocean.2017.10.007

Landry, M.R., Hassett, R.P., 1982. Estimating the grazing impact of marine micro-zooplankton. Mar. Biol. 67, 283–288. doi:10.1007/BF00397668

Landry, M.R., Kirshtein, J., Constantinou, J., 1995. A refined dilution technique for measuring the community grazing impact of microzooplankton, with experimental tests in the central equatorial Pacific. Mar. Ecol. Prog. Ser. 120, 53–63. doi:10.3354/meps120053

Langer, G., Nehrke, G., Jansen, S., 2007. Dissolution of *Calcidiscus leptoporus* coccoliths in copepod guts? A morphological study. Mar. Ecol. Prog. Ser. 331, 139–146. doi:10.3354/meps331139

Larsen, A., Egge, J.K., Nejstgaard, J.C., Di Capua, I., Thyrhaug, R., Bratbak, G., Thingstad, T.F., 2015. Contrasting response to nutrient manipulation in Arctic mesocosms are reproduced by a minimum microbial food web model. Limnol. Oceanogr. 60, 360–374. doi:10.1002/lno.10025

Larsen, A., Flaten, G.A.F., Sandaa, R.-A., Castberg, T., Thyrhaug, R., Erga, S.R., Jacquet, S., Bratbak, G., 2004. Spring phytoplankton bloom dynamics in Norwegian coastal waters: Microbial community succession and diversity. Limnol. Oceanogr. 49, 180–190. doi:10.4319/lo.2004.49.1.0180

Latasa, M., Cabello, A.M., Morán, X.A.G., Massana, R., Scharek, R., 2017. Distribution of phytoplankton groups within the deep chlorophyll maximum. Limnol. Oceanogr. 62, 665–685. doi:10.1002/lno.10452

Latasa, M., Morán, X.A.G., Scharek, R., Estrada, M., 2005. Estimating the carbon flux through main phytoplankton groups in the northwestern Mediterranean. Limnol. Oceanogr. 50, 1447–1458. doi:10.4319/lo.2005.50.5.1447

Leblanc, K., Quéguiner, B., Diaz, F., Cornet, V., Michel-Rodriguez, M., Durrieu de Madron, X., Bowler, C., Malviya, S., Thyssen, M., Grégori, G., Rembauville, M., Grosso, O., Poulain, J., de Vargas, C., Pujo-Pay, M., Conan, P., 2018.

Nanoplanktonic diatoms are globally overlooked but play a role in spring blooms and carbon export. Nat. Commun. 9, 1–12. doi:10.1038/s41467-018-03376-9

León, P., Walsham, P., Bresnan, E., Hartman, S.E., Hughes, S., Mackenzie, K., Webster, L., 2018. Seasonal variability of the carbonate system and coccolithophore *Emiliania huxleyi* at a Scottish Coastal Observatory monitoring site. Estuar. Coast. Shelf Sci. doi:10.1016/j.ecss.2018.01.011

Lessard, E.J., Murrell, M.C., 1998. Microzooplankton herbivory and phytoplankton growth in the northwestern Sargasso Sea. Aquat. Microb. Ecol. 16, 173–188. doi:10.3354/ame016173

Lewin-Epstein, Ohad., Aharonov, Ranit., Hadany, Lilach., 2017. Microbes can help explain the evolution of host altruism. Nat. Commun. 8, 14040. doi: 10.1038/ncomms14040

Liu, H., Aris-Brosou, S., Probert, I., De Vargas, C., 2010. A time line of the environmental genetics of the haptophytes. Mol. Biol. Evol. 27, 161–176. doi:10.1093/molbev/msp222

Löder, M.G.J., Meunier, C., Wiltshire, K.H., Boersma, M., Aberle, N., 2011. The role of ciliates, heterotrophic dinoflagellates and copepods in structuring spring plankton communities at Helgoland Roads, North Sea. Mar. Biol. 158, 1551-1580.

Lovejoy, C., Vincent, W.F., Bonilla, S., Roy, S., Martineau, M.J., Terrado, R., Potvin, M., Massana, R., Pedrós-Alió, C., 2007. Distribution, phylogeny, and growth of cold-adapted picoprasinophytes in arctic seas. J. Phycol. 43, 78–89. doi:10.1111/j.1529-8817.2006.00310.x

Lynn, D. H. 2008. The Ciliates Protozoa. Characerization, Classification, and Guide to the Literature, 3rd ed. Springer, Dordrecht.

MacRae, R.A., Fensome, R. a., Williams, G.L., 1996. Fossil dinoflagellate diversity, originations, and extinctions and their significance. Can. J. Bot. 74, 1687–1694. doi:10.1139/b96-205

Malin, G., Turner, S., Liss, P., Holligan, P., Harbour, D., 1993. Dimethylsulphide and dimethylsulphoniopropionate in the Northeast atlantic during the summer coccolithophore bloom. Deep. Res. Part I 40, 1487–1508. doi:10.1016/0967-0637(93)90125-M

Malitsky, S., Ziv, C., Rosenwasser, S., Zheng, S., Schatz, D., Porat, Z., Ben-Dor, S., Aharoni, A., Vardi, A., 2016. Viral infection of the marine alga *Emiliania huxleyi* triggers lipidome remodeling and induces the production of highly saturated

triacylglycerol. New Phytol. 210, 88–96. doi:10.1111/nph.13852

Manly, B. F. J. 1974, A model for certain types of selection experiments. Biometrics, 30, 281-294.

Marañón, E., 2015. Cell Size as a Key Determinant of Phytoplankton Metabolism and Community Structure. Ann. Rev. Mar. Sci. 7, 241–264. doi:10.1146/annurev-marine-010814-015955

Marañón, E., González, N., 1997. Primary production, calcification and macromolecular synthesis in a bloom of the coccolithophore *Emiliania huxleyi* in the North Sea. Mar. Ecol. Prog. Ser. 157, 61–77. doi:10.3354/meps157061

Margalef, R., 1997. Turbulence and marine life. Sci. Mar. 61, 109–123.

Margalef, R., 1978. Life-forms of phytoplankton as survival alternatives in an unstable environment. Oceanol. Acta 1, 493–509.

Martinez Martinez, J., Schroeder, D.C., Larsen, A., Bratbak, G., Wilson, W.H., 2007. Molecular dynamics of *Emiliania huxleyi* and cooccurring viruses during two separate mesocosm studies. Appl. Environ. Microbiol. 73, 554–562. doi:10.1128/AEM.00864-06

Mayers, K.M.J., Poulton, A.J., Daniels, C.J., Wells, S.R., Woodward, E.M.S., Tarran, G.A., Widdicombe, C.E., Mayor, D.J., Atkinson, A., Giering, S.L.C., 2018. Growth and mortality of coccolithophore during spring in a temperate Shelf Sea (Celtic Sea, April 2015). Prog. Oceanogr. 0–1. doi:10.1016/j.pocean.2018.02.024

Mayers, T.J., Bramucci, A.R., Yakimovich, K.M., Case, R.J., 2016. A bacterial pathogen displaying temperature-enhanced virulence of the microalga *Emiliania huxleyi*. Front. Microbiol. 7:892, 1–15. doi:10.3389/fmicb.2016.00892

Menden-Deuer, S., Lessard, Evelyn J., 2000. Carbon to volume relationships for dinoflagellates, diatoms and other protist plankton. Limnol. Oceanogr., 45 (3), 569-579.

Monier, A., Pagarete, A., de Vargas, C., Allen, M.J., Read, B., Claverie, J.-M., Ogata, H., 2009. Horizontal gene transfer of an entire metabolic pathway between a eukaryotic alga and its DNA virus. Genome Res. 19, 1441–9. doi:10.1101/gr.091686.109

Monteiro, F.M., Bach, L.T., Brownlee, C., Bown, P., Rickaby, R.E.M., Poulton, A.J., Tyrrell, T., Beaufort, L., Dutkiewicz, S., Gibbs, S., Gutowska, M.A., Lee, R., Riebesell, U., Young, J., Ridgwell, A., 2016. Why marine phytoplankton calcify. Sci.

Adv. 2, 1–14. doi:10.1126/sciadv.1501822

Moore, C.M., Mills, M.M., Achterberg, E.P., Geider, R.J., LaRoche, J., Lucas, M.I., McDonagh, E.L., Pan, X., Poulton, A.J., Rijkenberg, M.J.A., Suggett, D.J., Ussher, S.J., Woodward, E.M.S., 2009. Large-scale distribution of Atlantic nitrogen fixation controlled by iron availability. Nat. Geosci. 2, 867–871. doi:10.1038/ngeo667

Moore, C.M., Mills, M.M., Arrigo, K.R., Berman-Frank, I., Bopp, L., Boyd, P.W., Galbraith, E.D., Geider, R.J., Guieu, C., Jaccard, S.L., Jickells, T.D., La Roche, J., Lenton, T.M., Mahowald, N.M., Marañón, E., Marinov, I., Moore, J.K., Nakatsuka, T., Oschlies, A., Saito, M.A., Thingstad, T.F., Tsuda, A., Ulloa, O., 2013. Processes and patterns of oceanic nutrient limitation. Nat. Geosci. 6, 701–710. doi:10.1038/ngeo1765

Morison, F., Menden-Deuer, S., 2017. Doing more with less? Balancing sampling resolution and effort in measurements of protistan growth and grazing-rates. Limnol. Oceanogr. Methods 15, 794–809. doi:10.1002/lom3.10200

Morison, F., Menden-Deuer, S., 2015. Early spring phytoplankton dynamics in the subpolar north atlantic: The influence of protistan herbivory. Limnol. Oceanogr. 60, 1298–1313. doi:10.1002/lno.10099

Muller, H., Schlegel, A., 1999. Responses of three fresh water planktonic ciliates with different feeding modes to cryptophyte and diatom prey. Aquat. Microb. Ecol. 17, 49-60.

Müller, M.N., Antia, A.N., LaRoche, J., 2008. Influence of cell cycle phase on calcification in the coccolithophore *Emiliania huxleyi.* Limnol. Oceanogr. 2008, 506–512. doi:10.4319/lo.2008.53.2.0506

Müller, M.N., Lebrator, M., Riebesell, U., Barcelos e Ramos, J., Schulz, K. G., Blanco-Ameijeiras, S., Sett, S., Eisenhauer, A., Stoll, H. M. 2014. Influence of temperature and $CO_2$ on the strontium and magnesium composition of coccolithophore calcite. Biogeosci. 11, 1065-1075. doi: 10.5194/bg-11-1065-2014

Müller, M.N., Trull, T.W., Hallegraeff, G.M., 2017. Independence of nutrient limitation and carbon dioxide impacts on the Southern Ocean coccolithophore *Emiliania huxleyi.* ISME J. 11, 1777–1787. doi:10.1038/ismej.2017.53

Nagata, T., Kirchman, D.L., 1992. Release of macromolecular organic complexes by heterotrophic marine flagellates. Mar. Ecol. Prog. Ser. 83, 233–240. doi:10.3354/meps083233

Nejstgaard, J.C., Frischer, M.E., Simonelli, P., Troedsson, C., Brakel, M., Adiyaman, F., Sazhin, A.F., Artigas, L.F., 2008. Quantitative PCR to estimate copepod feeding. Mar. Biol. 153, 565–577. doi:10.1007/s00227-007-0830-x

Nejstgaard, J.C., Gismervik, I., Solberg, P.T., 1997. Feeding and reproduction by *Calanus finmarchicus*, and microzooplankton grazing during mesocosm blooms of diatoms and the coccolithophore *Emiliania huxleyi*. Mar. Ecol. Prog. Ser. 147, 197–217. doi:10.3354/meps147197

Nejstgaard, J.C., Naustvoll, L.J., Sazhin, A., 2001. Correcting for underestimation of microzooplankton grazing in bottle incubation experiments with mesozooplankton. Mar. Ecol. Prog. Ser. 221, 59–75. doi:10.3354/meps221059

Nelson, D.M., Tréguer, P., Brzezinski, M.A., Leynaert, A., Quéguiner, B., 1995. Production and dissolution of biogenic silica in the ocean: Revised global estimates, comparison with regional data and relationship to biogenic sedimentation. Global Biogeochem. Cycles 9, 359–372. doi:10.1029/95GB01070

Neukermans, G., Oziel, L., Babin, M., 2018. Increased intrusion of warming Atlantic waters leads to rapid expansion of temperate phytoplankton in the Arctic. Glob. Chang. Biol. 1–9. doi:10.1111/gcb.14075

Nielsdóttir, M.C., Moore, C.M., Sanders, R., Hinz, D.J., Achterberg, E.P., 2009. Iron limitation of the postbloom phytoplankton communities in the Iceland Basin. Global Biogeochem. Cycles 23, 1–13. doi:10.1029/2008GB003410

Nissen, C., Vogt, M., Munnich, M., Gruber, N., Haumann, F. A. 2018. Factors controlling coccolithophore biogeography in the Southern Ocean, Biogeosci. Discuss. In review. doi: https://doi.org/10.5194/bg-2018-157

Not, F., Latasa, M., Marie, D., Cariou, T., Vaulot, D., Simon, N., 2004. A single species, *Micromonas pusilla* (Prasinophyceae), dominates the eukaryotic picoplankton in the Western English Channel. Appl. Environ. Microbiol. 70, 4064–4072. doi:10.1128/AEM.70.7.4064

Oksanen, J., Blanchet, F. G., Friendly, M., Kindt, R., Legendre, P., McGlinn, D., Minchin, P. R., O'Hara, R. B., Simpson, G. L., Solymos, P., Stevens, M. H. H., Szoecs, E., Wagner, H. 2016. vegan: Community Ecology Package.

Olson, M.B., Strom, S.L., 2002. Phytoplankton growth, microzooplankton herbivory and community structure in the southeast Bering Sea: Insight into the formation and temporal persistence of an *Emiliania huxleyi* bloom. Deep. Res. Part II Top. Stud.

Oceanogr. 49, 5969–5990. doi:10.1016/S0967-0645(02)00329-6

Opik, H., Flynn, K.J., 1989. The digestive process of the dinoflagellate *Oxyrrhis marina* Dujardin, feeding on the chlorophyte, *Dunaliella primolecta* Butcher: a combined study of ultratructure and free amino acids. New Phytol. 113, 143–151.

Paasche, E., Brutak, S., 1994. Enhanced calcification in the coccolithophorid *Emiliania huxleyi* (Haptophycaea) under phosphorus limitation, Phycologia, 33, 324-330.

Paasche, E., 2002. A review of the coccolithophorid *Emiliania huxleyi* (Prymnesiophyceae), with particular reference to growth, coccolith formation, and calcification-photosynthesis interactions. Phycologia 40, 503–529.

Pagarete, A., Allen, M.J., Wilson, W.H., Kimmance, S.A., de Vargas, C., 2009. Host-virus shift of the sphingolipid pathway along an *Emiliania huxleyi* bloom: survival of the fattest. Environ. Microbiol. 11, 2840–8. doi:10.1111/j.1462-2920.2009.02006.x

Pearson, A. Lipidomics for Geochemistry. 2014. In Holland, H. D., Turekian, K. K (Eds), Treatise on Geochemistry, Elsevier, Oxford, 291-336.

Perrin, L., Probert, I., Langer, G., Aloisi, G. 2016. Growth of the coccolithophore *Emiliania huxleyi* in light- and nutrient-limited batch reactors: relevance for the BIOSOPE deep ecological niche of coccolithophores. Biogeosci. 13, 5983-6001.

Pingree, R.D., Sinha, B., Griffiths, C.R., 1999. Seasonality of the European slope current (Goban Spur) and ocean margin exchange. Cont. Shelf Res. 19, 929–975. doi:10.1016/S0278-4343(98)00116-2

Pond, D.W., Harris, R.P., Brownlee, C., 1995. A microinjection technique using a pH-sensitive dye to determine the gut pH of *Calanus helgolandicus*. Mar. Biol. 123 (1), 75-79.

Popendorf, K. J., Fredricks, H. F., Van Mooy, B. A. S. 2013. Molecular ion-independent quantification of polay glycerolipid classes in marine plankton using triple quadrupole MS. Lipids, 48, 185-195.

Poulton, A.J., Adey, T.R., Balch, W.M., Holligan, P.M., 2007. Relating coccolithophore calcification rates to phytoplankton community dynamics: Regional differences and implications for carbon export. Deep Sea Res. Part II Top. Stud. Oceanogr. 54, 538–557. doi:10.1016/j.dsr2.2006.12.003

Poulton, A.J., Charalampopoulou, A., Young, J.R., Tarran, G.A., Lucas, M.I., Quartly, G.D., 2010. Coccolithophore dynamics in non-bloom conditions during late summer

in the central Iceland Basin (July-August 2007) 55, 1601–1613. doi:10.4319/lo.2010.55.4.1601

Poulton, A.J., Painter, S.C., Young, J.R., Bates, N.R., Bowler, B., Drapeau, D., Lyczsckowski, E., Balch, W.M., 2013. The 2008 *Emiliania huxleyi* bloom along the Patagonian Shelf: Ecology, biogeochemistry, and cellular calcification. Global Biogeochem. Cycles 27, 1023–1033. doi:10.1002/2013GB004641

Poulton, A.J., Stinchcombe, M.C., Achterberg, E.P., Bakker, D.C.E., Dumousseaud, C., Lawson, H.E., Lee, G. a., Richier, S., Suggett, D.J., Young, J.R., 2014. Coccolithophores on the north-west European shelf: Calcification rates and environmental controls. Biogeosciences 11, 3919–3940. doi:10.5194/bg-11-3919-2014

Poulton, A.J., Young, J.R., Bates, N.R., Balch, W.M., 2011. Biometry of detached *Emiliania huxleyi* coccoliths along the Patagonian Shelf. Mar. Ecol. Prog. Ser. 443, 1–17. doi:10.3354/meps09445

Poulton, A.J., Holligan, P.M., Charalampopoulou, A., Adey, T.R., 2017a. Coccolithophore ecology in the tropical and subtropical Atlantic Ocean: New perspectives from the Atlantic meridional transect (AMT) programme. Prog. Oceanogr. 1–21. doi:10.1016/j.pocean.2017.01.003

Poulton, A.J., Davis, C. E., Daniels, C. J., Mayers, K. M. J., Harris, C., Tarran, G. A., Widdicombe, C. E., Woodward, E. M. S. 2017b. Seasonal phosphorus and carbon dynamics in a temperate shelf sea (Celtic Sea). Prog. Oceanogr. doi: https://doi.org/10.1016/j.pocean.2017.11.001

Pree, B., Kuhlisch, C., Pohnert, G., Sazhin, A.F., Jakobsen, H.H., Paulsen, M.L., Frischer, M.E., Stoecker, D., Nejstgaard, J.C., Larsen, A., 2016a. A simple adjustment to test reliability of bacterivory rates derived from the dilution method. Limnol. Oceanogr. Methods 14, 114–123. doi:10.1002/lom3.10076

Pree, B., Larsen, A., Egge, J.K., Simonelli, P., Madhusoodhanan, R., Tsagaraki, T.M., Våge, S., Erga, S.R., Bratbak, G., Thingstad, T.F., 2016b. Dampened copepod-mediated trophic cascades in a microzooplankton-dominated microbial food web: A mesocosm study. Limnol. Oceanogr. 1–14. doi:10.1002/lno.10483

R Core Team, 2015. R. A Language and Environment for Statistical Computing.

Raven, J.A., Crawfurd, K., 2012. Environmental controls on coccolithophore calcification. Mar. Ecol. Prog. Ser. 470, 137–166. doi:10.3354/meps09993

Raffi, I., Backman, J., Fornaciari, E., Palike, H., Domenico, R.H., Lourens, L., Hilgen, F., 2006. A review of calcareous nannoplankton astrobiochronology encompassing the past 25 million years. Quart. Sci. Rev. 25, 3113–3137.

Ray, J.L., Althammer, J., Skaar, K.S., Simonelli, P., Larsen, A., Stoecker, D., Sazhin, A., Ijaz, U.Z., Quince, C., Nejstgaard, J.C., Frischer, M., Pohnert, G., Troedsson, C., 2016. Metabarcoding and metabolome analysis of copepod grazing reveals feeding preference and linkage to metabolite classes in dynamic microbial plankton communities. Mol. Ecol. doi:10.1111/mec.13844

Read, B. a, Kegel, J., Klute, M.J., Kuo, A., Lefebvre, S.C., Maumus, F., Mayer, C., Miller, J., Monier, A., Salamov, A., Young, J., Aguilar, M., Claverie, J.-M., Frickenhaus, S., Gonzalez, K., Herman, E.K., Lin, Y.-C., Napier, J., Ogata, H., Sarno, A.F., Shmutz, J., Schroeder, D., de Vargas, C., Verret, F., von Dassow, P., Valentin, K., Van de Peer, Y., Wheeler, G., Dacks, J.B., Delwiche, C.F., Dyhrman, S.T., Glöckner, G., John, U., Richards, T., Worden, A.Z., Zhang, X., Grigoriev, I. V, 2013. Pan genome of the phytoplankton *Emiliania* underpins its global distribution. Nature 499, 209–13. doi:10.1038/nature12221

Rees, A.P., Hope, S.B., Widdicombe, C.E., Dixon, J.L., Woodward, E.M.S., Fitzsimons, M.F., 2009. Alkaline phosphatase activity in the western English Channel: Elevations induced by high summertime rainfall. Estuar. Coast. Shelf Sci. 81, 569–574. doi:10.1016/j.ecss.2008.12.005

Rees, A.P., Woodward, E.M.S., Robinson, C., Cummings, D.G., Tarran, G.A., Joint, I., 2002. Size-fractionated nitrogen uptake and carbon fixation during a developing coccolithophore bloom in the North Sea during June 1999. Deep. Res. Part II Top. Stud. Oceanogr. 49, 2905–2927. doi:10.1016/S0967-0645(02)00063-2

Ribera d'Alcalà, M., Conversano, F., Corato, F., Licandro, P., Mangoni, O., Marino, D., Mazzocchi, M.G., Modigh, M., Montresor, M., Nardella, M., Saggiomo, V., Sarno, D., Zingone, A., 2004. Seasonal patterns in plankton communities in a pluriannual time series at a coastal Mediterranean site (Gulf of Naples): an attempt to discern recurrences and trends. Sci. Mar. 68, 65–83. doi:10.3989/scimar.2004.68s165

Richier, S., Achterberg, E. P., Dumousseaud, C., Poulton, A. J., Suggest, D. J., Tyrrell, T., Zubkov, M. V., Moore, C. M. 2014. Carbon cycling and phytoplankton responses within highly-replicated shipboard carbonate chemistry manipulation experiments conducted around Northwest European Shelf Seas, Biogeosci. 11, 3489-3534.

Riebesell, U., Bach, L.T., Bellerby, R.G.J., Monsalve, J.R.B., Boxhammer, T., Czerny, J.,

Larsen, A., Ludwig, A., Schulz, K.G., 2017. Ocean acidification can impair competitive fitness of a predominant pelagic calcifier. Nat. Geosci. 10, 19–24. doi:10.1002/humu.22915.This

Riebesell, U., Zondervan, I., Rost, B., Tortell, P.D., Zeebe, R.E., Morel, F.M., 2000. Reduced calcification of marine plankton in response to increased atmospheric CO2. Nature 407, 364–7. doi:10.1038/35030078

Riegman, R., Noordeloos, A.A.M., Cadee, G.C., 1992. Phaeocystis blooms and eutrophication of the continental coastal zones of the North Sea. Mar. Biol. 479–484.

Riegman, R., Stolte, W., Noordeloos, A. a M., Slezak, D., 2000. Nutrient uptake and alkaline phosphatase (EC 3:1:3:1) activity of *Emiliania huxleyi* (Prymnesiophyceae) during growth under N and P limitation in continuous cultures. J. Phycol. 36, 87–96. doi:10.1046/j.1529-8817.2000.99023.x

Rivero-Calle, S., Gnanadesikan, A., Del Castillo, C.E., Balch, W.M., Guikema, S.D., 2015. Multidecadal increase in North Atlantic coccolithophores and the potential role of rising CO2. Science (80-. ). 350, 1533–1537. doi:10.1016/j.dsr.2009.08.007

Robinson, C., Widdicombe, C.E., Zubkov, M. V., Tarran, G.A., Miller, A.E.J., Rees, A.P., 2002. Plankton community respiration during a coccolithophore bloom. Deep. Res. Part II Top. Stud. Oceanogr. 49, 2929–2950. doi:10.1016/S0967-0645(02)00064-4

Roelke, D.L., Grover, J.P., Brooks, B.W., Glass, J., Buzan, D., Southard, G.M., Fries, L., Gable, G.M., Schwierzke-Wade, L., Byrd, M., Nelson, J., 2011. A decade of fish-killing *Prymnesium parvum* blooms in Texas: Roles of in flow and salinity. J. Plankton Res. 33, 243–253. doi:10.1093/plankt/fbq079

Rost, B., Riebesell, U., Burkhardt, S., Sultemeyer, D., 2003. Carbon acquisition of bloom-forming marine phytoplankton. Limnol. Oceanogr. 48 (1), 55-67.

Rost, B. Riebesell, U. 2004. Coccolithophores and the biological pump: responses to environmental changes, in Thierstein & Young 2004 (eds), Coccolithophores from molecular processes to global impact, Thierstein, H.R. and Young, J.R. (Eds.), Springer, Berlin, 99-125.

Saiz, E., Calbet, A., 2007. Scaling of feeding in marine calanoid copepods. Limnol. Oceanogr. 52, 668-676. doi:10.4319/lo.2007.52.2.0668

Salo, Violeta., Simo, Rafel., Calbet, Albert., 2010. Revisiting the dilution technique to quantify the role of microzooplankton in DMS(P) cycling: laboratory and field tests. J. Plankton Res. 32 (9), 1255 – 1267.

Sanders, R. W. 1991. Mixotrophic protists in marine and freshwater ecosystem. J. Protozool. 38, 76-81.

Schaafsma, F.L., Peperzak, L., 2013. Phytoplankton growth inhibited by the toxic and bacterivorous ciliate *Uronema marinum* (Protozoa, Ciliophora). Mar. Ecol. Prog. Ser. 475, 35–48. doi:10.3354/meps10124

Schiebel, R., Brupbacher, U., Schmidtko, S., Nausch, G., Waniek, J.J., Thierstein, H.R., 2011. Spring coccolithophore production and dispersion in the temperate eastern North Atlantic Ocean. J. Geophys. Res. Ocean. 116, 1–12. doi:10.1029/2010JC006841

Schmoker, C., Hernández-León, S., Calbet, A., 2013. Microzooplankton grazing in the oceans: Impacts, data variability, knowledge gaps and future directions. J. Plankton Res. 35, 691–706. doi:10.1093/plankt/fbt023

Seymour, J. R., Simo R., Ahmed, T. Stocker, R. 2010. Chemoattraction to dimethylsulfoniopropionate throughout the marine microbial food web. Science, 329, 342-345.

Sharples, J., Moore, C.M., Hickman, A.E., Holligan, P.M., Tweddle, J.F., Palmer, M.R., Simpson, J.H., 2009. Internal tidal mixing as a control on continental margin ecosystems. Geophys. Res. Lett. 36, 1–5. doi:10.1029/2009GL040683

Sharples, J., Tweddle, J.F., Green, J.A.M., Palmer, M.R., Kim, Y.N., Hickman, A.E., Holligan, P.M., Moore, C.M., Rippeth, T.P., Simpson, J.H., Krivtsov, V., 2007. Spring-neap modulation of internal tide mixing and vertical nitrate fluxes at a shelf edge in summer. Limnol. Oceanogr. 52, 1735–1747. doi:10.4319/lo.2007.52.5.1735

Sheward, R.M., Poulton, A.J., Gibbs, S.J., Daniels, C.J., Bown, P.R., 2017. Physiology regulates the relationship between coccosphere geometry and growth phase in coccolithophores. Biogeosciences 14, 1493–1509. doi:10.5194/bg-14-1493-2017

Sigman, D.M., Boyle, E.A., 2000. Glacial/interglacial variations In atmospheric carbon dioxide. Nature 407, 859–869. doi:10.1038/35038000

Sikes, C.S., Wilbur, K.W., 1982. Functions of coccolith formation. Limnol. Oceanogr. 27, 18–26.

Simpson, J. H., Sharples J. 2012. Introduction to the Physical and Biological Oceanography of Shelf Sea, Cambridge University Press.

Sintes, E., del Giorgio, P.A., 2010. Community heterogeneity and single-cell digestive

activity of estuarine heterotrophic nanoflagellates assessed using lysotracker and flow cytometry. Environ. Microbiol. 12, 1913–1925. https://doi.org/10.1111/j.1462-2920.2010.02196.x

Skovgaard, A., Legrand, C., Hansen, P.J., Granéli, E., 2003. Effects of nutrient limitation on food uptake in the toxic haptophyte *Prymnesium parvum*. Aquat. Microb. Ecol. 31, 259–265. doi:10.3354/ame031259

Smith, H.E.K., Poulton, A.J., Garley, R., Hopkins, J., Lubelczyk, L.C., Drapeau, D.T., Rauschenberg, S., Twining, B.S., Bates, N.R., Balch, W.M., 2017. The influence of environmental variability on the biogeography of coccolithophores and diatoms in the Great Calcite Belt. Biogeosciences 14, 4905–4925. doi:10.5194/bg-14-4905-2017

Smyth, T. J., Atkinson, A., Widdicombe, S., Frost, M., Allen, I., Fishwick, J., Queiros, A., Sims, D., Barange, M. 2015. The Western Channel Observatory. Prog. Oceanogr. 137, B, 335-341.

Smyth, T.J., Fishwick, J.R., Al-Moosawi, L., Cummings, D.G., Harris, C., Kitidis, V., Rees, A., Martinez-Vicente, V., Woodward, E.M.S., 2010. A broad spatio-temporal view of the Western English Channel observatory. J. Plankton Res. 32, 585–601. doi:10.1093/plankt/fbp128

Smyth, T.J., Tyrell, T., Tarrant, B., 2004. Time series of coccolithophore activity in the Barents Sea, from twenty years of satellite imagery. Geophys. Res. Lett. 31, 2–5. doi:10.1029/2004GL019735

Stoecker, D.K., Hansen, P.J., Caron, D.A., Mitra, A., 2017. Mixotrophy in the Marine Plankton. Ann. Rev. Mar. Sci. 9, 311–335. doi:10.1146/annurev-marine-010816-060617

Stoecker, D.K., Nejstgaard, J.C., Madhusoodhanan, R., Pohnert, G., Wolfram, S., Jakobsen, H.H., Šulčius, S., Larsen, A., 2015. Underestimation of microzooplankton grazing in dilution experiments due to inhibition of phytoplankton growth. Limnol. Oceanogr. 60, 1426–1438. doi:10.1002/lno.10106

Strauss, R. E. 1979. Reliability estimates for Ivlevv's electivity index, the forage ratio, and a proposed linear index of food selection. Transactions of the Americans Fisheries Society, 108, 344-352.

Strom, S.L., Bright, K.J., 2009. Inter-strain differences in nitrogen use by the coccolithophore *Emiliania huxleyi*, and consequences for predation by a planktonic ciliate. Harmful Algae 8, 811–816. doi:10.1016/j.hal.2007.10.005

Strom, S.L., Bright, K.J., Fredrickson, K.A., Cooney, E.C., 2017. Phytoplankton defenses : Do *Emiliania huxleyi* coccoliths protect against microzooplankton predators ? Limnol. Oceanogr. 0, 1–11. doi:10.1002/lno.10655

Sullivan, L.J., 2010. Gut evacuation of larval *Mnemiopsis leidyi* A. Agassiz (Ctenophora, Lobata). J. Plankton Res. 32, 69–74. doi:10.1093/plankt/fbp100

Suttle, C.A., 2005. Viruses in the sea. Nature 437, 356–61. doi:10.1038/nature04160

Takahashi, K., Ling, H.Y., 1984. Particle Selectivity of Pelagic Tintinnid Agglutination. Mar. Mic 9, 87–92.

Tarran, G.A., Heywood, J.L., Zubkov, M. V., 2006. Latitudinal changes in the standing stocks of nano- and picoeukaryotic phytoplankton in the Atlantic Ocean. Deep. Res. Part II Top. Stud. Oceanogr. 53, 1516–1529. doi:10.1016/j.dsr2.2006.05.004

Taylor, J. R. 1982. An introduction to error analysis. University Science Books, Sausalito, California, pp. 327.

Teixeira, I.G., Figueiras, F.G., 2009. Feeding behaviour and non-linear responses in dilution experiments in a coastal upwelling system. Aquat. Microb. Ecol. 55, 53–63. doi:10.3354/ame01281

Tyrrell, T., Merico., A. 2004. *Emiliania huxleyi* bloom observations and the conditions that induce them, in Thiersten, H. R., Young, J. R. (Eds) Coccolithophores from Molecular Processes to Global Impact, Spring, Berlin.

Unrein, F., Gasol, J.M., Not, F., Forn, I., Massana, R., 2014. Mixotrophic haptophytes are key bacterial grazers in oligotrophic coastal waters. ISME J. 8, 164–176. doi:10.1038/ismej.2013.132

Utermöhl, H. 1958. Zur vervollkommung der quantitativen Phytoplankton Methodik. Mitteil. Int. Verein. Theor. Angew. Limnol. 9, 1-38.

Valiadi, M., Iglesias-Rodriguez, D., 2013. Understanding Bioluminescence in Dinoflagellates—How Far Have We Come? Microorganisms 1, 3–25. doi:10.3390/microorganisms1010003

Van Mooy, B. a S., Fredricks, H.F., Pedler, B.E., Dyhrman, S.T., Karl, D.M., Koblízek, M., Lomas, M.W., Mincer, T.J., Moore, L.R., Moutin, T., Rappé, M.S., Webb, E. a, 2009. Phytoplankton in the ocean use non-phosphorus lipids in response to phosphorus scarcity. Nature 458, 69–72. doi:10.1038/nature07659

Vardi, A., Haramaty, L., Van Mooy, B. a S., Fredricks, H.F., Kimmance, S.A., Larsen, A.,

Bidle, K.D., 2012. Host-virus dynamics and subcellular controls of cell fate in a natural coccolithophore population. Proc. Natl. Acad. Sci. U. S. A. 109, 19327–32. doi:10.1073/pnas.1208895109

Vardi, A., Van Mooy, B.A.., Fredricks, H.F., Popendorf, K.J., Ossolinski, J.E., Haramaty, L., Bidle, K.D., 2009. Viral Glycosphingolipids Induce Lytic Infection and Cell Death in Marine Phytoplankton. Science. 326, 861–865.

Verity, P. G., 1988. Chemosensory behaviour in marine planktonic ciliates. Bull. Mar. Sci. 43, 772-782.

von Dassow, P., Ogata, H., Probert, I., Wincker, P., Da Silva, C., Audic, S., Claverie, J.-M., de Vargas, C., 2009. Transcriptome analysis of functional differentiation between haploid and diploid cells of *Emiliania huxleyi*, a globally significant photosynthetic calcifying cell. Genome Biol. 10, R114. doi:10.1186/gb-2009-10-10-r114

Widdicombe, C.E., Eloire, D., Harbour, D., Harris, R.P., Somerfield, P.J., 2010. Long-term phytoplankton community dynamics in the Western English Channel. J. Plankton Res. 32, 643–655. doi:10.1093/plankt/fbp127

Winter, A., Henderiks, J., Beaufort, L., Rickaby, R.E.M., Brown, C., 2013. Poleward expansion of the coccolithophore *Emiliania huxleyi*. J. Plankton Res. 36, 316–325. doi:10.1093/plankt/fbt110

Winter, A., Jordan, R., Roth, P. 1994. Biogeography of living coccolithophores in ocean waters. In Winter, A., Siesser, W. (Eds), Coccolithophores. Cambridge University Press, Cambridge, 161-177.

Winter, A., Stockwell, D., Hargraves, P.E., 1986. Tintinnid agglutination of coccoliths: A selective or random process? Mar. Micropaleontol. 10, 375–379. doi:10.1016/0377-8398(86)90038-1

Woodward, E. M. S., Rees, A. 2001. Nutrient distributions in an anticyclonic eddy in the northeast Atlantic Ocean, with reference to nanomolar ammonium concentrations, Deep Res. Part II, 48, 4, 775-793.

Young, E.F., Brown, J., Aldridge, J.N., Horsburgh, K.J., Fernand, L., 2004. Development and application of a three-dimensional baroclinic model to the study of the seasonal circulation in the Celtic Sea. Cont. Shelf Res. 24, 13–36. doi:10.1016/j.csr.2003.09.003

Young, J.R., Andruleit, H., Probert, I., 2009. Coccolith function and morphogenesis: Insights from appendage-bearing coccolithophores of the family syracosphaeraceae

(haptophyta). J. Phycol. 45, 213–226. doi:10.1111/j.1529-8817.2008.00643.x

Young, J.R., Geisen, M., Cros, L., Kleijne, a, Sprengel, C., Probert, I., Østergaard, J., 2003. A guide to extant coccolithophore taxonomy . J. Nannoplankt. Res. 125.

Young, J. R., Henriksen, K. 2003. Biomineralization within vesicles: the calcite of coccoliths. Rev. in Mineral. And Geochem. 54, 189-215.

Young, J.R., Ziveri, P., 2000. Calculation of coccolith volume and its use in calibration of carbonate flux estimates. Deep. Res. Part II Top. Stud. Oceanogr. 47, 1679–1700. doi:10.1016/S0967-0645(00)00003-5

Young, J. R. 1994. Functions of coccoliths. In Winter, A., Siesser, W. G. (Eds). Coccolithophores. Cambridge University Press, Cambridge, 63-82.

Zhang, S., Liu, H., Ke, Y., Li, B., 2017. Effect of the Silica Content of Diatoms on Protozoan Grazing. Front. Mar. Sci. 4, 1–10. doi:10.3389/fmars.2017.00202

Ziveri, P., de Bernardi, B., Baumann, K.H., Stoll, H.M., Mortyn, P.G., 2007. Sinking of coccolith carbonate and potential contribution to organic carbon ballasting in the deep ocean. Deep. Res. Part II 54, 659–675. doi:10.1016/j.dsr2.2007.01.006

Ziveri, P., Baumann, K. H., Bockel, B., Bollmann, J., Young, J. R. 2004. Biogeography of selected holocene coccoliths in the Atlantic Ocean. In Thierstein, H. R., Young, J. R. (Eds) Coccolithophores From Molecular Processes to Global Impact, 403-428.

Zöllner, E., Hoppe, H.-G., Sommer, U., Jürgens, K., 2009. Effect of zooplankton-mediated trophic cascades on marine microbial food web components (bacteria, nanoflagellates, ciliates). Limnol. Oceanogr. 54, 262–275. doi:10.4319/lo.2009.54.1.0262

Zondervan, I. Rost, B., Riebesell, U. 2002. Effect of $CO_2$ concentration on the PIC/POC ratio in the coccolithophore *Emiliania huxleyi* grown under light-limiting conditions and different daylengths. J. Exp. Mar. Bio. Ecol. 272, 55-70.